THE 2010 POLAR AERONOMY AND RADIO SCIENCE (PARS) SUMMER SCHOOL

Edward J. Kennedy, et al.

NorthWest Research Associates, Inc.
4118 148th Ave. NE
Redmond, WA 98052

52'F gego dgt 2011

Interim Report

AIR FORCE RESEARCH LABORATORY
Space Vehicles Directorate
3550 Aberdeen Ave SE
AIR FORCE MATERIEL COMMAND
KIRTLAND AIR FORCE BASE, NM 87117-5776

DTIC COPY

NOTICE AND SIGNATURE PAGE

Using Government drawings, specifications, or other data included in this document for any purpose other than Government procurement does not in any way obligate the U.S. Government. The fact that the Government formulated or supplied the drawings, specifications, or other data does not license the holder or any other person or corporation; or convey any rights or permission to manufacture, use, or sell any patented invention that may relate to them.

This report was cleared for public release by the 377 ABW Public Affairs Office and is available to the general public, including foreign nationals. Copies may be obtained from the Defense Technical Information Center (DTIC) (http://www.dtic.mil).

AFRL-RV-PS-TR-2011-0170 HAS BEEN REVIEWED AND IS APPROVED FOR PUBLICATION IN ACCORDANCE WITH ASSIGNED DISTRIBUTION STATEMENT.

//signed//
_____
Craig Selcher, AFRL/RVBXI

//signed//
_____
Joel Mozer, RVB Division Chief

This report is published in the interest of scientific and technical information exchange, and its publication does not constitute the Government's approval or disapproval of its ideas or findings.

REPORT DOCUMENTATION PAGE

1. REPORT DATE *(DD-MM-YYYY)*	2. REPORT TYPE	3. DATES COVERED *(From - To)*
32-34-2011	Interim Report	01 Aug 2010 – 31 Jul 2011

4. TITLE AND SUBTITLE	5a. CONTRACT NUMBER
The 2010 Polar Aeronomy and Radio Science (PARS) Summer School	FA8718-08-C-0049
	5b. GRANT NUMBER
	5c. PROGRAM ELEMENT NUMBER 62601F

6. AUTHOR(S)	5d. PROJECT NUMBER
Edward J. Kennedy, A. Lee Snyder, James A. Secan	4827
	5e. TASK NUMBER
	5f. WORK UNIT NUMBER 837152

7. PERFORMING ORGANIZATION NAME(S) AND ADDRESS(ES)	8. PERFORMING ORGANIZATION REPORT NUMBER
NorthWest Research Associates, Inc. 4118 148th Ave. NE Redmond, WA 98052	NWRA-SEA-11-R425

9. SPONSORING / MONITORING AGENCY NAME(S) AND ADDRESS(ES)	10. SPONSOR/MONITOR'S ACRONYM(S)
Air Force Research Laboratory Space Vehicles Directorate 3550 Aberdeen Avenue, SE Kirtland AFB, NM 87117-5776	AFRL/RVBXI
	11. SPONSOR/MONITOR'S REPORT NUMBER(S) AFRL-RV-PS-TR-2011-0170

12. DISTRIBUTION / AVAILABILITY STATEMENT

Approved for public release; distribution is unlimited. (377ABW-2011-1475, dtd 14 Oct 2011)

13. SUPPLEMENTARY NOTES

14. ABSTRACT
The Polar Aeronomy and Radio Science (PARS) Summer School offers graduate students the opportunity to participate in a two week program consisting of scientific lectures and tutorials on the earth''s upper atmosphere and ionosphere at the University of Alaska, Geophysical Institute, and experimental research at the High frequency Active Auroral Research Program (HAARP) Research Station at Gakona, Alaska. The 2010 PARS Summer School, conducted over the period July 12 – 22, 2010, included a total of 21 students and 14 advisors or visiting scientists representing 12 universities. During the research period at the HAARP facility, students conducted a wide variety of experiments ranging from the study of methods and generation efficiency for Extremely Low Frequency (ELF) waves, to the study of Field Aligned Irregularities (FAI) and their influence on Global Positioning System (GPS) accuracy. This report discusses the organization and execution of the 2010 PARS Summer School and presents summaries of the research carried out by each of the participating graduate students.

15. SUBJECT TERMS
Ionosphere, Ionospheric modification, Ionospheric irregularities, Ionospheric optical emissions, Ionospheric scintillation, HAARP, Stimulated Electromagnetic Emissions (SEE)

16. SECURITY CLASSIFICATION OF:			17. LIMITATION OF ABSTRACT	18. NUMBER OF PAGES	19a. NAME OF RESPONSIBLE PERSON Craig Selcher
a. REPORT Unclassified	**b. ABSTRACT** Unclassified	**c. THIS PAGE** Unclassified	Unlimited	82	**19b. TELEPHONE NUMBER** *(include area code)*

i

This page intentionally left blank.

Table of Contents

List of Figures

Approved for public release; distribution is unlimited.

List of Tables

Preface and Acknowledgements

The 2010 PARS Summer School was conducted at the University of Alaska Fairbanks Geophysical Institute (UAF/GI) and at the HAARP Research Station, Gakona, AK over the period 12-22 July 2010. The first week of the summer school took place at UAF/GI and consisted of a daily lecture series. The campaign portion of the summer school, which took place in Gakona, is envisioned as an opportunity for university graduate students to visit the HAARP facility and become familiar with using it for research purposes by planning, executing and reporting on experiments of their own design. The format of the activity required that each student be assisted by a mentor. Five operational days from 18 to 22 July were included in order to take advantage of a wide variety of background ionospheric conditions and to provide ample time for each student to investigate variations within their experiment plan. The campaign period also included daily meetings at which tutorials or presentations were provided by a mentor or other visiting scientist. Students were encouraged to provide interim results of their experiments during these daily meetings.

We would like to acknowledge the participation of each of the mentors and other visiting scientists who provided tutorials and daily consultative guidance to the students. We also want to acknowledge the HAARP facility"s staff and the transmitter system operators. The often complex and sophisticated transmitter and antenna beam operations and frequent experiment revisions required expertise and dedicated effort that was greatly appreciated by all participants. We particularly recognize the efforts of the following individuals who set up each of the experiments and operated the transmitter and antenna array during the campaign.

Dr. Mike McCarrick	Chief Scientist and operator
Dr. Helio Zwi	Software engineer and operator
David Seafolk-Kopp	Software engineer and operator
Ben Uscinski	Software engineer and operator

We also gratefully acknowledge the significant time and effort invested by Dr. Brenton Watkins of the Geophysical Institute who operated the HAARP Modular UHF Ionospheric Radar during the campaign.

Less visible but equally as important to the campaign"s success were the contributions by the site support staff who provided support services, transmitter and diagnostic maintenance and assisted individual researchers in equipment set up data retrieval. The 100% availability of the transmitter system during this campaign was a direct result of the work invested by the following staff members and we are grateful for their contributions:

Marty Karjala	HAARP Site Manager
Deana Rietveld	HAARP Admin Assistant
Jay Scrimshaw	HAARP Senior Electrical Engineer
Travis Million	HAARP Power Engineer
Tracy Coon	HAARP Associate Electrical Engineer
Dave Coon	HAARP Associate Electrical Engineer
Stef Scribner	HAARP Maintenance Technician
Josh Geldersma	HAARP Maintenance Technician

This page is intentionally left blank.

1.   Background: The 2010 HAARP-PARS Summer School

Each year since 2000, a program called the Polar Aeronomy and Radio Science (PARS) Summer School has been conducted to acquaint graduate level university students with many of the scientific facilities located in Alaska. Traditionally, this program which is sponsored by HAARP, the National Science Foundation and the University of Alaska Fairbanks (UAF) begins with a week of lectures and tutorials at the UAF"s Geophysical Institute (UAF/GI) in Fairbanks, AK and includes visits to some of the University"s research facilities including the Poker Flat Research Range (PFRR). At the end of this week, students and their mentors travel to the HAARP Research Station in Gakona for a four to five day research campaign. This portion of the activity provides an opportunity for the students to become familiar with the HAARP facility by using it for research purposes, planning and executing experiments of their own design in close cooperation with the facility operators. The period at the HAARP facility includes daily meetings at which tutorials or presentations are provided by mentors or other visiting scientists. Students are encouraged to provide interim results of their experiments during these daily meetings to obtain feedback and encouragement from their peers. Beginning in 2009, the traditional PARS Summer School is held biennially with a shortened, experimental program at HAARP called the Summer Student Research Campaign (SSRC) held in the intervening years.

The selection process for the PARS program begins with an announcement in one or more scientific journals. The application process includes submission of a research proposal for an experiment to be conducted at the HAARP facility and participants are selected by the UAF/GI. Transportation to Alaska and between facilities and lodging during the school are arranged for successful applicants by UAF/GI. The format of the summer school requires that each student be assisted by a mentor who may be their university advisor or a government or civilian scientist.

The 2010 PARS Summer School was organized and executed jointly by the UAF/GI and NorthWest Research Associates (NWRA). UAF/GI planned all of the school"s activities that took place in Fairbanks. NWRA was responsible for the experimental portion of the program at HAARP, including planning the program, developing the campaign schedule, coordinating with the UAF as necessary, and directing the research campaign activities.

2.   Overview of the 2010 PARS Summer School

The 2010 PARS Summer School was conducted over the period July 12 – 22, 2010. The theme of the school was Ionospheric Plasma Physics and the participants included a total of 21 students and 14 mentors or visiting scientists representing 12 universities.

2.1.   The PARS Lecture Program at the University of Alaska, Fairbanks Geophysical Institute

The tutorial and lecture portion of the 2010 PARS Summer School took place during the period Monday July 12 to Friday July 16. Students and mentors arrived in Fairbanks on Monday and were welcomed by the Director, Dr. Roger Smith, during an evening dinner. The lecture program started at the Geophysical Institute on Tuesday morning with introductory lectures on the atmosphere, ionosphere, and magnetosphere, followed by a tour of the institute. Wednesday"s program was devoted to a full day of plasma physics topics. The lectures on Thursday and Friday covered special topics related to diagnostics of ionospheric plasmas and to the subject of ionospheric plasma heating. On Thursday afternoon the group traveled to Poker Flat Research Range for a tour of the facility. The lecture session ended on Friday afternoon and Saturday was

a break day for travel to the HAARP Research Station in Gakona. A complete list of lectures (both at the Geophysical Institute and at HAARP) is provided in Table 1.

Table 1: PARS Summer School Lecture Program

Date	Lecture Title	Presenter	Location
July 13	The Neutral Atmosphere	Roger Smith	UAF/GI
	The Ionosphere	Bill Bristow	UAF/GI
	The Magnetosphere	Antonius Otto	UAF/GI
	Geophysical Institute Tour	Roger Smith	UAF/GI
July 14	Ionospheric Plasma Physics	Antonius Otto	UAF/GI
	Resonances, Index of Refraction & Dispersion Relations	Bill Bristow	UAF/GI
	Plasma Instabilities	Jim Sheerin	UAF/GI
	Wave Propagation and Ray Tracing	Bill Bristow	UAF/GI
July 15	Optical Diagnostics of Plasmas	Don Hampton	UAF/GI
	RF Heating of Plasmas	Spencer Kuo	UAF/GI
	Tour of Poker Flat Research Range		
July 16	Plasma Waves Excited by High Power Radio Waves	Paul Bernhardt	UAF/GI
	D-region absorption of HF Waves	Robb Moore	UAF/GI
	Radio Diagnostics of Plasmas	Brenton Watkins	UAF/GI
July 18	Welcome to HAARP	Paul Kossey	HAARP
	HAARP Facility Description and Capabilities	Edward Kennedy	HAARP
July 19	Space Weather	Dwight Decker	HAARP
July 20	Ionospheric Effects on GPS	Jade Morton	HAARP
July 21	ELF/VLF Generation with HAARP	Morris Cohen	HAARP
July 22	Students present results of their experiments		HAARP

2.2.   PARS Experiments at the HAARP Research Station, Gakona, AK

Following the break day on July 17, the Summer School participants arrived at the HAARP Research Station on Sunday, July 18 where they were welcomed and introduced to the facility through technical and administrative briefings during which the experiment schedule was distributed. Students and mentors were then given a tour of the facility and research operations began immediately afterward. The program of activities at the HAARP facility over the period July 18-22 included a daily meeting consisting of a facility update, a space weather summary and forecast, a review of prior day experiments (including an opportunity for students to present interim results), a review of current day experiments and a daily tutorial.

Student research experiments were conducted on each of the five days at HAARP. The total operations time of 51.2 hours included 19 student experiments and three special experiments requested by the HAARP program. The total time allocated to each experiment was spread over several days to mitigate the day-to-day variations of ionospheric parameters on experimental results.

Each student was required to present a description of his or her experiment during one of the early daily meetings. On the last day of the summer school, each student presented a summary briefing to the assembled group, including the objective, the procedures and initial results. Students were also required to prepare a preliminary report of their experimental results; these summaries are included in Section 3 of this report.

2.3.   Campaign Planning and Schedule Development

As a part of the application process, students were required to submit a proposal for an experiment to be conducted at HAARP. In addition to their use by UAF/GI in the selection process, these proposals were also used by NWRA for campaign planning and by the HAARP staff to develop operating procedures. Two of the proposers had requested operation in the frequency ranges 4040 - 4300 kHz and 2850 – 3100 kHz, neither of which is within the normal HAARP spectrum allocation. A request for temporary frequency assignment was submitted to the Joint Frequency Management Office (JFMO) at Elmendorf AFB and the request was approved early in June. The frequency ranges that were available for use at HAARP during the 2010 PARS Summer School are shown below in Table2.

Table 2: Frequency Allocations for the HAARP Research Station In Effect During the 2010 PARS Summer School

2.650-2.850 kHz	Permanent
2.850-3.100 kHz	Temporary
3.155-3.400 kHz	Permanent
4.040-4.438 kHz	Temporary
4.438-4.650 kHz	Permanent
4.750-4.995 kHz	Permanent
5.005-5.450 kHz	Permanent
5.730-5.950 kHz	Permanent
6.765-7.000 kHz	Permanent
7.300-8.100 kHz	Permanent
9.040-9.995 kHz	Permanent

At the request of the HAARP program managers, additional experiments from the Naval Research Laboratory, UAF/GI and Stanford University were also included in the campaign period. An initial campaign schedule was developed based on a prioritized set of parameters including satellite pass times, specific time-of-day requirements, and F-layer critical frequency predictions.

A PARS Summer School campaign website had been previously set up with useful information such as the HAARP data rights policy, safety information for visitors to the site, visit request procedures and information about using the chat room during the research. The initial schedule was posted in a password-protected section of the website on July 14. The schedule posted on the website was adjusted regularly throughout the campaign as real time changes were made or new experiments were added.

As previously mentioned, the development of a campaign schedule is based on several factors including requests for specific times associated with satellite passes, requests for specific ionospheric conditions, or the availability of specific diagnostic instruments. Each of these factors is discussed in greater detail in the following sections.

Satellite Passes

Development of the experiment schedule begins with consideration of satellite times since these times are fixed and known in advance. During the 2010 PARS Summer School, the only satellite passes proposed for experiments were those for the DEMETER satellite. Because of the DEMETER orbit, passes were scheduled for both the overhead (at HAARP) cases and for the conjugate point cases.

Ionospheric Conditions

The success of many of the experiments was dependent on specific ionospheric conditions. For a large number of the experiments, operation at a frequency at or just below the F-region or E-region critical frequency is essential. To assist in the schedule development, a prediction of F-region critical frequency (f_0F_2) was prepared using the ITS78 ionospheric model. A sunspot number (SSN) of 10 was used for this calculation since the Summer School experiment campaign took place near solar minimum. Figure 1 shows the results of this prediction. (For comparison, the actual 12 month smoothed sunspot number centered on July 2010 was 16.7; the observed variation of f_0F_2 as a function of time for each of the days during the experiment campaign is given in Appendix A, in Figure A3.). In Figure 1, the yellow horizontal bands show the frequency ranges allocated for HAARP operations during the campaign period.

Several observations can be made from Figure 1. First, as a consequence of the long daylight hours in Alaska during the summer, the f_0F_2 could be expected to remain above the higher (>4 MHz) HAARP permanent frequency allocations for a large number of daily hours during the afternoon and extending into the late evening. Even at its lowest point near 04:00 local time, the f_0F_2 remains above HAARP allocations. However, the figure shows that those experiments requiring operation at or just below the f_0F_2 would not be possible during the times 06:00 – 08:00 ADT and from 23:00 – 02:00 ADT because of the lack of operating frequency allocations in the 3.4 – 4.04 MHz range.

One of the experiments (P03) focused on investigating the formation of field–aligned irregularities in the E-region. The E-region reaches maximum ionization density at approximately local noon, which for the HAARP facility in mid-July is 1345 ADT. The E-region

4

critical frequency at this time is approximately 3 MHz and effective experiments can be conducted using a combination of the HAARP permanent and temporary frequency assignments if they are centered on this time.
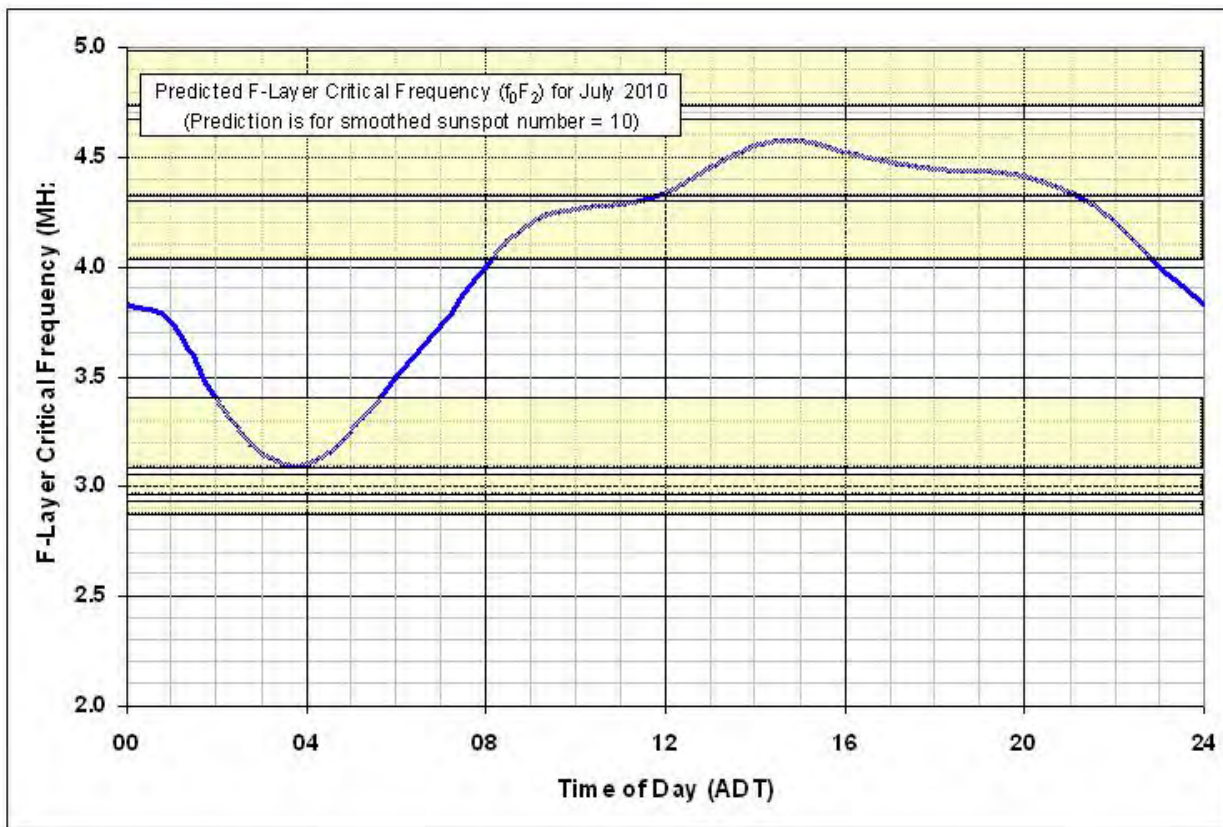
Figure 1: Prediction of F-region critical frequency (f₀F₂) as a function of time of day (in Alaska Daylight Time) for July 2010

Several of the proposers requested that their experiment be scheduled during times of the day when the auroral electrojet is most likely to be present in order to maximize the likelihood of good ELF generation. The occurrence of an overhead auroral electrojet is correlated with disturbed ionospheric conditions driven by solar activity and quantified by the planetary Kp index. A review of the Kp record for several solar cycles prior to the Summer School experimentation period did not disclose any repeating pattern to suggest that favorable ELF generation should occur on any particular campaign day.

Through many years of operation using HAARP, it has been observed that under moderate geomagnetic conditions, the most productive hours for ELF generation are those just prior to local magnetic midnight. During this time period, the auroral oval (and coincident electrojet) is north of, but moving toward HAARP as the earth rotates the magnetic pole toward the longitude of HAARP. Generally, absorption is low as the electrojet moves southward over the HAARP facility (evidenced by low riometer absorption and an increasing, positive H magnetic field component shown on the magnetometer). For higher Kp, these events generally take place earlier in the evening. For very high Kp or at later times, the auroral oval may move to the south of HAARP (as evidenced by a negative magnetic field H component indicating a westward electrojet current) and there is a greater likelihood of increased absorption due to auroral

precipitation, with the result that ELF signal generation may decrease. Therefore, ELF generation experiments requiring an electrojet are generally scheduled for the hours just prior to the closest approach of the auroral oval (21:00 – 02:00 ADT).

Availability of Diagnostic Instruments

The two main diagnostic instruments requested in the proposals were the HAARP Modular Ionospheric Radar (MUIR) and the SuperDARN facility located on Kodiak Island, AK. The MUIR, which is located on-site at the HAARP facility, is operated by the UAF/GI for all research. The MUIR was requested for nearly all of the daytime (high f_0F_2) experiments and for many of the evening experiments.

SuperDARN was requested by those experiments investigating field-aligned irregularities in the F-region. In general, assignment of dedicated (also termed "discretionary") time from SuperDARN requires submission of the request 90 days in advance. Because SuperDARN (Kodiak) is managed by UAF/GI, scheduling of discretionary time for the HAARP experimentation period was integral to the overall PARS Summer School planning and all of the participants requesting SuperDARN in their proposals were able to access relevant data.

Students from MIT and Boston University brought a new instrument to this campaign to support their experiment and set it at the HAARP facility"s most distant diagnostic pad. This instrument, called the Geomagnetic Observatory System (GMOS) is capable of measuring very small fluctuations in the geomagnetic field.

Two other groups brought specialized instruments which were installed at locations away from the HAARP facility. A new digital HF receiver was set up by scientists from the Naval Research Laboratory and used by the students from Virginia Tech at a location approximately 8 miles southwest of the HAARP facility. Students from the University of Florida installed two new ELF receivers. The first receiver was installed at a hunting lodge at mile 28.5 of the Nabesna Road in the Wrangell St. Elias National Park. A second receiver was installed at Tok, AK.

Operator Endurance and Facility Limitations

The scientists, engineers and technicians who operate the HAARP transmitter and supporting infrastructure are dedicated personnel who, nevertheless, have endurance limitations. Typically, the facility can be operated for periods of 10 to 12 hours before the operators require a break. In addition, some equipment failures can be expected in normal operation and the site personnel require transmitter down times measured in hours in order to bring the facility back to full capability. Because of the number of experiments that made up this campaign and with the desire to provide a minimum of 2.5 hours per student, the daily operating time was nearly 14 hours on three of the days.

2.4. Special Experiments

Three additional experiments were conducted during the PARS Summer School experiment campaign. These experiments were scheduled to take advantage of the presence of HAARP operators and staff and to use time that might otherwise not be productive to the student experiments. A description of each of these special experiments is given below.

Evaluation of an Advanced HF Receiver

A new, digital, 4-channel high frequency (HF) receiver was installed at a location approximately 8 miles from the facility by scientists from the Naval Research Laboratory. The receiver, which

was developed for Over The Horizon Radar (OTH-R) applications provided a new capability to study Stimulated Electromagnetic Emission (SEE) spectra with data updating much more rapidly than in the traditional frequency-sweeping receivers. The objective of the experiment was to evaluate and demonstrate the receiver's potential as a diagnostic device for future ionospheric heating experiments. A secondary objective was to examine the magnitude and polarizations of ionospherically reflected HF signals for a variety of frequencies and polarizations transmitted by HAARP for OTH-R applications.

ELF detection using the DEMETER satellite

A special experiment was inserted into the schedule to take advantage of the DEMETER satellite prior to the end of that program. The onboard receiver and orbital parameters of DEMETER made it particularly useful in the study of ELF wave generation and propagation. In the experiments conducted during the PARS Summer School, DEMETER was used to receive ELF signals leaking out of the Earth-Ionosphere waveguide as the satellite approached HAARP in its orbit, to monitor the previously observed focused propagation along the magnetic field line over HAARP, and to look for ELF signals that propagated along the magnetic field line to the southern hemisphere at the conjugate point of HAARP.

Modular UHF Ionospheric Radar (MUIR)

Several time blocks were assigned to experiments focusing on evaluating the performance of the HAARP MUIR to better define its capabilities and limitations as a diagnostic tool to be used by scientists participating in research campaigns at the HAARP facility.

2.5. Final PARS Summer School Experiment Schedule

The experimental campaign schedule was set up to begin on the afternoon of July 18 following the students' arrival at HAARP and the introductory briefings, and to end early on July 22 to allow a final session in which the students could present results of their experiments to the complete group. Beginning and ending times for each day were constrained by the total campaign hours allocated by program managers, by the number of hours facility staff could operate continuously, by the optimum time for E-region experiments occurring near local noon, and by the need to cover electrojet experiments during the period leading up to local midnight. The pass times for the DEMETER satellite, which varied from day to day but were generally clustered around 20-21 UTC and 06-07 UTC, were consistent with the previous constraints and resulted in a daily schedule beginning at 20:00 UTC (12:00 ADT) and ending at 09:30 UTC (01:30 ADT).

Table 3 is a listing of all of the experiments as executed during the 2010 PARS Summer School. The table shows the date and time that the experiment was conducted, the proposal number of the experiment, the section of this report where a quick-look report of the experiment can be found, and the principal investigator.

Table 3: PARS Summer School Research Schedule as Executed

Date UTC	Start UTC	Stop UTC	Experiment Number	Q-L Report Section	Principal Investigator
7/18/2010	20:53:00	20:55:30	P00	*	San Antonio
	21:10:00	21:29:30	P19	*	Piddyachiy
	22:00:00	22:29:30	P10	3.10	Liang
	22:30:00	22:53:30	P18	3.3	Bordikar
	23:00:00	23:59:30	P05	3.1	Adham
7/19/2010	0:00:00	0:59:30	P04	3.15	Roe
	1:00:00	1:53:30	P17	3.6	Fu
	2:00:00	2:53:30	P16	3.11	Mahmoudian
	3:00:00	3:29:30	P02	3.7	Gancarz
	3:30:00	3:41:30	P18	3.3	Bordikar
	3:45:00	4:14:36	P12	3.17	Webb
	4:15:00	5:26:30	P18	3.3	Bordikar
	5:30:00	5:59:30	P01	3.9	Hu
	6:00:00	6:39:30	P09	3.5	Cheng
	6:45:00	7:05:00	P19	*	Piddyachiy
	7:15:00	8:59:30	P08	3.8	Hsu
	9:00:00	9:29:30	P14	3.16	Wang
	20:04:00	20:24:00	P19	*	Piddyachiy
	20:37:00	20:59:30	P19	*	Piddyachiy
	21:00:00	22:29:30	P03	3.13	Nossa
	22:30:00	23:59:59	P07	3.14	Pradipta
7/20/2010	0:00:00	0:29:30	P07	3.14	Pradipta
	0:32:00	1:58:00	P02	3.7	Gancarz
	1:58:30	1:59:30	P11	***	Blaes
	2:00:00	2:29:30	P21	**	Moore
	2:32:30	3:44:30	P06	3.12	Triplett
	3:45:00	4:14:30	P10	3.10	Liang
	4:15:00	4:58:00	P21	**	Moore
	4:58:30	4:59:30	P11	***	Blaes
	5:00:00	5:29:30	P12	3.17	Webb
	5:31:00	5:37:30	P20	*	Watkins
	5:38:00	5:58:00	P19	*	Piddyachiy
	5:58:30	5:59:30	P11	***	Blaes
	6:00:00	6:58:00	P01	3.9	Hu
	6:58:30	6:59:30	P11	***	Blaes
	7:00:00	7:29:30	P09	3.5	Cheng
	7:30:00	7:58:00	P12	3.17	Webb
	7:58:30	7:59:30	P11	***	Blaes

Date UTC	Start UTC	Stop UTC	Experiment Number	Q-L Report Section	Principal Investigator
7/20/2010	8:00:00	8:29:30	P09	3.5	Cheng
	8:30:00	8:58:00	P12	3.17	Webb
	8:58:30	8:59:30	P11	***	Blaes
	9:00:00	9:29:30	P14	3.16	Wang
	20:00:00	20:30:00	P20	*	Watkins
	20:34:00	20:54:00	P19	*	Piddyachiy
	20:58:30	20:59:30	P11	***	Blaes
	21:07:00	21:27:00	P19	*	Piddyachiy
	21:28:30	21:29:30	P11	***	Blaes
	21:30:00	22:29:30	P03	3.13	Nossa
	22:30:00	23:29:30	P07	3.14	Pradipta
	23:30:00	23:58:00	P02	3.7	Gancarz
	23:58:30	23:59:30	P11	***	Blaes
7/21/2010	0:07:00	0:58:00	P05	3.1	Adham
	0:58:30	0:59:30	P11	***	Blaes
	1:00:00	1:58:00	P04	3.15	Roe
	1:58:30	1:59:30	P11	***	Blaes
	2:00:00	2:14:30	P21	**	Moore
	2:15:00	3:44:30	P06	3.12	Triplett
	3:45:00	4:14:30	P10	3.10	Liang
	4:15:00	4:58:00	P05	3.1	Adham
	4:58:30	4:59:30	P11	***	Blaes
	5:00:00	5:09:30	P05	3.1	Adham
	5:10:00	5:58:00	P04	3.15	Roe
	5:58:30	5:59:30	P11	***	Blaes
	6:07:00	6:27:00	P19	*	Piddyachiy
	6:28:30	6:29:30	P11	***	Blaes
	6:30:00	6:58:00	P01	3.9	Hu
	6:58:30	6:59:30	P11	***	Blaes
	7:00:00	7:29:30	P15	3.2	Agrawal
	7:30:00	7:58:00	P12	3.17	Webb
	7:58:30	7:59:30	P11	***	Blaes
	8:00:00	8:29:30	P15	3.2	Agrawal
	8:30:00	8:58:00	P09	3.5	Cheng
	8:58:30	8:59:30	P11	***	Blaes
	9:00:00	9:29:30	P14	3.16	Wang
	20:00:00	21:29:00	P08	3.8	Hsu
	21:31:00	21:58:00	P20	*	Watkins
	21:58:30	21:59:30	P11	***	Blaes
	22:00:00	22:49:30	P03	3.13	Nossa
	22:50:00	22:58:00	P03	3.13	Nossa

Date UTC	Start UTC	Stop UTC	Experiment Number	Q-L Report Section	Principal Investigator
7/21/2010	22:58:30	22:59:30	P11	***	Blaes
	23:00:00	23:57:30	P17	3.6	Fu
7/22/2010	0:00:00	0:58:00	P16	3.11	Mahmoudian
	0:58:30	0:59:30	P11	***	Blaes
	1:02:00	1:29:30	P02	3.7	Gancarz
	1:30:00	1:53:30	P18	3.3	Bordikar
	1:58:30	1:59:30	P11	***	Blaes
	2:00:00	2:29:30	P20	*	Watkins
	2:30:00	3:40:00	P06	3.12	Triplett
	3:45:00	4:14:30	P10	3.10	Liang
	4:15:00	4:59:30	P17	3.6	Fu
	5:00:00	5:47:30	P16	3.11	Mahmoudian
	5:50:00	6:30:00	P01	3.9	Hu
	6:37:00	6:57:00	P19	*	Piddyachiy
	6:58:30	6:59:30	P11	***	Blaes
	7:00:00	7:58:00	P15	3.2	Agrawal
	7:58:30	7:59:30	P11	***	Blaes
	8:00:00	8:29:30	P10	3.10	Liang
	8:30:00	8:58:00	P09	3.5	Cheng
	8:58:30	8:59:30	P11	***	Blaes
	9:00:00	9:06:30	P14	3.16	Wang
	9:07:00	9:19:30	P15	3.2	Agrawal
	9:20:00	9:29:30	P13	3.4	Braun
	18:30:00	18:49:30	P03	3.13	Nossa
	18:50:00	19:09:30	P03	3.13	Nossa
	19:10:00	19:29:30	P00	*	San Antonio
	19:30:00	19:59:30	P21	**	Moore
	20:00:00	20:29:30	P06	3.12	Triplett
	20:30:00	20:49:00	P19	*	Piddyachiy
	21:01:00	21:29:30	P20	*	Watkins
	21:30:00	21:59:30	P00	*	San Antonio
	22:00:00	22:29:30	P21	**	Moore

*	Additional experiment, not a part of the Summer School research group.
**	Substitute experiment inserted during the campaign.
***	Experiment to evaluate new ELF receiver; QL report not required. PI was also co-PI on experiment P10.

Figure 2 is a high-level, graphical representation of the campaign schedule as executed. The columns in this figure represent dates in Alaska Daylight Time (ADT). Each horizontal row represents a 15 minute time block out of the 24 hour day. Blue shading identifies the date and time blocks in which an experiment was conducted.

Experiment Schedule for the PARS 2010 HAARP Research Period

ADT	UTC	18-Jul Sunday	19-Jul Monday	20-Jul Tuesday	21-Jul Wednesday	22-Jul Thursday
10:00	18:00					
10:15	18:15					
10:30	18:30					
10:45	18:45					
11:00	19:00					
11:15	19:15					
11:30	19:30					
11:45	19:45					
12:00	20:00					
12:15	20:15					
12:30	20:30					
12:45	20:45					
13:00	21:00					
13:15	21:15					
13:30	21:30					
13:45	21:45					
14:00	22:00					
14:15	22:15					
14:30	22:30					
14:45	22:45					
15:00	23:00					
15:15	23:15					
15:30	23:30					
15:45	23:45					
16:00	0:00					
16:15	0:15					
16:30	0:30					
16:45	0:45					
17:00	1:00					
17:15	1:15					
17:30	1:30					
17:45	1:45					
18:00	2:00					
18:15	2:15					
18:30	2:30					
18:45	2:45					
19:00	3:00					
19:15	3:15					
19:30	3:30					
19:45	3:45					
20:00	4:00					
20:15	4:15					
20:30	4:30					
20:45	4:45					
21:00	5:00					
21:15	5:15					
21:30	5:30					
21:45	5:45					
22:00	6:00					
22:15	6:15					
22:30	6:30					
22:45	6:45					
23:00	7:00					
23:15	7:15					
23:30	7:30					
23:45	7:45					
0:00	8:00					
0:15	8:15					
0:30	8:30					
0:45	8:45					
1:00	9:00					
1:15	9:15					
1:30	9:30					
1:45	9:45					

ADT	UTC	Sun 18-Jul	Mon 19-Jul	Tue 20-Jul	Wed 21-Jul	Thu 22-Jul

Alaska Daylight Time Date

Figure 2: The 2010 PARS Summer School conceptual operation schedule

In Figure 2, the blue shaded area shows the time allocated for experiments on each of the experimental days at the HAARP Research Station.

Figure 3 shows the proportion of time allocated to individual experiments. This chart includes not only the experiments conducted by the students but also the special experiments that were included in the schedule.
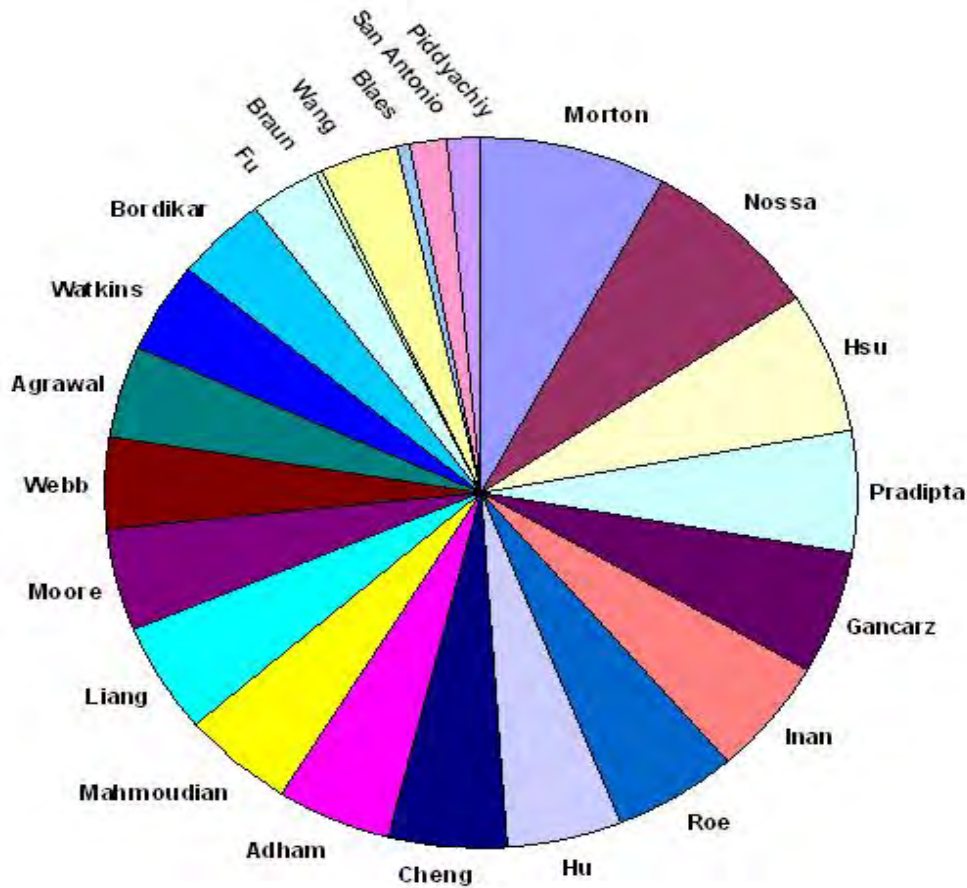
Figure 3: Division of total available campaign time by Principal Investigator for the 2010 PARS Summer School

Twenty-two unique experiments (including the three special experiments) were conducted during the campaign. There were 21 students present during the campaign along with 14 mentors or visiting scientists representing 12 universities. The total operations time allocated to students was 45 hours which provided an average time per student experiment of approximately 2.4 hours. A photograph of the PARS Summer School participants, taken during a tour of the HAARP high power transmitter and phased antenna array, is shown in Figure 4.
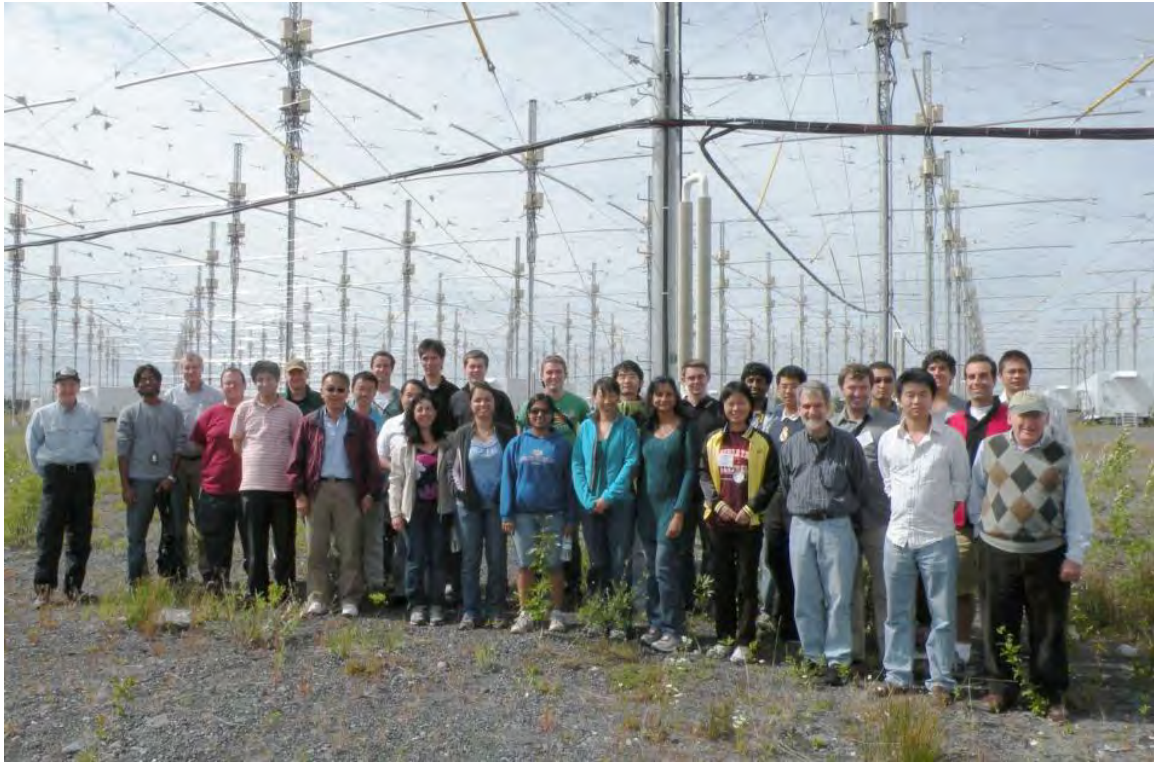
Figure 4: Photograph of the 2010 PARS Summer School participants

2.6   Daily Group Meetings

The traditional PARS Summer School is comprised of a week of lectures and tutorials at the UAF/GI in Fairbanks followed by a research period at the HAARP Facility. In order to retain the valuable learning aspect of the summer school, the daily activity schedule included a meeting consisting of a repeating agenda designed to promote group interaction. The daily meetings followed the standard format of:

- Facility Operational Status Update
- Review of Geomagnetic / Space Weather Conditions
- Review of Prior Day Experiments
- Experiment Plans for Current Day
- Lecture or Tutorial

The operational update provided information on status of the HAARP transmitter and on-site diagnostic instruments. A comprehensive review of prior day and predicted geomagnetic and space weather conditions was presented by a site scientist for the purpose of planning or modifying the current day experiment schedule. Students (or mentors) were then given the opportunity to present quick-look results of their prior-day experiments to the group. Those who were scheduled to conduct experiments on the current day were then polled to confirm that they were prepared and that their equipment, if any, was ready. The daily meeting concluded with a presentation provided by a visiting scientist or mentor on a subject relevant to ionospheric interaction or on the use of the instruments at the HAARP facility.

3.0. Preliminary Campaign Results

All principal investigators were asked to submit quick-look reports in a standard format describing the research objective, the procedure or observation technique, and preliminary results. Submission of the reports was requested within 6 weeks of the end of the campaign. All of the student participants and several PIs for the special experiments submitted the requested reports. Although some investigators reported that there was insufficient time to analyze the data, many of the students were able to show significant results. All of the submitted quick-look reports are included in the following sections.

3.1. MUIR Studies of Aspect Angle Dependence of Plasma Waves at HAARP

3.1.1. Investigators

N. Adham, R.Roe, J. P. Sheerin (mentor), *Eastern Michigan University, Ypsilanti, MI*
B. Watkins, W. Bristow, J. Spaleta, *Geophysical Institute, University of Alaska, Fairbanks, Fairbanks, AK*
C. Selcher, P. Bernhardt, G. San Antonio, *Naval Research Laboratory, Washington, DC*

3.1.2. Objective

The full HAARP IRI was operated at low-duty cycle to generate and study Langmuir plasma waves recorded in the MUIR UHF backscatter spectra (the HF-induced plasma line or HFPL) for a wide range of HF pointing angles. High time resolution (3.3 ms) achieved in the MUIR spectra enabled the study of the development of HFPL spectra during each HF pulse. Stimulated electromagnetic emissions (SEE) spectra were recorded for comparison to MUIR radar backscatter from plasma waves.

3.1.3. Observation Technique

The full HAARP IRI was operated at full power (3444 kW) in O-mode at 4.5 MHz, and using the temporary frequency allocation granted, 4.3 MHz (third gyroharmonic) while keeping the ionosphere overdense. Based on our previous results, an HF pulse width (ON) of 50 ms in an IPP of 12 - 15 sec (for a low-duty cycle of 0.3 - 0.5%), was necessary and sufficient to prevent onset of artificial field-aligned irregularities (AFAI), thus enabling comparison to theoretical predictions for HFPL spectra. The HF pump pointing was varied in zenith in 3° steps from vertical to magnetic zenith (14°) in the magnetic meridian. MUIR recorded the downshifted plasma line spectra with 250 kHz bandwidth (sufficient to record expected outshifted plasma line, OPL) and 3.3 ms resolution. The MUIR radar recorded the HFPL spectra along zenith angles at the magnetic zenith, and for the first time, rapid scans from 9 to 15 degrees south of vertical. The Kodiak SuperDARN HF radar was operated to monitor ionospheric conditions and any development of AFAI. The HAARP ionospheric data instruments (e.g. ionosonde) diagnostics were used for density profile, absorption measurements, and ionospheric conditions.

3.1.4. Preliminary Results

HAARP HF zenith angle pointing was varied stepwise and pulse-to-pulse typically from zero to magnetic zenith. The HFPL spectra are expected to be characterized by strong cascades when observed by MUIR along the magnetic zenith. Our results confirm these observations. For spectra taken with HAARP pointed near the Spitze angle (Z ~ 7° zenith angle) and with MUIR

pointed along the magnetic zenith, we observe strong plasma wave echoes as expected. Results shown (Figure 5) show the strongest plasma line backscatter when HAARP is pointed a 7° zenith and then 11° zenith illustrating the importance of refraction of the HF pump into the MUIR radar-favorable direction. These results lend experimental support to predictions based on computer simulation of refracted HF pump beam.

Figure 6 shows the MUIR real-time display of PL recorded during zenith scans of HAARP (7, 11, 14 degrees) with MUIR operated in a rapid pulse-to-pulse scan mode at 9, 15, 24 degrees zenith. This reproduces the result in Figure 5 and reveals the strong interaction region at 24 degrees. The existence and location of this second interaction region has been verified in several experiments now and by computer simulation. Analysis of this data and comparison to coordinated SEE receiver observations continues.
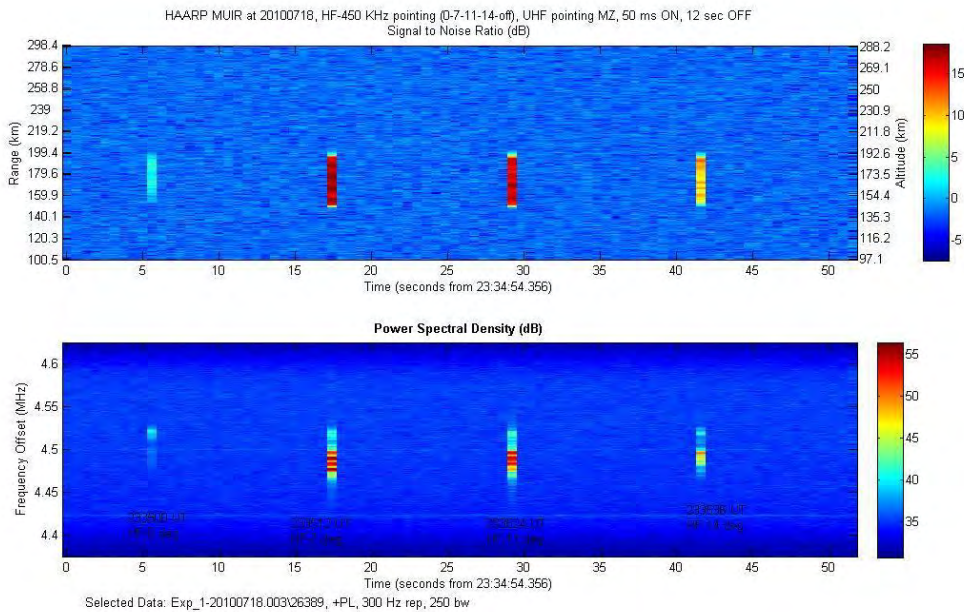
Figure 5: MUIR Plasma Line backscatter for single 50 ms HF pulses

Figure 5 shows MUIR plasma line back scatter for single 50 ms HF pulses at 0, 7, 11 and 14 degrees of zenith angle respectively (labeled in the figure). This data was recorded with MUIR diagnostic radar pointed at magnetic zenith. The strongest return occurs when HAARP is pointed at 7° zenith and then 11° zenith.
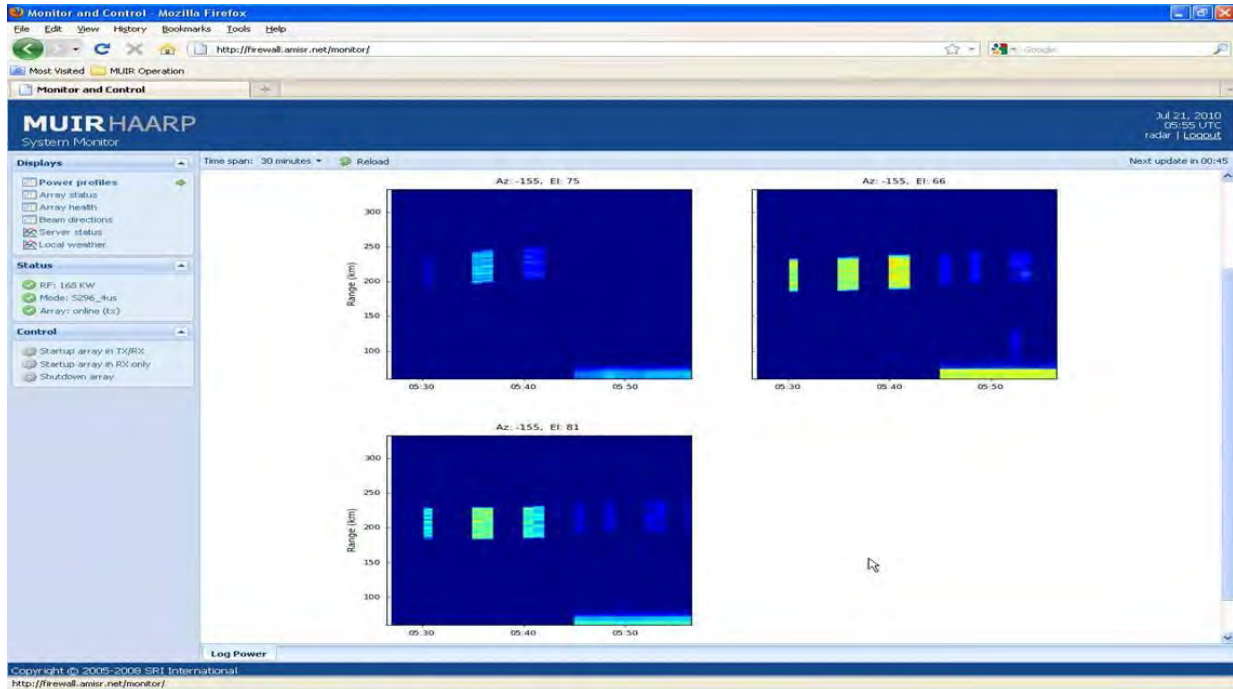
Figure 6: MUIR plasma line backscatter for several HAARP and MUIR pointing angles

Figure 6 shows the MUIR real-time display of plasma line as HAARP scans 7°, 11°, 14° zenith and MUIR pointing (clockwise from upper left) 15°, 24°, 9°. There is a second interaction region observed at 24° as revealed in previous experiments.

3.2. Dual Beam ELF/VLF Wave Generation at HAARP

3.2.1. Investigators

D. Agrawal, R. Moore (Mentor), *University of Florida, Gainesville, FL*

3.2.2. Objective

The main objective of this experiment is to determine the dominant ELF/VLF source region by performing TOA (Time of Arrival) analysis, which will give us vertical ranging information about the source location. We also want to test and validate the Dual-Beam HF heating model, which indicate that simultaneous heating of the ionosphere by a CW HF wave and a modulated HF wave produces lower ELF/VLF magnitudes than during periods without CW heating.

3.2.3. Observation Technique

Two broadband (300Hz – 45kHz) ELF/VLF receivers were deployed. The first receiver, shown in Figure 7, was located at Sportsmen's Paradise Lodge at mile 28.5 of the Nabesna Road in the Wrangell St. Elias National Park off the Tok Cutoff Highway between Tok and Glennallen. The Paradise site proved to be exceptional, as there were no power lines and the data received were comparable to those obtained at the University of Florida (UF) Antarctica sites, in terms of Signal-to-Noise ratio (SNR). The other receiver was deployed in Tok, Alaska.

These receivers (along with the previously installed UF receiver located at Sinona Creek) were used to detect the ELF/VLF waves generated by HAARP. Each receiver system consists

Figure 7: Photograph of ELF/VLF receiver as installed at Paradise, Alaska to detect the ELF/VLF signals generated by the HAARP HF

of two orthogonal magnetic loop antennas oriented to detect the radial magnetic field at ground level, a preamplifier, a line receiver, and a digitizing computer. Radial and azimuthal components of the magnetic field were monitored continually. The receivers are sensitive to magnetic fields with frequencies ~500 Hz to ~45 kHz. Data were sampled at 100 kHz with 16-bit resolution.

During periods between 0700-0730 and 0800-0830 UTC on 21 July 2010 and 0700-0800 UTC and 0900-0920 UTC on 22 July 2010, the HAARP IRI antenna system was used in a split array configuration. The array was split into two 6x15 North-South sub-arrays, each with a peak power of 1800 kW. One sub-array was used to generate ELF/VLF waves by modulated ionospheric heating at 4.5 MHz (X-mode polarization). Frequency time ramps were used, by stepping the frequency from 1-5 kHz for a total ramp duration of 8 seconds, using sinusoidal amplitude modulation. Simultaneously, the second beam of the HAARP HF transmitter was used in a CW ON-OFF mode. The array continually heated the same patch of ionosphere at peak power at 3.25 MHz (CW, X-mode) for a period of 8 seconds. A lower HF frequency was selected for the CW beam so that the CW beam pattern would be broader than that of the modulated 4.5 MHz HF beam. The 8 second CW transmission block was followed by an 8-second period without CW heating (i.e., the first beam continued to modulate at 4.5 MHz while the second beam was OFF). This pattern was continued for the entire transmission block.

3.2.4. Preliminary Results

This experiment allowed for the detection of the total propagation delay between HAARP and ELF/VLF signal detection on the ground. The time-of-arrival (TOA) was measured under dual-beam heating conditions. Figures 8 and 9 show the amplitude-normalized TOA traces for

Sportsmen's Paradise lodge, comparing CW ON and CW-OFF times. Differences of several dB are observed between CW-ON and CW-OFF times (not shown), but only generic differences can be observed between the two runs in terms of TOA (near 100 μsec). We are compiling statistics on the rest of the runs to determine whether further differences may be detected.
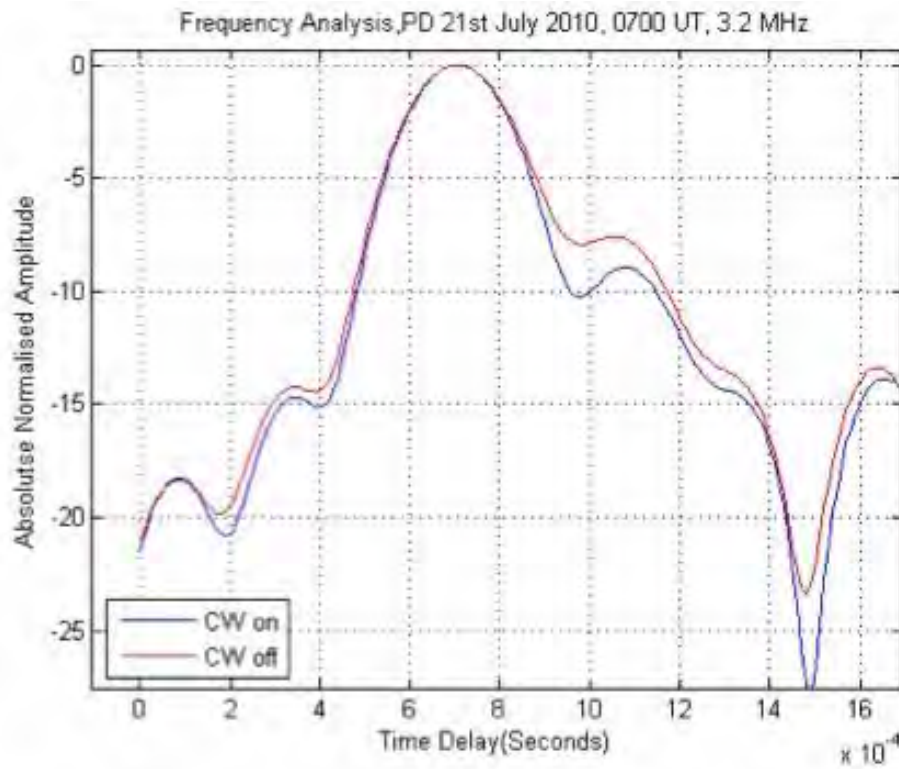
Figure 8: Time of arrival (TOA) measured at Sportsman's Lodge displayed on a zoomed-out scale
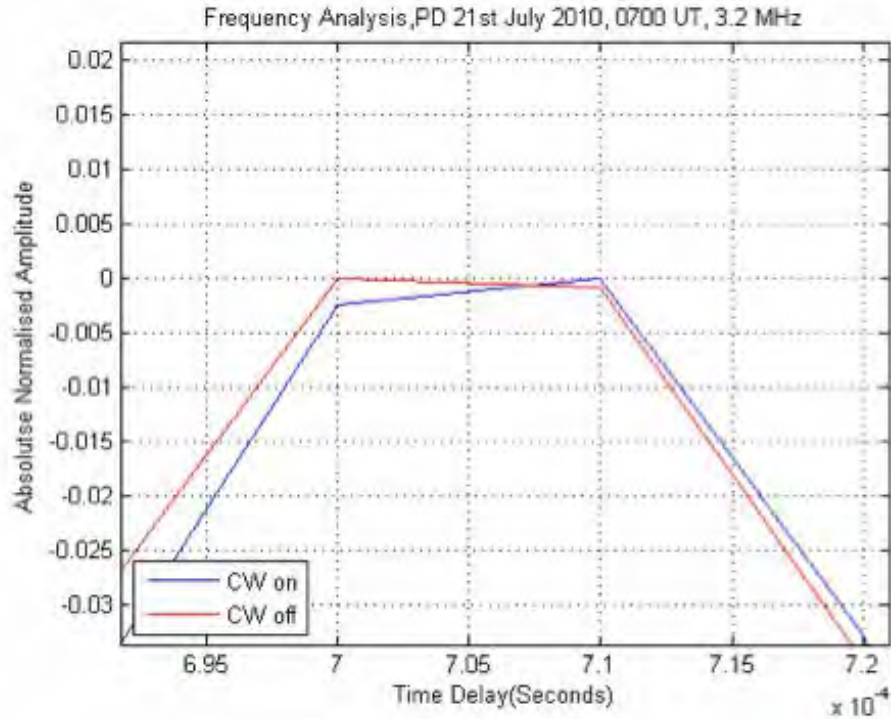
Figure 9: Time of arrival (TOA) measured at Sportsman's Lodge displayed on a zoomed-in scale

3.3. Investigation of Ion Bernstein Scatter Generation Near the 2nd Cyclotron Harmonic in SEE

3.3.1. Investigators

M. Bordikar, W. Scales (Mentor), *Virginia Tech, Blacksburg, VA*
P. Bernhardt (Mentor), S. Briczinski, G. San Antonio, C. Selcher, *Naval Research Laboratory, Washington, DC*
E. Nossa, *Cornell University, Ithaca, NY*

3.3.2. Objective

Recent unsatisfactorily explained observations at HAARP have shown a new decay mechanism in which possible decay of the electromagnetic pump wave into ion Bernstein-type modes (rather than lower hybrid modes) is present. Such new Stimulated Electromagnetic Emission (SEE) features obviously may have important diagnostic consequences for ion composition and ion behavior in the heated volume as well as information on the ambient magnetic field. The objective of this experiment is to shed light on the new SEE feature. It should be noted that this is a physically different process than the recently observed magnetized stimulated Brillouin scatter. The experiment is to explore this proposition in further detail by sweeping the pump frequency through the second electron cyclotron harmonic frequency and observe the behavior of the creation and hopefully suppression of this new so-called oxygen Bernstein decay instability.

This experiment addressed the following fundamental questions:

1) Are these oxygen lines suppressed in a similar manner as the Downshifted Maximum (DM)?

2) Do they exist both above and below the gyroharmonic as the DM?

3) If so, what are the differences in the spectral structure above and below the gyroharmonic?

4) In general how does the behavior compare to the DM behavior near a gyroharmonic and what can be learned to further advance the understanding of the physical processes associated with SEE?

3.3.3. Observation Technique

Generate ion Bernstein modes with HAARP operating at the 2nd gyroharmonic frequency. Figure 10 shows a conceptual drawing of the experiment.

Frequency – Step through from 2.75 MHz – 2.85 MHz in steps of 0.02 MHz, Then step through from 2.85 MHz – 2.95 MHz in steps of 0.02 MHz

Beam pointing – Magnetic zenith and Vertical

Polarization – O mode wave.

Power – Decrease HAARP radiated power level in steps of 6dB starting with full power 3.6 MW.

Transmitter duty cycle – 1 minute on and 1 minute off

The experiment was performed on 18 July 2010 from 2230 – 2250 UTC, on 19 July 2010 from 0330- 0340 UTC and 0414-0530 UTC and on 22 July 2010 from 0130-0154 UTC.
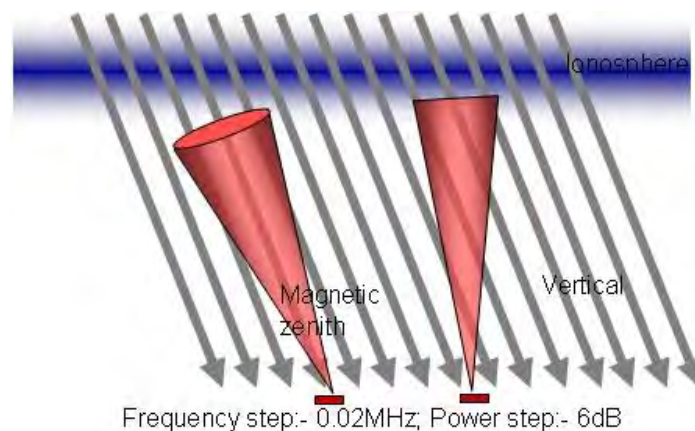
Figure 10: Conceptual diagram of experiment setup

A spectrum analyzer with a four channel receiver was used to collect the SEE data. Also the 30 MHz VHF radar located at Homer, AK was used during the experiment run on 22 July to obtain range time intensity (RTI).

3.3.4. Preliminary Results

Data obtained in a SEE experiment on 28 October 2008 at HAARP have shown a new decay mechanism in which possible decay of the electromagnetic pump wave into ion Bernstein-type modes (rather than lower hybrid modes) was present. The spectrum plots in Figure 11 show both Stokes and Anti-Stokes ion Bernstein modes at approximately 50 Hz apart. The ion Bernstein lines can also be seen in the two dimensional spectrum.
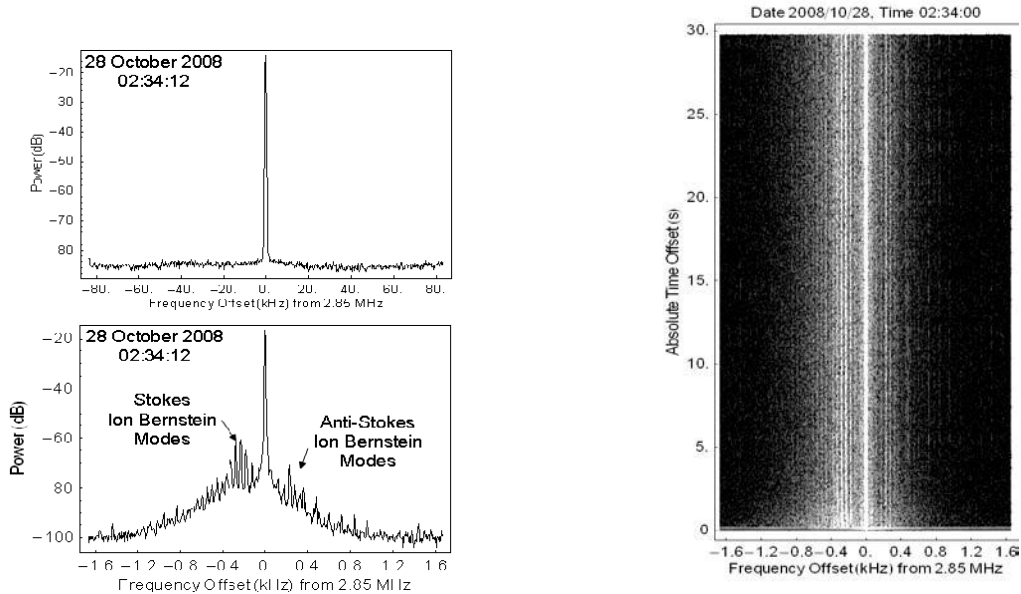
Figure 11: Results of the 28 October 2008 experiment at HAARP

The preliminary results from the 2010 PARS experiment also confirms the existence of the ion Bernstein modes. Figure 12 shows the results for the run conducted on 19 July 2010 at 0517 UTC. The pump frequency was 2.79 MHz using 0.9 MW of radiated power and with the antenna beam pointed vertically. The ion Bernstein modes (indicated by arrows in Figure 12) can be seen with a frequency separation of approximately 50 Hz.
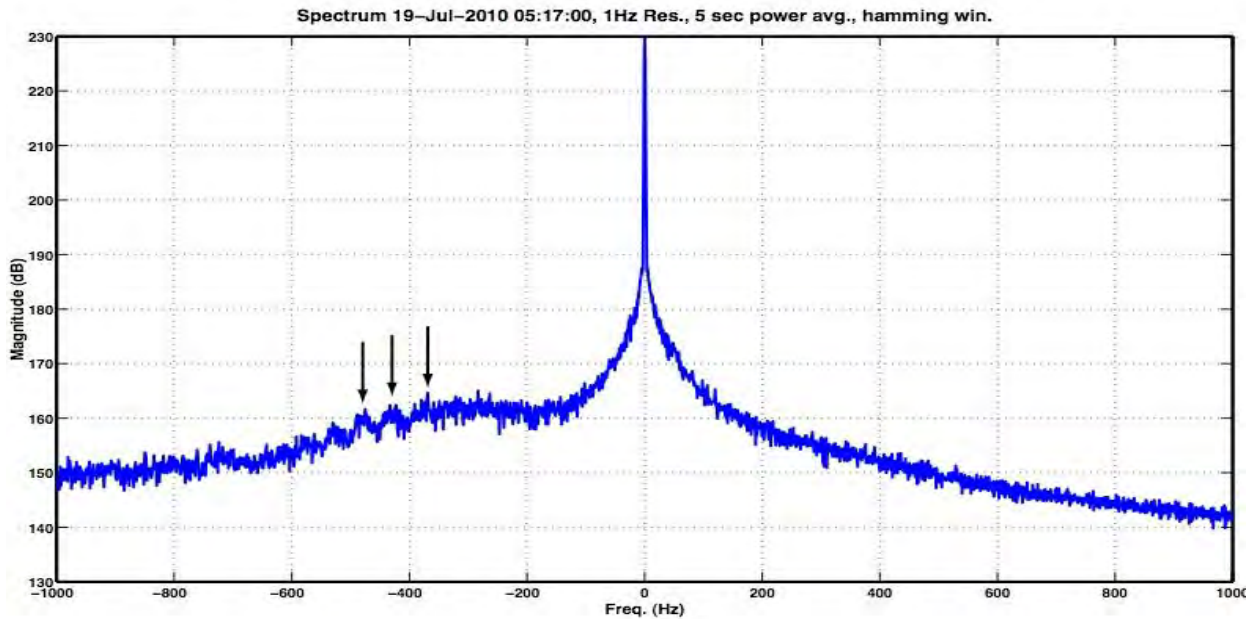
Figure 12: Frequency spectrum for 19 July 2010

We are currently processing additional data. The analysis may show more well-defined gyroharmonic structuring and probably Stokes and anti-Stokes Bernstein modes. Figure 13 shows range time intensity from the 30 MHz radar at Homer, AK for 22 July 2010 between 0130 – 0200 UTC. The HAARP frequency was stepped from 2.85 MHz – 2.95 MHz at full power and with the antenna beam positioned vertically and at magnetic zenith. The cycle was repeated for 0.9 MW power. The range time intensity plot shows a bite out for heating at magnetic zenith and full power indicating the presence of a sporadic E layer.
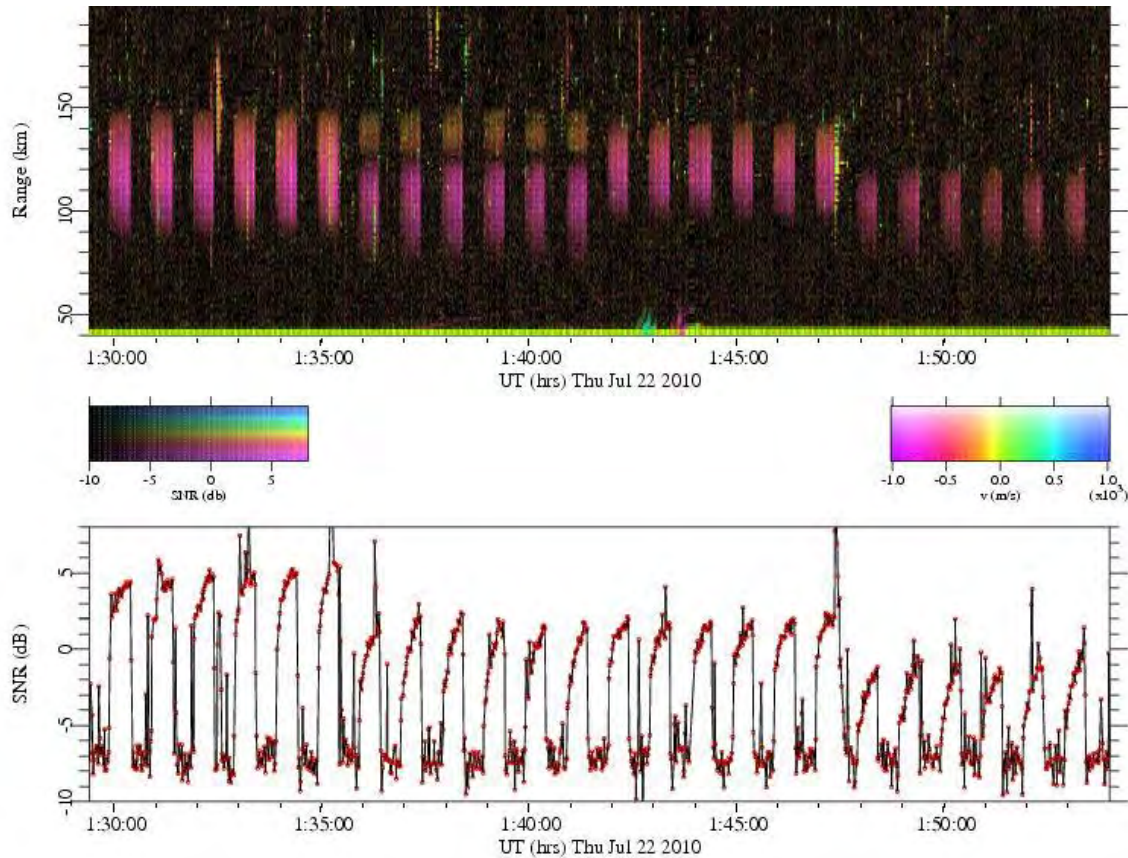
Figure 13: RTI from the 30 MHz Radar at Homer, AK

3.4. Time of Arrival Observations of ELF/VLF Waves Generated by Modulated HF Heating at HAARP

3.4.1. Investigators

E. Braun and S. Fujimaru, *University of Florida, Gainesville, FL*
R. Moore (Mentor), *University of Florida, Gainesville, FL*

3.4.2. Objective

The High Frequency Active Auroral Research Program transmitter was used to modulate electrojet currents present above Gakona, AK in order to produce ELF and VLF waves. These transmissions were repeated with different HF power levels and different HF frequencies in order to test the time of arrival (TOA) method and determine experimental limits for the method's ranging resolution.

3.4.3. Observation Technique

Several VLF antennas, at Paradise Sportsmen's Lodge, Tok, and Sinona Creek, recorded the ELF/VLF waves as they were received at that location. The systems include 2 orthogonal crossed loop antennas, a GPS antenna and receiver for timing, and a pre-amplifier and receiver system for the antennas. Data were sampled at 100 kHz with 16-bit resolution.

3.4.4. Preliminary Results

Figure 14 shows the results of data analysis from the Paradise Sportsman˝s Lodge using the TOA method. The peaks correspond to the time of arrival of each of the frequencies and power levels, respectively. It shows that the changes to the heated region induced by HF power level and HF frequency differences are detectable and that the TOA method is viable in this application. The stars on the figure indicate interpolated peak value arrival times. At 3.2 MHz, ELF/VLF generated using 100% power arrives after the ELF/VLF generated using 50% power, indicating that 100% power was generated at a slightly higher altitude. The same is observed at 5.8 MHz, except that the relative time difference between the two is approximately double. These observations indicate that the TOA method is sensitive enough to detect the ELF/VLF source variations that occur by doubling the HF power and by approximately doubling the HF frequency.
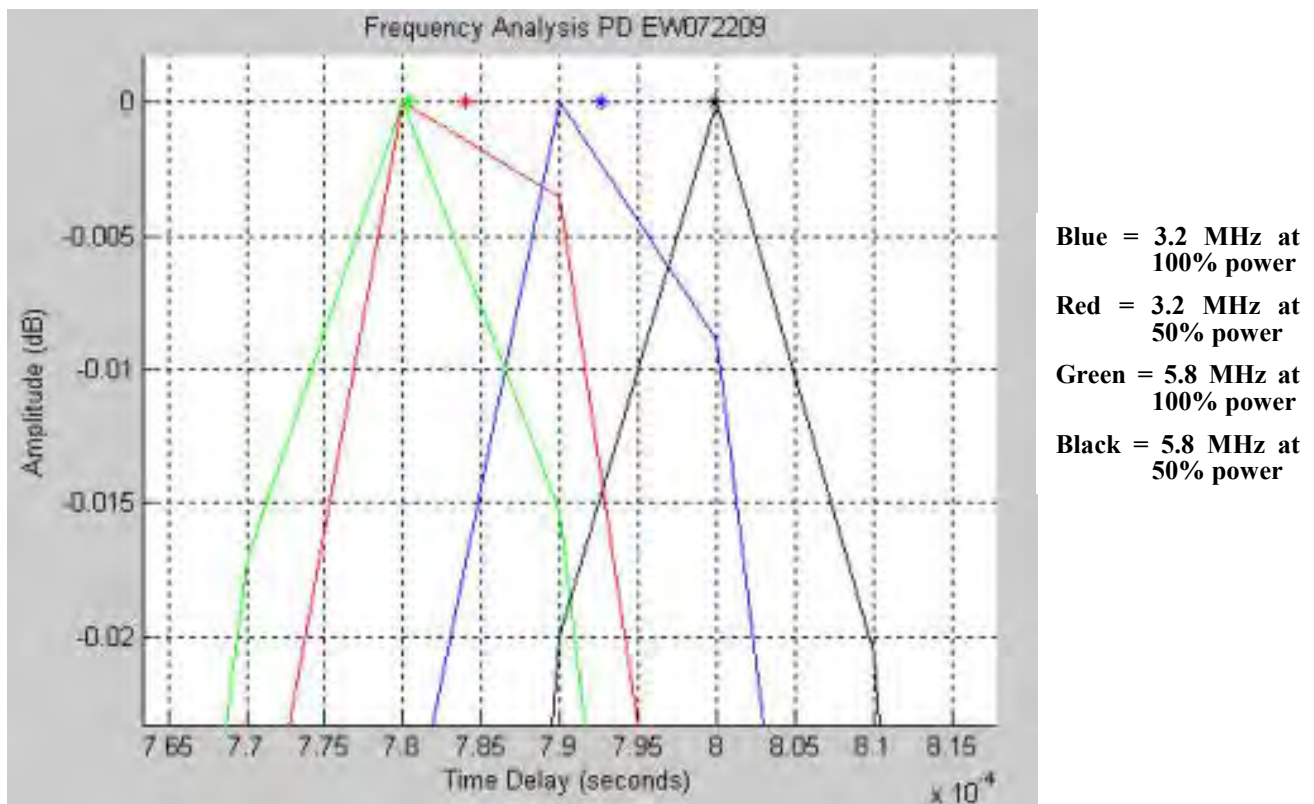
Figure 14: Data from the Paradise receiver E/W channel showing a comparison for three cases of HF frequency and radiated power

3.5. VLF Wave Generation by the X-mode HF Heater: Beat Wave and Split Beam Schemes

3.5.1. Investigators

Wei-Te Cheng, Will Hsu, Spencer Kuo (Mentor), *Polytechnic Institute of New York University, Brooklyn, NY*
Arnold Snyder, *NorthWest Research Associates, Stockton Springs, ME*
Chia-Lie Chang, *BAE Systems - Technology Solutions, Arlington, VA*

3.5.2. Objective

On 4 April, 2010, in the presence of a moderate electrojet, relatively intense VLF waves were generated by the beat wave approach. The results show that the spectral intensity of the VLF radiation increases with the beat wave frequency. The proposed experiment is to confirm the previous experimental results and to compare with the conventional electrojet modulation approach.

Experiments were conducted with the HF heater transmitting at 3.2 MHz, X-mode polarization along the geomagnetic zenith at full power level. The antenna array was split to radiate two beams. In the beat wave scheme, the two beams both run in CW mode, but radiate at slightly different frequencies, 3.2 MHz and 3.2 MHz + Δf, where Δf is the frequency of the VLF wave generated by the beat wave. In the split beam scheme, one beam runs in the CW mode while the other is amplitude-modulated at a VLF frequency. The dependencies of the VLF wave intensity on the beat frequency of the beat wave scheme and on the modulation frequency of the split beam scheme were explored. The experimental results from two different days show correlation on the trend of the dependencies.

3.5.5. Observation Technique

The experiments were monitored by the HAARP Digisonde, Fluxgate Magnetometer, and ELF/VLF receivers. The Digisonde acquired fast cadence, low resolution ionograms interleaved with skymaps.

3.5.6. Preliminary Results

Experiments were conducted from 19 to 21 July 2010 in different time slots. On 19 July from 0600 to 0620 UTC, the HAARP transmitter operated at 3.2 MHz using X-mode and transmitting the beat wave modulation frequency from 2.5 KHz to 22.5 kHz with 90 seconds ON and 30 seconds OFF. From 0620 to 0640, the HAARP transmission was modulated in the same fashion with the split beam modulation. On 20 July 2010 from 0700 to 0730 UTC, the heater was operated in the split beam mode using modulation frequencies from 2.5 kHz to 22.5 kHz with 2 minutes ON and 1 minute OFF. From 0800 to 0830 UTC, the HAARP transmitter was operated with beat wave modulation. On 21 July 2010 from 0830 to 0900 UTC, the HAARP transmitter was modulated with a duty cycle of 90 seconds ON and 30 seconds OFF, with beat wave frequencies from 3.5 kHz to 23.5 kHz. On 22 July, the heater was modulated in the same manner using the split beam scheme.

The magnetic power spectral density of the VLF wave was recorded during the experiment period. These data were integrated over the frequency bandwidth to obtain the magnetic field intensity of the wave. Ionograms taken during the experiments indicated that the ionosphere was moving upward. Therefore, the radiation intensity is calibrated by the variation of the height at 3.2 MHz. Since the heater power is inversely proportional to the square of the height and the radiation amplitude is inversely proportional to the height of the radiation source (~ at 3.2 MHz), the calibration factor is proportional to the cube of the height.

For the beat wave modulation, the results of 19 July from 0600 to 0620 UTC and 21 July from 0830 to 0900 UTC are shown in Figure 15(a) and 15(b). Both figures show that the signal intensity increases with frequency in the low frequency regime and decreases with frequency in the high frequency regime. The peak appears to be in the region between 11.5 and 12.5 kHz..

For the split beam modulation, the results of 19 July from 0620 to 0640 UTC and 22 July from 0830 to 0900 UTC are shown in Figures 16(a) and 16(b). The trends of the frequency dependencies of the two plots are less obvious and no conclusions can be drawn. This may be due to different ionospheric conditions.
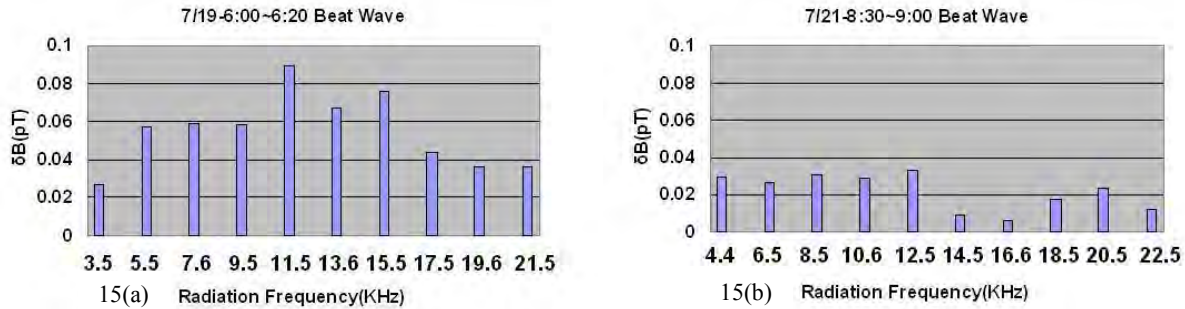
Figure 15: Field intensity for the beat wave generation scheme
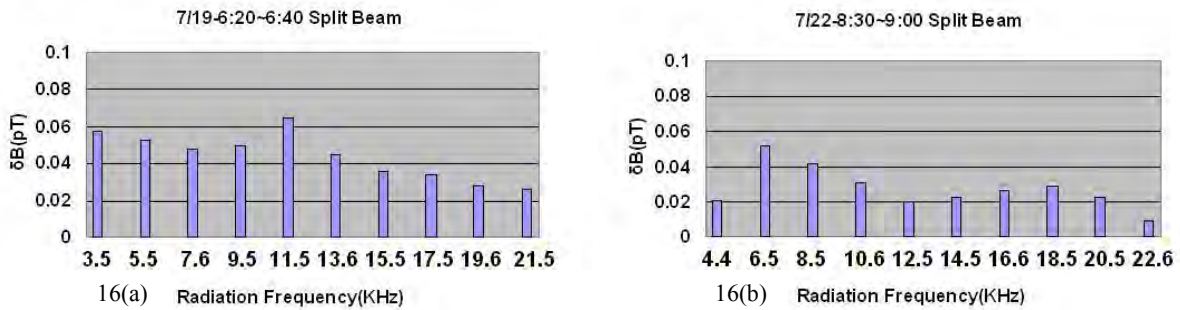
Figure 16: Field intensity for the split beam generation scheme

3.6.   Heater Beam Angle Effect on Simulated Brillouin Scatter in Magnetized Ionospheric Plasma

3.6.1. Investigators

H. Fu, W. Scales (Mentor), *Virginia Tech, Blacksburg, VA*
P. Bernhardt (Mentor), S. Briczinski, G. San Antonio, C. Selcher), *Naval Research Laboratory, Washington, DC*

3.6.2. Objective

The HAARP 3.6 MW HF transmitter is used to excite low frequency electrostatic waves by magnetized stimulated Brillouin scatter (MSBS) near the reflection resonance region or the upper hybrid resonance regions. The pump wave (O mode) may excite either electrostatic ion acoustic (IA) or electrostatic ion cyclotron (EIC) waves depending on the wave propagation relative to the ambient magnetic field. This proposed experiment aims to look more thoroughly at a broader range of heater beam angle effects on IA and EIC waves generated by MSBS as shown in Figure 17.
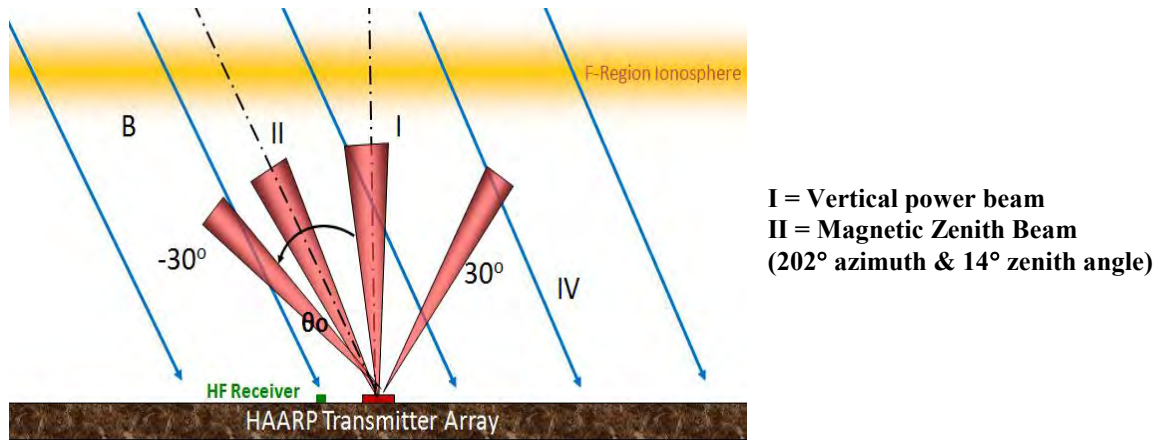
Figure 17: Stimulated Electromagnetic Emission (SEE) measurement with varying antenna radiation beam angle

3.6.3. Observation Technique

The HAARP transmitter was operated on 19 July 2010 between 0100 and 0150 UTC using a pump frequency of 4.5 MHz at O-mode and 5.254 MHz at X-mode and again on 22 July between 0415 and 0459 UTC using 4.1 MHz, 4.2 MHz, and 4.3 MHz with O-mode polarization. The time history of electromagnetic backscattered waves by the HAARP transmitter was recorded with a 4-channel spectrum analyzer SEE receiver, which was located 13 km from the HAARP transmitter. This receiver, which employed two cross dipole antennas, was also able to measure the polarization. In addition, diagnostics data were collected simultaneously by the University of Alaska SuperDARN radar facility on Kodiak Island and by the MUIR ionospheric radar located at the HAARP facility.

3.6.4. Preliminary Results

Preliminary results presented here are based on the data obtained from the SEE receiver. Data acquired from the SuperDARN and MUIR diagnostics during the July 2010 PARS campaign were not yet available.

The SEE spectra with O-mode polarization are shown in Figure 18 for various HAARP antenna beam angles. The data were obtained on 22 July 2010 between 0415 and 0459 UTC. For the pump frequency at 4.2 MHz in Figure 18(a), for all three beam angle cases, we can observe the spectral lines about $\pm f1 = 9.5$ Hz, which appear to be quite symmetric. For the beam pointing case of 202° azimuth and 21° zenith angle, two other spectral lines are also observed at about $f2 = 26$ Hz and $f3 = 52$ Hz. For the case of 202° azimuth and 28° zenith angles (too far from magnetic zenith), only $\pm f1$ are observed. It is believed that the excitation of the f2 and f3 spectral lines is near the threshold.

A similar result is seen for the pumping frequency at 4.1 MHz as shown in Figure 18(b) in the sense that the $f2 = 26$ Hz and $f3 = 52$ Hz spectrum lines are only observed in the case of 202° azimuth and 21° zenith angle. It also appears that the strength of the f1 spectral line may be varying with the heater power beam angle.

These spectral lines are in the frequency range of ion acoustic and electrostatic ion cyclotron waves. For the X-mode transmissions in this campaign, we did not observe any SEE spectrum using a pumping frequency 5.254 MHz.

Further analysis about the wave normal angle with magnetic field and altitude will be conducted in the future.
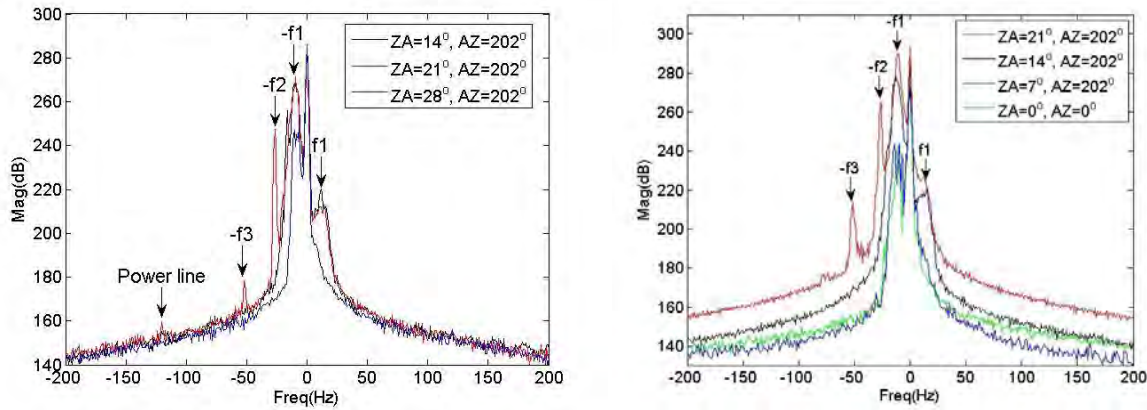
Figure 18: SEE spectra near the HF pump frequency for various antenna beam pointing angles

3.7.   Measurements of HF Wave-Induced Micropulsations Using GMOS

3.7.1. Investigators

J. Gancarz, R. Pradipta, and Min-Chang Lee (Mentor), *Massachusetts Institute of Technology, Cambridge, MA*

K. Hu, *Boston University, Boston, MA*

3.7.2. Objective

We have conducted several previous experiments to investigate the generation of large plasma sheets by HAARP heater waves via thermal filamentation instabilities [Cohen et al., 2008 & 2009]. These large plasma sheets generated by HAARP have different configurations, depending upon the polarizations (i.e., O or X-mode) of the heater waves. One striking feature of thermal filamentation instabilities, which we focus on in this experiment using our new instrument, the Geomagnetic Observatory System (GMOS), is the simultaneous excitation of sheet-like plasma density fluctuations (δn) and geomagnetic field fluctuations (δB). The physical process can be simply understood as follows. The differential Joule heating resulting from the interactions of HF heater waves and excited high frequency sidebands, yields a thermal pressure force on electrons. The thermal pressure force (denoted by f_T) leads to a f_T **X** $\mathbf{B}_0$ drift motion of electrons and, consequently, induces a net current perpendicular to both the background magnetic field $\mathbf{B}_0$ and the wave vector **k** of the excited plasma density irregularities. Therefore, magnetic field fluctuations ($\delta\mathbf{B}$) associated with micropulsations are excited along the background magnetic field ($\mathbf{B}_0$ designated as the z-axis) simultaneously with the density irregularities in both O- and X-mode heating processes. The excited magnetic field fluctuations ($\delta\mathbf{B}$) have three components

designated as $\delta\mathbf{B}_D$, $\delta\mathbf{B}_H$, and $\delta\mathbf{B}_Z$. Based on the above explanation of the simultaneous excitations of δn and $\delta\mathbf{B}$, we can expect that $\delta\mathbf{B}_D$ and $\delta\mathbf{B}_Z$ (or $\delta\mathbf{B}_H$ and $\delta\mathbf{B}_Z$) will be highly correlated in O-mode (or X-mode, respectively) heating experiments. We will use GMOS to take data for this correlation study.

3.7.3. Observation Technique

The experiment is ideally conducted during the daytime with reasonably high f_0F_2 and no spread F. The HAARP IRI is operated with two separate and independent antenna subarrays.

      Subarray A = 6 elements X 8 elements (northeast corner of the IRI)
      Subarray B = 7 elements X 7 elements (southwest corner of the IRI)

The HAARP transmitter is operated over a one hour cycle consisting of:

      <u>For the first 20 minutes</u>

      Subarray A is operated in CW mode, antenna beam vertical, O-mode polarization, HF frequency = 2.8 MHz.; Subarray B is operated in pulsed mode (100 ms ON / 900 ms OFF), antenna beam vertical, O-mode polarization, HF frequency = 3.3 MHz

      <u>For the next 10 minutes</u>

      Subarray A is OFF; Subarray B is operated in pulsed mode (100 ms ON / 900 ms OFF), antenna beam vertical, O-mode polarization, HF frequency = 3.3 MHz.

      <u>For the next 20 minutes</u>

      Subarray A is operated in CW mode, antenna beam vertical, X-mode polarization, HF frequency = 2.8 MHz; Subarray B is operated in pulsed mode (100 ms ON / 900 ms OFF), antenna beam vertical, O-mode polarization, HF frequency = 3.3 MHz

      <u>For the next 10 minutes</u>

      Subarray A is OFF; Subarray B is operated in pulsed mode (100 ms ON / 900 ms OFF), antenna beam vertical, O-mode polarization, HF frequency = 3.3 MHz

The following diagnostic instruments were operated to collect data

      <u>HAARP Digisonde</u>

      1 ionogram and 4 F-region skymaps every 5 minutes.

      <u>HAARP MUIR</u>

      Antenna beam pointed vertical, plasma lines recorded @3.3 MHz using CLP

      <u>GPS/LEO Satellite Pass</u>

      Experiment schedule requested to include a satellite pass that can provide a measurement of TEC in the vicinity of the heated region. Ideal satellite pass would be in the middle or end of the experiment period.

      <u>SuperDARN</u>

      Data from 3 look directions (beam #2, #8, #14)

      <u>HAARP Magnetometer and Riometer</u>

Data obtained from normal operation of these instruments

GMOS/VLF Receiver

Operated by the investigators

3.7.4. Preliminary Results

The detailed correlation study of recorded magnetic field fluctuations ($\delta\mathbf{B}_D$, $\delta\mathbf{B}_H$, and $\delta\mathbf{B}_Z$) for this experiment is currently in process. Figure 19 showing the preliminary correlation analyses, η_{HZ} of $\delta\mathbf{B}_H$ and $\delta\mathbf{B}_Z$ and η_{DZ} of $\delta\mathbf{B}_D$ and $\delta\mathbf{B}_Z$ and Figure 20, which is a plot of normalized power for $\delta\mathbf{B}_D$, $\delta\mathbf{B}_H$, and $\delta\mathbf{B}_Z$ are both from our earlier experiments on 31 July 2008.

During the X-mode heating experiments, η_{HZ} of $\delta\mathbf{B}_H$ and $\delta\mathbf{B}_Z$ (the red curve in Figure 19) is much greater than η_{DZ} of $\delta\mathbf{B}_D$ and $\delta\mathbf{B}_Z$ (shown in blue). This indicates that large plasma sheets orthogonal to the meridional plane were favorably excited by X-mode heater waves. This indication is further supported by the temporal variations of the normalized power $\mu|\delta\mathbf{B}_H|^2$ and $\mu|\delta\mathbf{B}_Z|^2$ in 20, which show very similar patterns and features, as marked by red arrows in the figure.

It is expected from our theoretical analysis that, during the O-mode heating experiments, η_{DZ} of $\delta\mathbf{B}_D$ and $\delta\mathbf{B}_Z$ is much greater than η_{HZ} of $\delta\mathbf{B}_H$ and $\delta\mathbf{B}_Z$. This indicates that large plasma sheets parallel to the meridional plane were favorably excited by O-mode heater waves. We are currently in the process of analyzing the temporal variations of the normalized power $\mu|\delta\mathbf{B}_D|^2$ and $\mu|\delta\mathbf{B}_Z|^2$, which are expected to show very similar patterns and features, as seen in the case of X-mode heating seen in Figure 20.

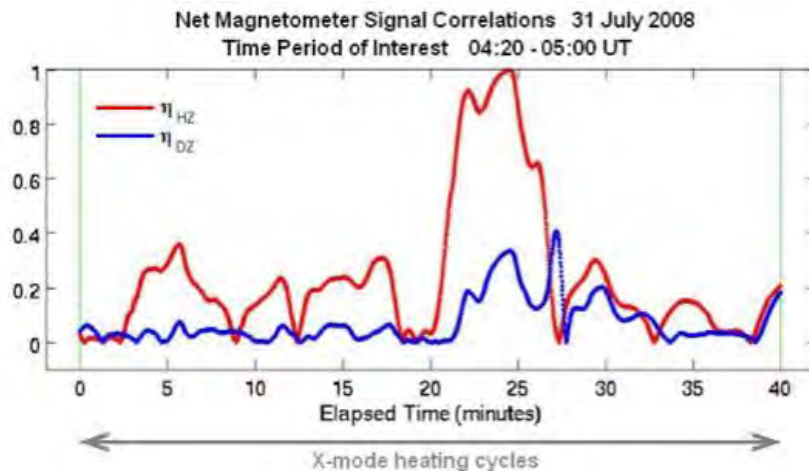**Figure 19: Magnetometer signal correlation versus experiment elapsed time**

Figure 19 shows the results when the heater is operated in X-mode, 1 minute ON and 30 seconds OFF for 7.5 minutes, 2 minutes ON and 30 seconds OFF for 12.5 minutes, 3 minutes ON and 30 seconds OFF for 17 minutes, and 4 minutes ON and 30 seconds OFF for 22.5 minutes. Note that the net H-Z correlation dominates over the net D-Z correlation.
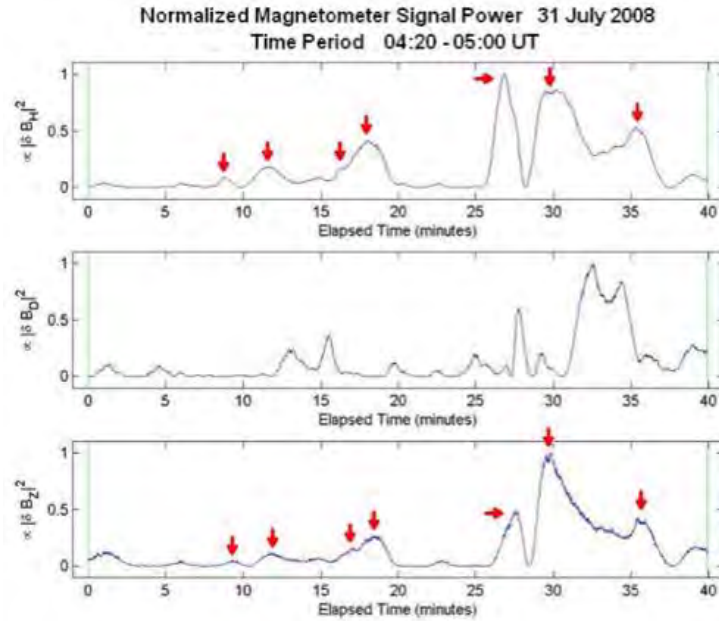
Figure 20: Normalized power for each magnetic field signal component showing an apparent correlation between the H and Z components of the magnetometer signal

In Figure 20, the red arrows mark several features present in both the H and Z components.

3.8. Ionospheric Modification by Under-Dense Heating

3.8.1. Investigators

W. Hsu, Wei-Te Cheng, and S. Kuo (Mentor), *Polytechnic Institute of New York University, Brooklyn NY*
Arnold Snyder, *NorthWest Research Associates, Stockton Springs, ME*

3.8.2. Objective

A recent work [Kuo and Snyder, GRL 37, L07101, 2010] has shown that by combining solar illumination in the solar noontime period with powerful HF heater waves, the HF heater modified the ionosphere more effectively.

The purpose of the experiment is to stimulate large region ionospheric modification via underdense heating in the presence of solar illumination and determine the recovery time of the ionosphere. The relevance of the threshold power of the HF heater will be examined.

3.8.3. Observation Technique

The experiments employed HAARP"s Digisonde and Fluxgate Magnetometer as diagnostic instruments. The Digisonde acquired fast cadence, low resolution ionograms interleaved with skymaps.

3.8.4. Preliminary Results

Experiments were conducted on 19 July 2010 from 0715 to 0900 UTC and on 21 July 2010 from 2000 to 2130 UTC at the HAARP Research Station in Gakona, AK. HAARP transmitted using X-mode at an HF frequency of 9.1 MHz, with the antenna beam pointed along the geomagnetic zenith and with modulations, duty cycles and power formats. The HAARP heater was operated

with a varying duty cycle and with down-stepped power for observing the recovery time of the electron density distribution and to identify the threshold power.

Figure 21 shows the results of the experiment conducted at a time with low solar illumination, on 19 July 2010, at Gakona, AK. The electron density distribution was modified by the HF heating and did not completely recover after the heater was turned off for three minutes. The heating caused both the bottomside and topside of the ionosphere to move up, and increased the plasma density. A similar experiment was conducted at noontime in the presence of high solar illumination. The experimental results are presented in Figure 22, which illustrates the evolution of the electron density distribution through a heater off-on-off period. Comparing Figure 22 with the results presented in Figure 21, the influence of solar illumination on the enhancement of the electron density distribution and to the up-moving of the ionosphere is clearly seen. The f_0F_2 increased from 4.65 MHz at 2033 UTC to 5.3 MHz to 2040 UTC. Recovery of the ionosphere was observed after the heating period ended, although the recovery was not completed in 6 minutes. However, these results are inconclusive since the background ionosphere was also changing at this time. The f_0F_2 dropped back to 4.8 MHz at 2046 UTC.
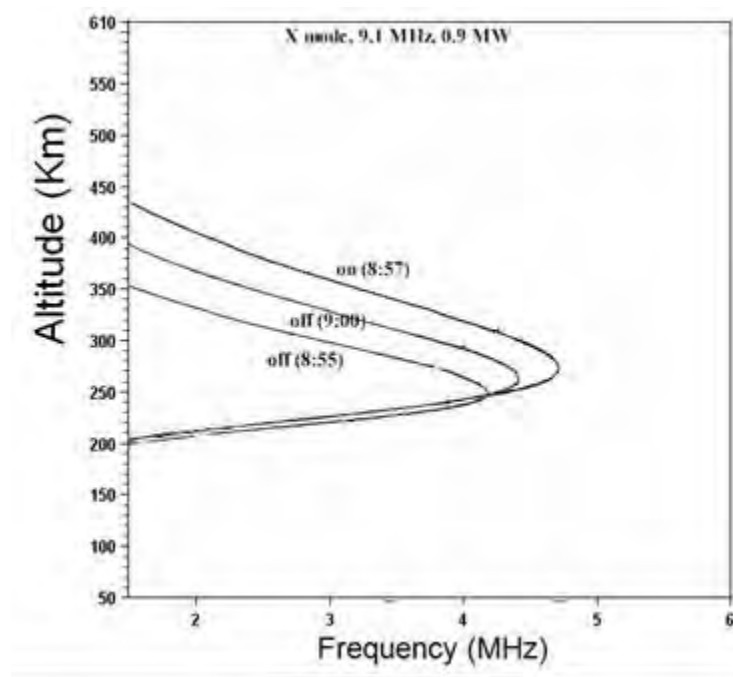

Figure 21: Comparison the electron density profiles in a heater off-on-off sequence recorded at 0855 UTC (off), 0857 UTC (ON), and 0900 UTC (OFF)
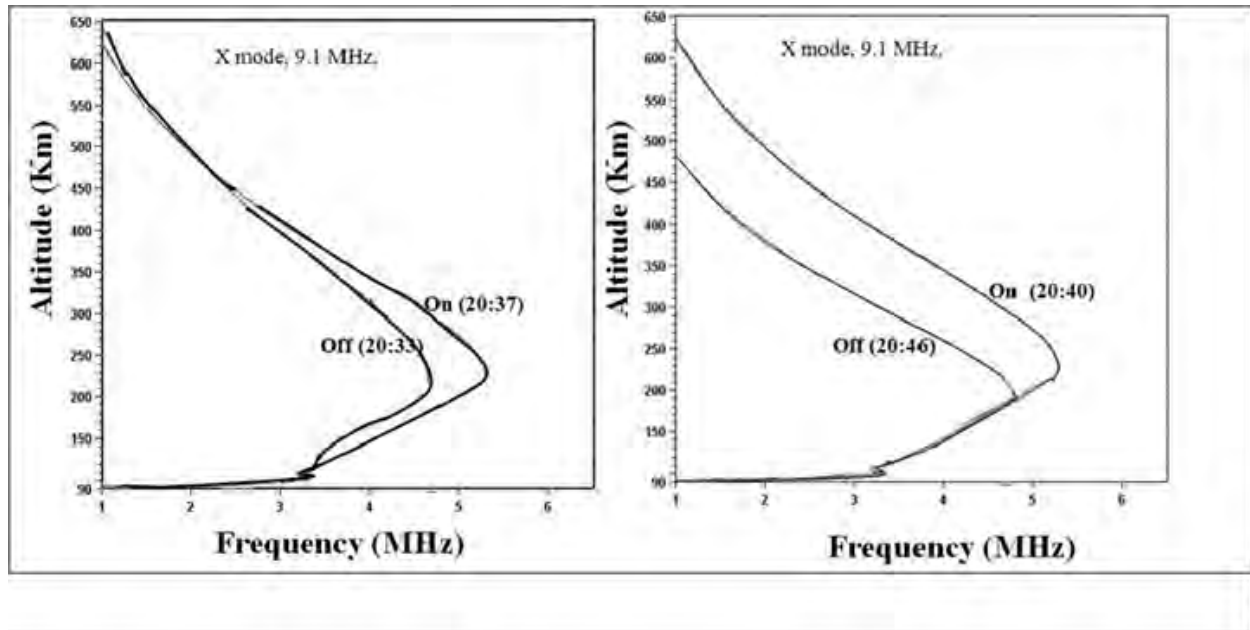
Figure 22: Evolution of the electron density profile through a heater off-on-off period from 2033 to 2046 UTC

3.9. Ionospheric Disturbances Caused by Electrojet-Radiated Whistler Waves

3.9.1. Investigators

K. Hu, J. Gancarz, R. Pradipta, and Min-Chang Lee (Mentor), *Massachusetts Institute of Technology, Cambridge, MA*

3.9.2. Objective

In our earlier HAARP experiments, we demonstrated that temporally modulated electrojet currents can mix with heater wave-excited density irregularities to form whistler mode currents, which generate whistler waves directly with much larger intensities and better directivity than a Hertzian electric or magnetic dipole can [Kuo et al., 2008]. Because whistler waves can be generated by the HAARP heater, we propose to investigate ionospheric plasma disturbances caused by electrojet-radiated whistler waves with the following scenario. It is expected that whistler waves directly produced by HAARP heater-modulated electrojet current can interact with ionospheric plasmas and energize electrons by two processes independently: (1) Parametric excitation of lower hybrid waves and field-aligned purely growing density irregularities via a four-wave interaction process [Labno et al., 2007] and (2) Direct acceleration of electrons by whistler waves [See et al., 2009]. The continuing propagation of these whistler waves from the ionosphere into the radiation belts can interact with trapped energetic charged particles and precipitate them into the lower ionosphere. The residual energies of these precipitated particles can be inferred from measured plasma lines [Pradipta et al., 2007]. The success of the proposed experiments relies on the presence of intense electrojet currents and appropriately selected modulation frequencies of HF heater waves. The aforementioned processes will be monitored by our new Geomagnetic Operation System (GMOS) instrument, which can measure low-frequency waves over a broad frequency range.

3.9.3. Observation Technique

Procedure

HAARP IRI operation:

X-mode polarization, beam pointed vertical, square wave AM

HF carrier frequency 2.8 MHz

Modulation frequency 4, 5, 6, 7, 7.5, 8, 9, 9.5 Hz

The proposed sequence:

- modulate at each frequency for 3 minutes

- heater OFF for 6 minutes

 Repeat

(C) Diagnostics Required

HAARP Digisonde >> 1 ionogram + 2 F-region skymaps + 2 E-region skymaps

Cadence: every 5 minutes

MUIR >> point in up-B direction, record ion line using uncoded pulse

SuperDARN >> 3 look directions (beam #2, #8, #14)

Magnetometer / Riometer >> routine measurements as usual

Our GMOS/VLF Receiver >> we will deploy & operate

(D) Conditions Required

The desirable ionospheric condition:

Nighttime, the presence of electrojet.

3.9.4. Preliminary Results

Figure 23 is a set of ion line data recorded by MUIR in our experiments with the heating sequence: 3 minutes each for 4Hz, 5Hz, 6Hz, 7Hz, 7.5Hz, 8Hz, 9Hz, 9.5Hz; and followed by 6 min OFF. The experiment slots were:

2010-07-19   05:30:00 - 05:59:30 UTC

2010-07-19   06:00:00 - 06:58:00 UTC

2010-07-21   06:30:00 - 06:58:00 UTC

The important implication is that HF heater-induced micropulsations caused significant ionospheric effects detected by MUIR. This is the first time we were able to operate our new

GMOS instrument together with MUIR. We are in the process of writing scripts to analyze data in a format that will permit a better understanding of the physics.
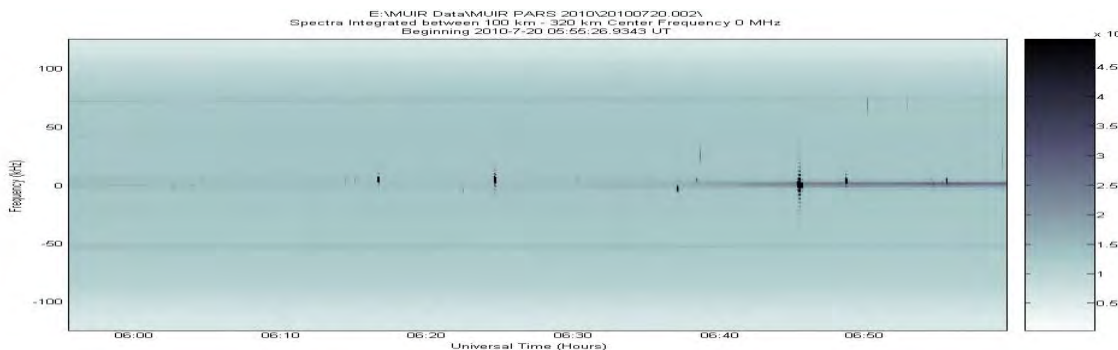

Figure 23: Ion line data obtained using MUIR

3.10.   Sferics Scattering by Local Heating of the Ionosphere

3.10.1. Investigators

C. Liang, P. Blaes and M. Cohen (Mentor), *Stanford University, Stanford, CA*

3.10.2. Objective

The scientific goal of the experiment is to investigate how sferics are scattered by the locally heated ionosphere. In comparison with the previous study of VLF transmitter signal scattering, this experiment setup has two major advantages. The first advantage lies in the broadband feature of sferics. The broadband nature makes sferics capable of carrying much more information about the scattering effect over a much wider range of frequencies. The second advantage comes from the fact that lighting strikes take place all over the world at the same time. These lighting strikes radiate sferics from all directions with respect to a locally heated region of ionosphere. These sferics meet the locally heated region of ionosphere at different angles and different propagation distances. These sferics and their scattered signals are recorded by VLF receivers at many locations and can be studied to provide much more detailed information about the local region of ionosphere.

3.10.3. Observation Technique

The experiment involved three facilities: the HAARP Research Station, the Vaisala National Lightning Detection Network (NLDN) and the Stanford AWESOME VLF receiver network in Alaska.

For each experiment, the half hour experiment time was divided into smaller segments, the HAARP HF beam being tuned to a different setting for each segment. The HF beam was always set to full power and X-mode polarization. The variable settings of the HAARP HF beams included modulation frequency, carrier frequency, beam angle and broad or narrow beam. VLF receivers were used to record the sferics during the experiment. NLDN data provided information on the time and location of lightning strikes during the experiment period.

From NLDN data and the receivers‟ locations, the sferics generated by a specific lightning strike can be identified in data from each VLF receiver. All sferics recorded at a receiver that fall in the

same HF beam setting and from a small region centered around a lightning cluster are summed together to form their average waveform. The average waveforms from different beam settings are compared to study the effectiveness of the experiment design.

Figure 24 shown below, illustrates the locations of Stanford AWESOME receivers (in blue dots) and the HAARP Facility (the red dot). Figure 25 is a summary plot of the NLDN data for the lightning strikes recorded during the experiment period on July 18th 2010.
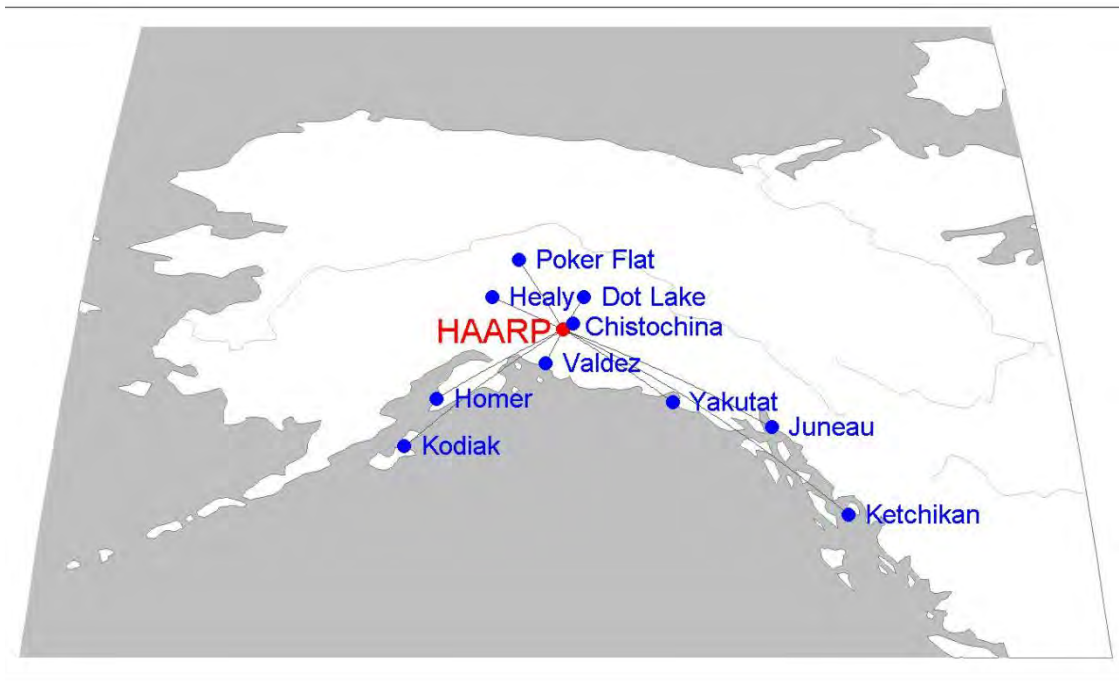
Figure 24: Map showing HAARP and locations of AWESOME receivers in Alaska
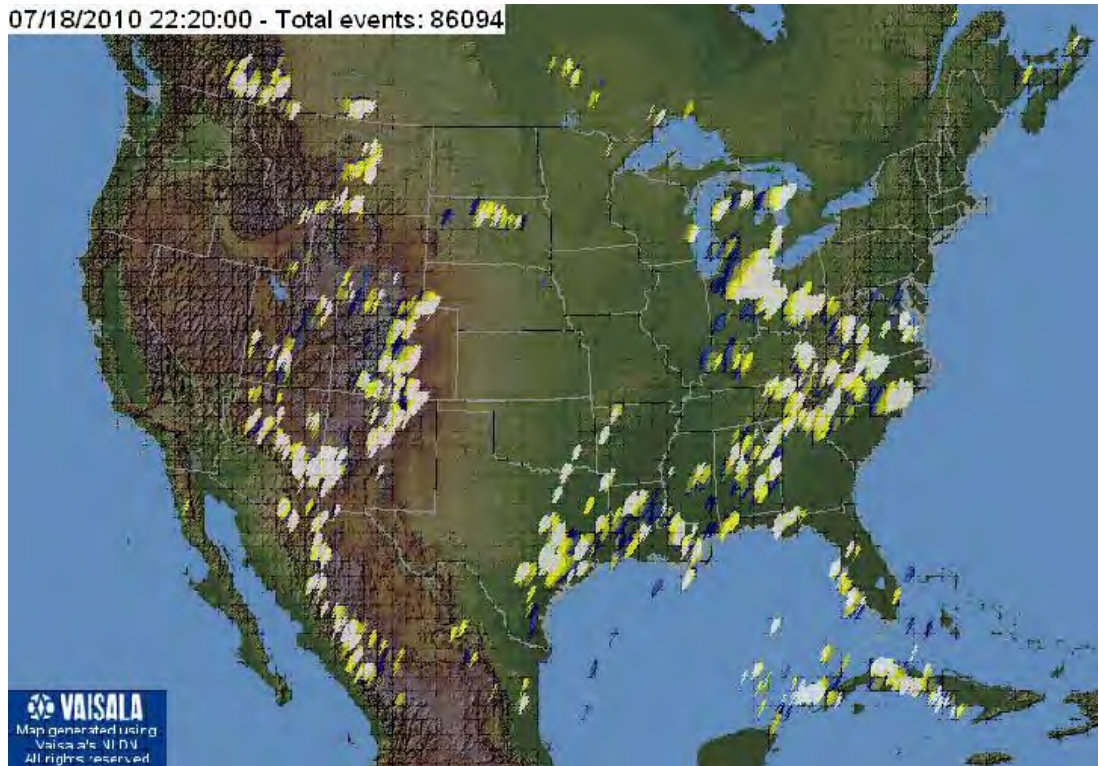
Figure 25: Summary plot of the NLDN data for lightning strikes that took place during the experiment

Example HAARP schedule:

The following HAARP schedule was used during the experiment on 18th July 2010.

The time of the experiment: 22:00:00 – 22:29:30 UTC

Experimental parameters used: X-mode heating at 2.8MHz, narrow beam with 30 degree tilt from vertical towards northeast.

Heating Pattern:

       5 min heating with no modulation;
       5 min no heating
       5 min heating with AM modulation at 5 kHz;
       5 min no heating
       5 min heating with AM modulation at 10 kHz;
       4.5 min heating with AM modulation at 15 kHz

3.10.4. Preliminary Results

The following figures compare average waveforms of sferics collected at two receiver stations originating from two chosen lightning clusters. (In the plots: PF = Poker Flat, CH = Chistochina)

Figure 26: Sferic waveforms from two lightning clusters collected at the Poker Flat and Chistochina receivers [clusters at latitude= 22.15, longitude -80.4]

Figure 27: Sferic waveforms from two lightning clusters collected at the Poker Flat and Chistochina receivers for a second cluster location [clusters at latitude= 34.5, longitude = -77.4]

It can be observed in these plots that the modification on the sferics" average waveforms by the locally heated ionosphere depends on the modulation frequencies of the HF beam. This trend consistently shows up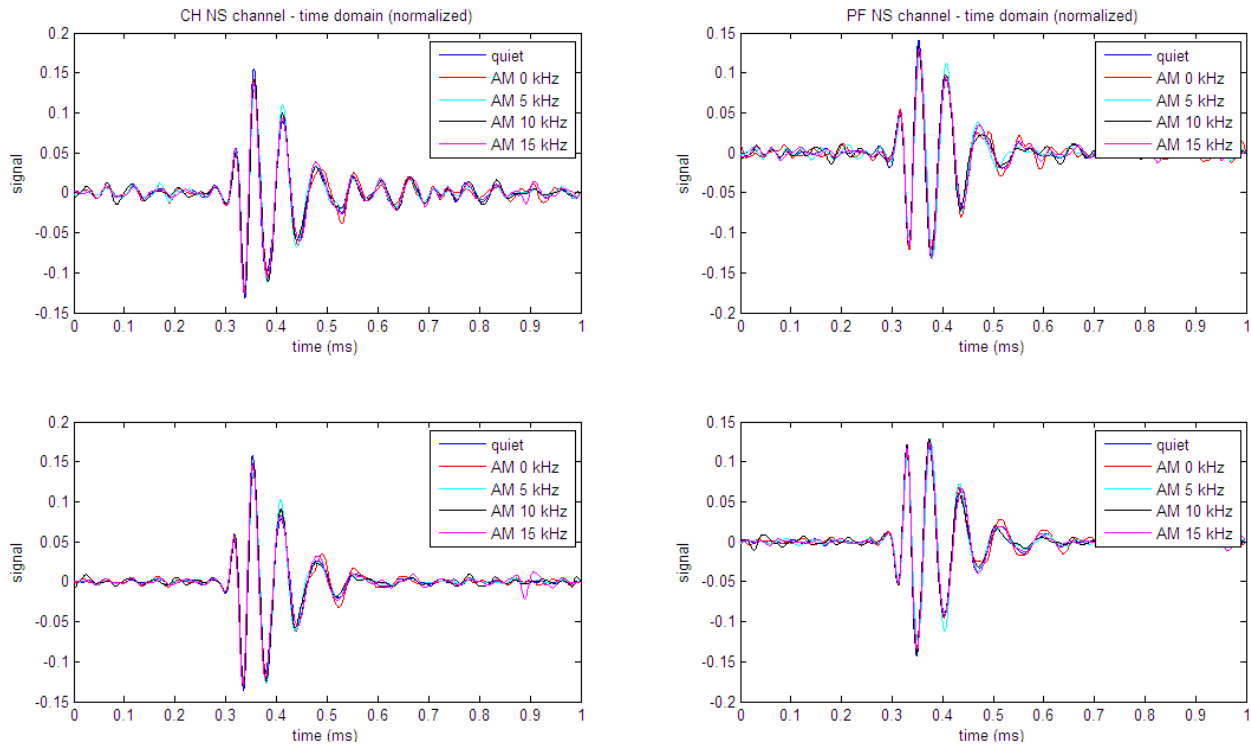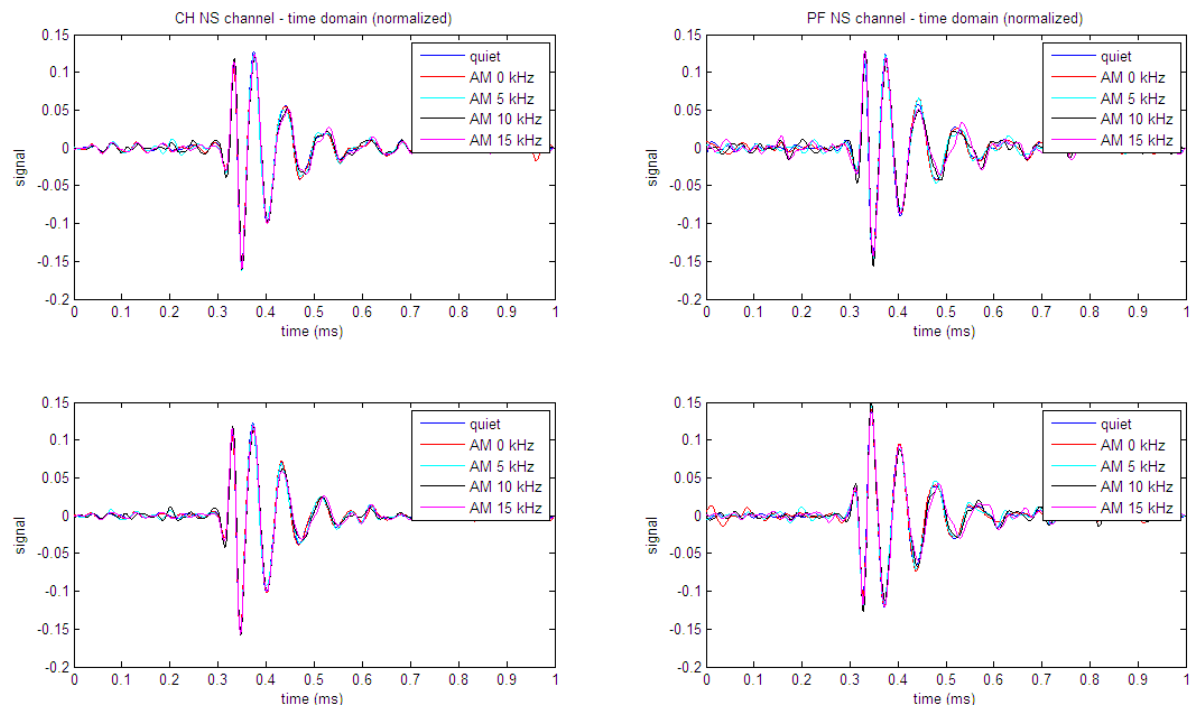 in data collected during experiments on different days at different receivers for lightning clusters centered at different locations. Future work is needed to find effective signal processing methods to better extract information from the data and to explain the modulation frequency dependence of modifications on the sferics average waveform due to scattering.

Acknowledgement:

This experiment would not have come about without the invaluable efforts of many faculty members, officers and staff members of both the University of Alaska and HAARP. Thanks to Patrick Blaes for his help and special thanks to Dr. Morris Cohen for his guidance and help.

3.11. Determination of the Excitation Threshold for Magnetized Stimulated Brillouin Scatter (MSBS) Using the HAARP Facility

3.11.1. Investigators

A. Mahmoudian and W. Scales (Adviser), *Virginia Tech, Blacksburg, VA*
C. Selcher, S. Briczinski, G. San Antonio, and P. Bernhardt (Mentor), *Naval Research Laboratory, Washington, DC*

3.11.2. Objective

Determining the threshold for Magnetized Stimulated Brillouin Scatter (MSBS) by stepping the power of the pump field may lead to useful diagnostics about MSBS. This experiment was done for two beam pointing configurations as shown in Figure 28. For the first case the heater beam is pointed along the magnetic field to study the threshold strength of the pump field to excite the Ion Acoustic (IA) MSBS process. In the second case, the heater beam is at an angle with respect to the magnetic field to study the threshold amplitude of the transmitter power for the Electrostatic Ion Cyclotron (EIC) MSBS process. The pump field frequency was set at 4.5 MHz and frequencies between 4.1-4.3 MHz (for the O-mode). The amplitude of the pump field affects the generation and strength of the multiple EIC harmonics or may generate upper sidebands. An additional goal of this experiment is to study the difference in threshold amplitude for the IA MSBS and EIC MSBS processes to determine which has the lower threshold amplitude. The variation of tilt angle between pump field and magnetic field will also be studied to determine the excitation threshold of IA MSBS process and EIC MSBS process.
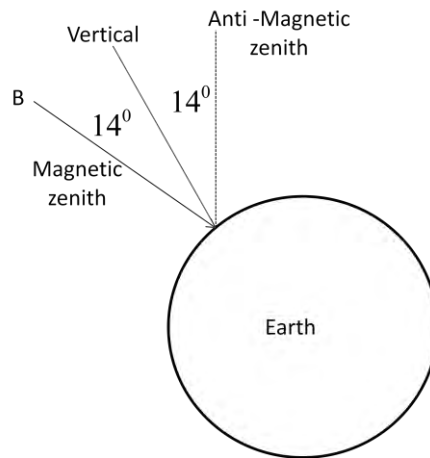
Figure 28: Beam pointing configurations used for the experiment

3.11.3. Observation Technique

Three diagnostics were implemented to study the Stimulated Electromagnetic Emission (SEE) spectrum produced by high power ionospheric heating: 1) A 4 channel spectrum analyzer SEE receiver, 2) the University of Alaska SuperDARN radar facility and, 3) the MUIR incoherent scatter radar. To measure the signals passing through the region of the ionosphere heated by

HAARP HF transmissions the four-channel spectrum analyzer fed from a spaced antenna array was used. This receiver has a uniform response and a wide frequency range and two crossed dipole antennas were used to measure the polarization.

3.11.4. Preliminary Results

In recent HAARP heating experiments it has been shown that during the Magnetized Stimulated Brillouin Scattering MSBS instability, the pumped electromagnetic wave will decay into an electromagnetic wave and a low frequency electrostatic wave (either an IA wave or an EIC wave).

According to the matching condition, the O-mode electromagnetic wave can excite either an IA wave with a frequency less than the ion cyclotron frequency for propagation along the magnetic field or an EIC wave just above the ion cyclotron frequency that propagates at an angle with respect to the magnetic field.

Using SEE spectral features, side bands which extend above and below the pump frequency can yield significant diagnostics for the modified ionosphere. It has been shown that the ion acoustic frequency offsets can be used to measure electron temperature in the heated ionosphere. It is also shown that MSBS can be used as a sensitive method to determine the ion species by measuring ion mass using the ion gyro frequency offset.

For the first day 19 July 2010, the experiment was set up for two modes, O-mode at 4.5 MHz and X-mode at 5.24 MHz, and for three beam angles (Magnetic zenith, vertical and Anti-magnetic zenith). For all cases the power is reduced in 3-dB steps. The experiment cycle for each case is 1 minute with 30 seconds heater on and 30 seconds heater off. Figure 29 shows the results for the experiment on 19 July in which transmitter power is reduced from 3.6 MW to 0.11 MW. The transmitter beam is pointed at zenith using O-mode polarization. This figure shows that reduction in transmitter power causes a weakening of the spectral lines that are offset from the pump frequency by the ion-acoustic frequency in the plasma.
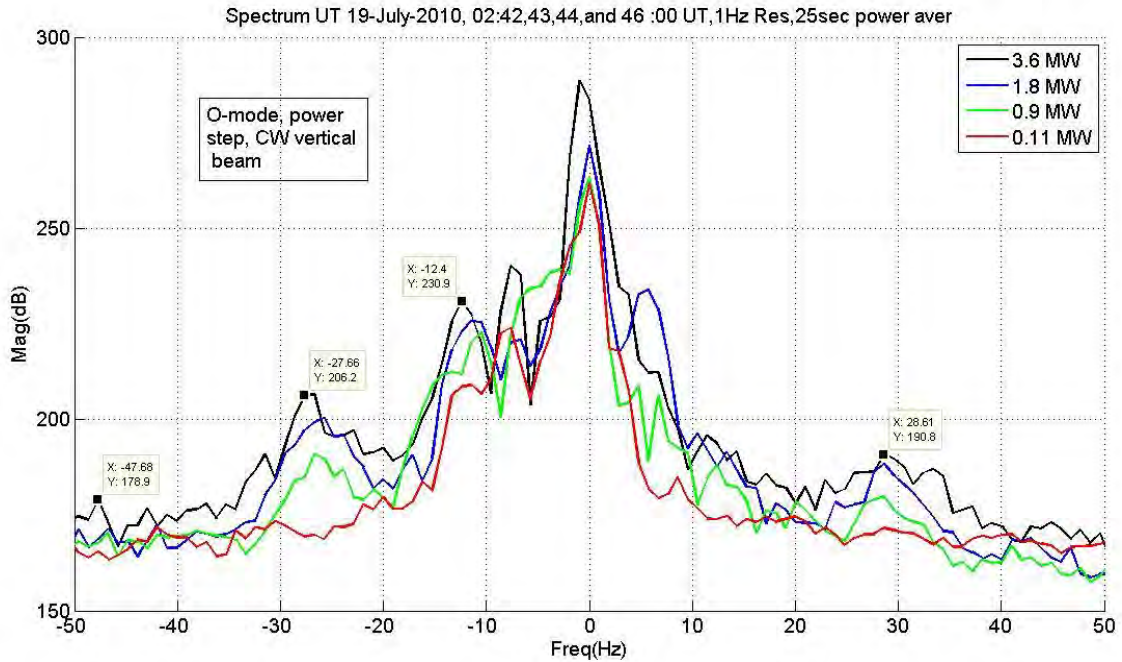
Figure 29: SEE spectrum for the HAARP power variation experiment conducted on 19 July 2010

Figure 30 below, shows that no SEE was observed for X-mode polarization. The 120 Hz spectral lines are the result of minute but detectable power supply ripple (AM modulation) in the HAARP transmitter. These lines were used effectively to verify the frequency calibration for the SEE spectral measurements.
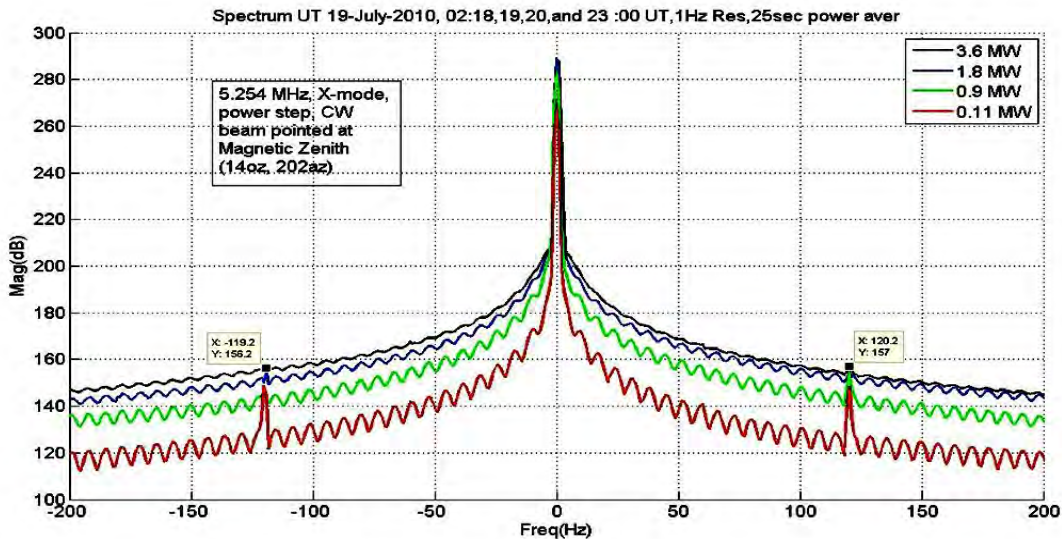
Figure 30: Chart showing no detectable SEE spectrum during experiments employing X-mode polarization

In the following two figures, plotted using data from the same experiment as Figure 3.11.2., the x-axis range is reduced to show the close-in SEE spectrum. Figure 3.11.4. shows the reduction in the amplitude of IA spectral lines (indicated by the arrows). Figure 3.11.5. shows the SEE at 02:42:00 which corresponds to the full power case. In this figure, the upshifted and downshifted spectral lines around 50Hz can be considered as EIC modes but further analysis needs to be done to verify these results.

Figure 31: Chart with narrower frequency range showing the variation in amplitude of the close-in ion acoustic lines as transmitter power is varied

Figure 32: Chart with narrower frequency range showing the close-in SEE spectral content for the case of HAARP transmitting at full power

3.12. Observation of Ionosphere Irregularities and Their Impact on GPS Measurements

3.12.1. Investigators

J. Triplett, P. Vikram, S. Peng, and J. Morton (Mentor), *Miami, University, Oxford, OH*
A. Vermuru W. Pelgrum (Mentor), *Ohio University, Athens, OH*

3.12.2. Objective

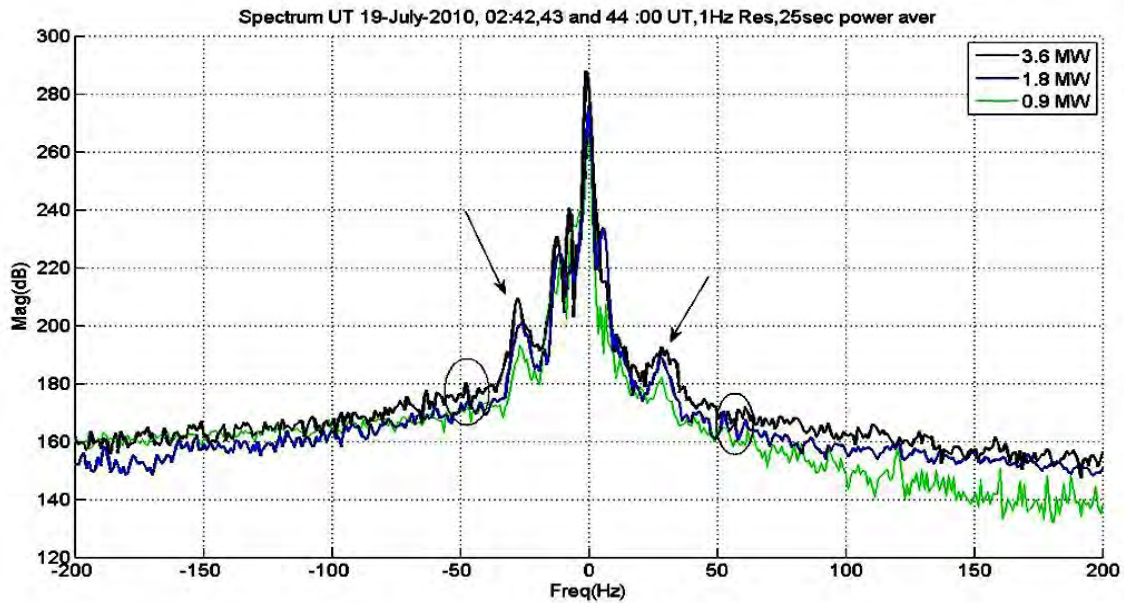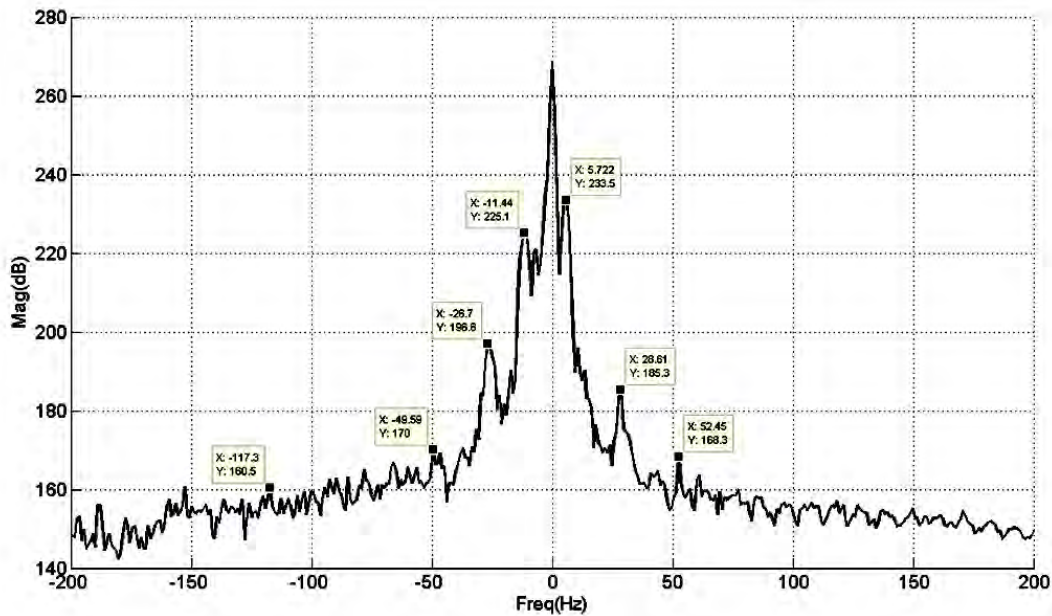The objective of the experiment is to obtain high quality raw RF samples of GPS signals to allow extensive processing of GPS signals propagating through the ionosphere‟s F2 region with significant irregularities present. The processed GPS signals will help our understanding of the temporal, spectral, and spatial behavior of GPS signal scintillations and support the development of robust GPS receivers that are capable of tracking GPS signals accurately and reliably under scintillation conditions.

3.12.3. Observation Technique

Based on experience gained from the 2009 student campaign, we re-configured our GPS receiver array setup as shown in Figure 33. The receiver equipment is set up inside a shelter located on HAARP Science Pad 3. Two antennas (Ant 1 and Ant 2) are mounted on the corner fence posts on the east fence. A third antenna (Ant 3) is set up on a pole located 240m west of Ant 1. Two Novatel OEM-V3 receivers are connected to Ant 2 and Ant 3. A GSV 4004B scintillation receiver, a custom GPS L1/L2C RF sampling device, and a modified USRP2 front end designed to collect raw GPS L5 and Russian‟s GLONASS satellite data is connected to Ant 1. Figure 34 shows photos of the receiver equipment rack inside the shelter, and the setup of Ant 1 and Ant 3.
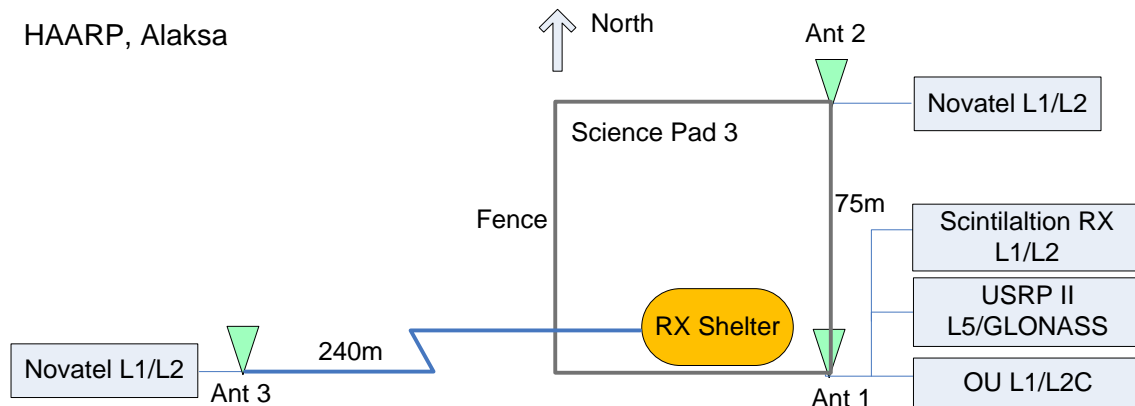
Figure 33: GNSS receiver array layout

Figure 34: Equipment setup inside the shelter (left), Ant 1 (middle), and Ant 3 (right)

3.12.4. Preliminary Results

A total of about 4 hours 45 minutes of HAARP operation time was allocated to our proposed experiments between 19 July and 22 July 2010. During these experiments, "O" mode polarization and the full power level of 3.6 MW with continuous wave (CW) were selected to heat the ionosphere. The operating frequency was selected to be 4.3 MHz which is the triple electron gyro-frequency and which happened to be slightly below the f_0F_2 critical frequency at the time of the operation. Several different combinations of heating power on-and-off patterns were experimented with. For example, on 19 July, there were two satellites, PRN 12 and PRN 25, whose signal path came near the magnetic zenith at HAARP. Figure 35 shows the satellite path between 2:00 and 3:45 UT. We alternately aimed the heating beam at PRN 12 and PRN 25 for 2.5 minutes each during the allocated time.
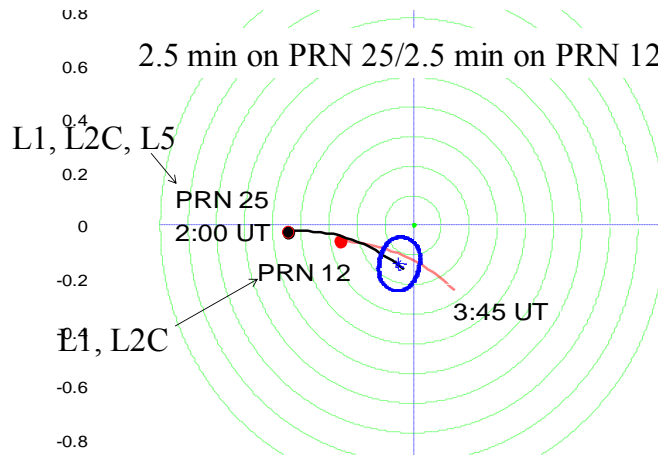
Figure 35: PRN 12 and 25 path above HAARP on July 19, 2:00-3:45UT

Figure 36 plots the relative Total Electron Content (TEC) along the PRN 25 signal propagation path measured by a Novatel receiver (red and black) and the GSV 4004B scintillation receiver (blue). The shaded areas correspond to the 2.5 minute period of heating power on the satellite path while the time in between the shaded areas depict the 2.5 minutes intervals when the beam was directed at PRN 12. The TEC measurements promptly responded to the heating on and off pattern. The heating effect resulted in a prompt rise of over 0.2 TEC unit.
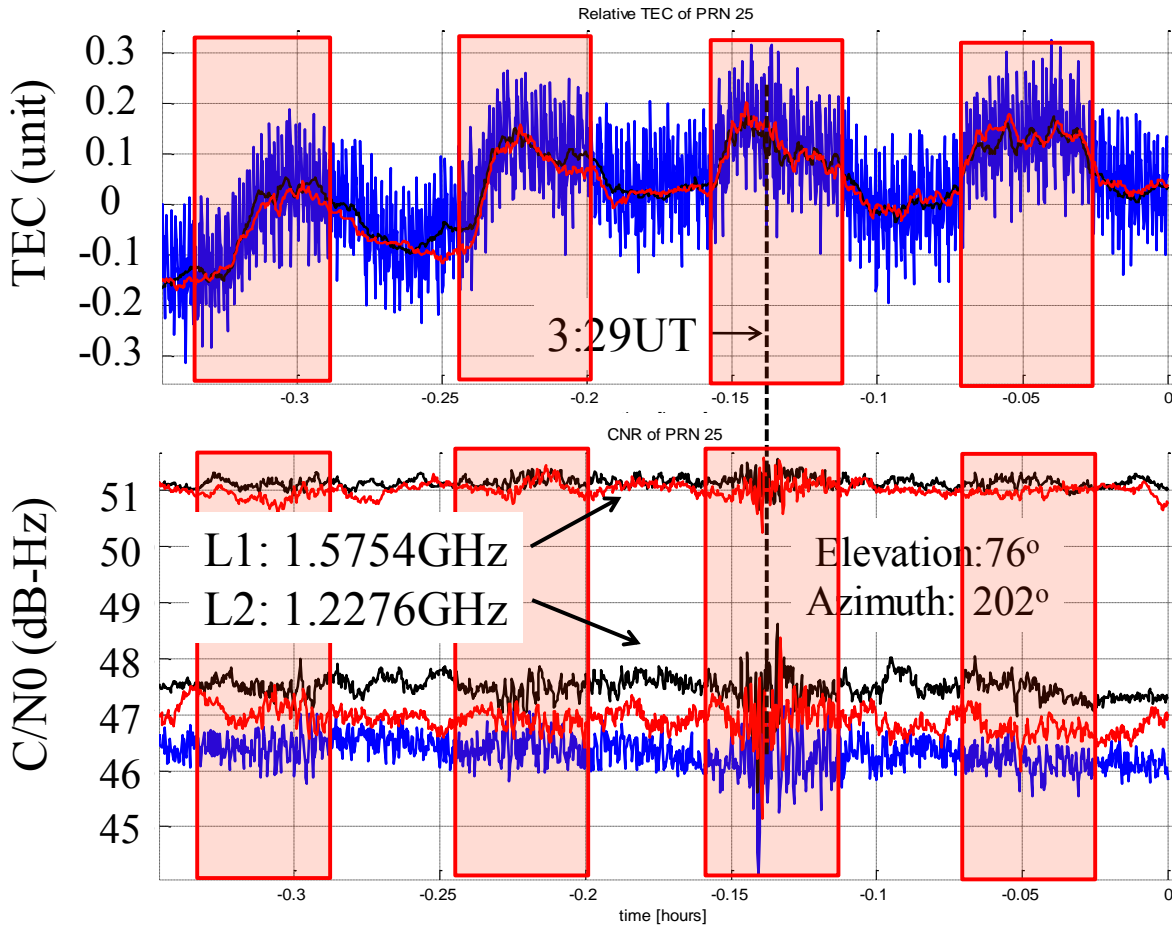
Figure 36: Relative TEC C/N$_0$ variations during the July 19 heating experiment

We were able to repeat this experiment on 21 July 2010. On 20 July 2010, a different heating scheme was applied where continuous heating power was applied to magnetic zenith for 8 minutes. Figure 37 plots the relative TEC and C/N$_0$ for this experiment. While we only saw mild C/N$_0$ fluctuations during this time, the wavelike structure shown in the relative TEC measurements indicates some interesting background dynamics stimulated by the heating.
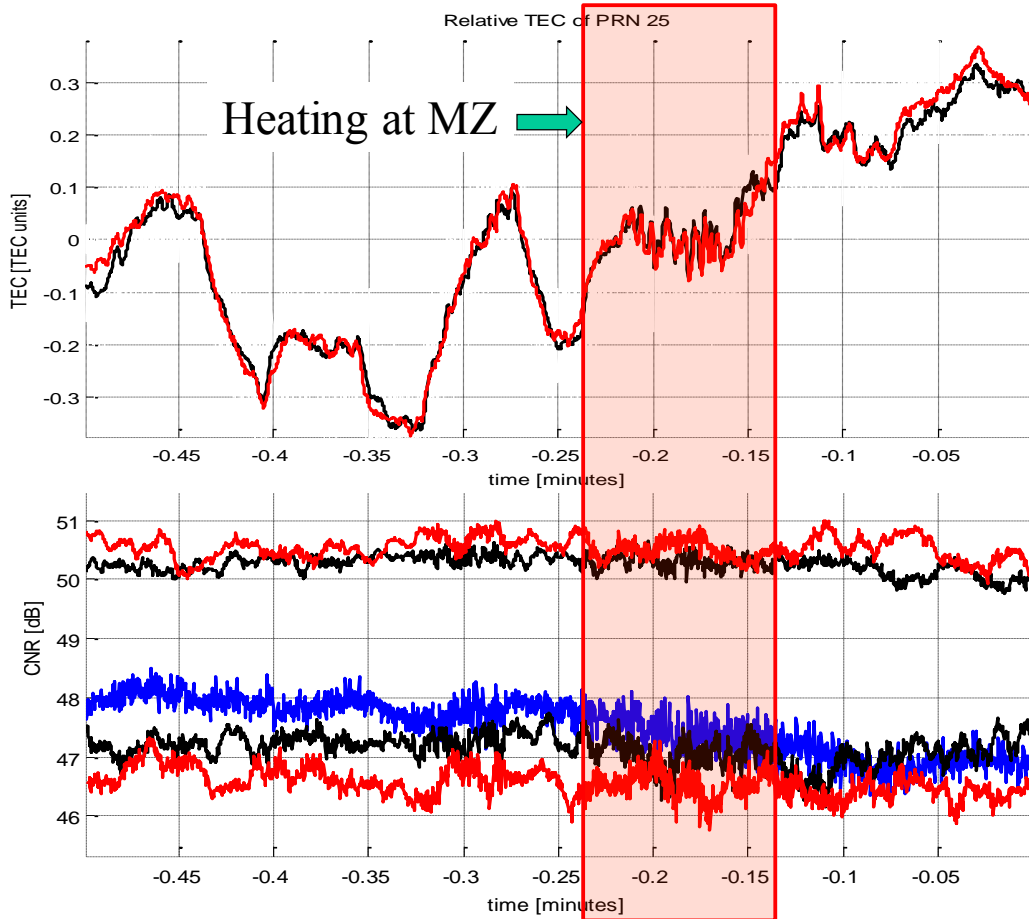
Figure 37: Relative TEC and C/N$_0$ during the 20 July 2010 experiment

We did not observe scintillation effects when the satellite path deviated from the magnetic zenith.

The raw RF data collected by the L1/L2C and USRP2 front ends are currently being processed and analyzed. An abstract has been submitted to the fall 2010 AGU meeting.

3.13. Exploring E Region Artificial FAI Generation

3.13.1. Investigators

E. Nossa and D. Hysell (Advisor), *Cornell University, Ithaca, NY*
R. Moore (Mentor), *University of Florida, Gainesville, FL*

3.13.2. Objective

The goal of this experiment was to explore the characteristics of the heating and the generation of the Artificial Field-aligned Irregularities (AFI) in the E region over HAARP. Previous experiments showed suppression at the second electron gyroharmonic at lower powers and yielded expressions and effects of preconditioning (Hysell et al 2010). With the experiments at the 2010 PARS Summer School, two specific topics were addressed:

1. The impact of heating above and below the second electron gyroharmonic and the power threshold for observing the suppression at the second gyroharmonic and the type of irregularity that it is involved.

2. The characterization of the nature of the preconditioning to establish the size of the filaments responsible for wave trapping.

3.13.3. Observation Technique

O-mode radiation is used to heat the E layer at the upper hybrid resonance height. The resulting irregularities are diagnosed using the 30 MHz imaging coherent scatter radar located near Homer, Alaska, which is looking perpendicular to the magnetic field **B** at an altitude of ~100 km over Gakona (denoted by "G") as shown in Figure 38 below. The detailed characteristics of the radar can be found in Hysell (2008).
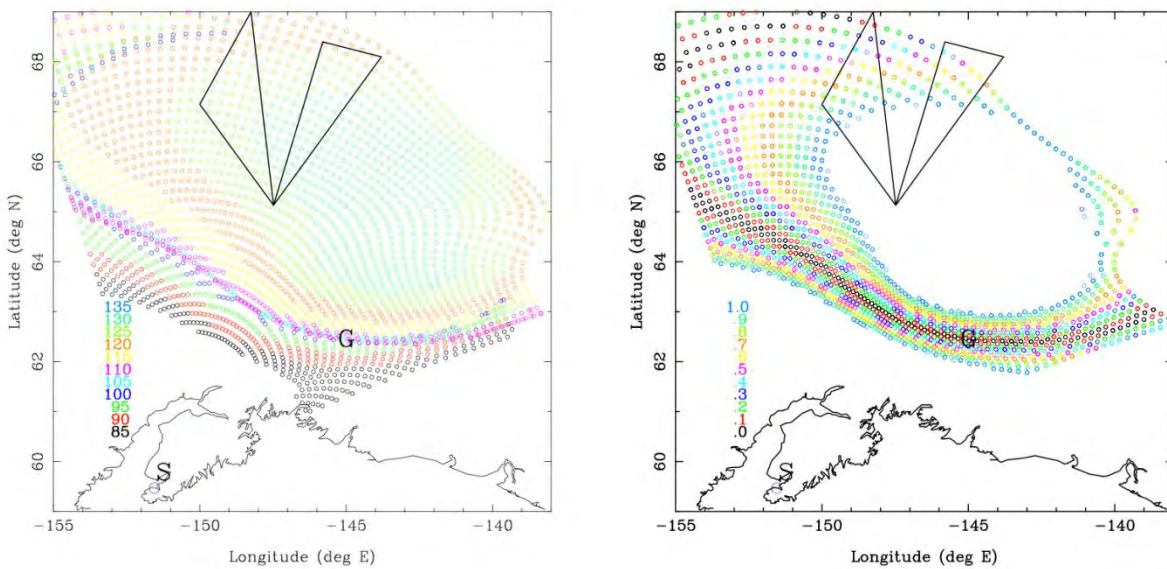
Figure 38: The 30 MHz coherent scatter radar, deployed at the NOAA Kasitsna Bay Laboratory in Homer, AK, near the town of Seldovia (denoted as "S" on the map)

In Figure 38, the left panel shows ray tracing indicating the altitude of the locus of perpendicularity. The right panel shows the magnetic aspect angle at an altitude of 110 km.

The heating frequencies were selected to match summer mid-day E layer conditions, where the critical frequency is relatively high.

3.13.4. Preliminary Results

Experiment 1: Instabilities present when heating at $2\Omega_e$

Suppression of the second gyroharmonic frequency ($2\Omega_e$) at the upper hybrid resonance height in the E layer was detected during previous experiments performed during the Summer Student Research Campaign (SSRC) and BRIOCHE campaigns at HAARP in 2009. This suppression was observed at modest power levels only, which suggested a strong correlation with one of the two types of irregularities acting at the upper-hybrid height: the thermal oscillation two stream instability (TOTSI) and the resonance instability. Using amplitude modulated (AM) pulses, it was determined that the resonance instability started at 17% of full power (Hysell et al, 2010). A

natural correlation between TOTSI and the suppression seemed evident. However, experiments were needed to prove this hypothesis.

To observe the instabilities separately, frequency modulated (FM) pulses around $2\Omega_e$ were used. The 3 minute pulses go from 2.95 MHz to 3.05 MHz and then back to 2.95 MHz, each at a different power. The F_oE at the time of the experiment was just over the highest frequency in the sweep. The value of $2\Omega_e = 3.0235$ MHz was calculated using the IGRF11 ionospheric model for the specific time at 100 km over HAARP (B = 53992.5 nT). Results are shown in the figures below.
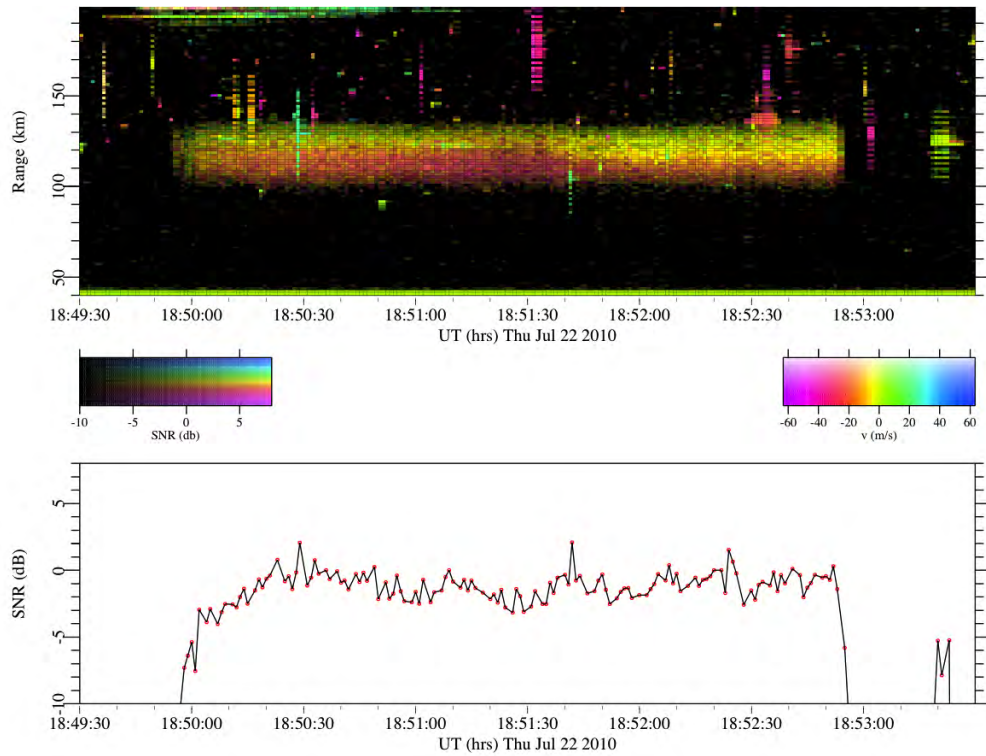

Figure 39: Experiment to detect the instabilities present during heating at $2\Omega_e$ (pulses at 15% of full power)

Figure 39 shows pulse with 15% of full power, where it is assumed that only TOTSI is present. The second gyroharmonic heating intervals correspond to 18:51:02 and 18:51:50, where the suppression is barely observed.
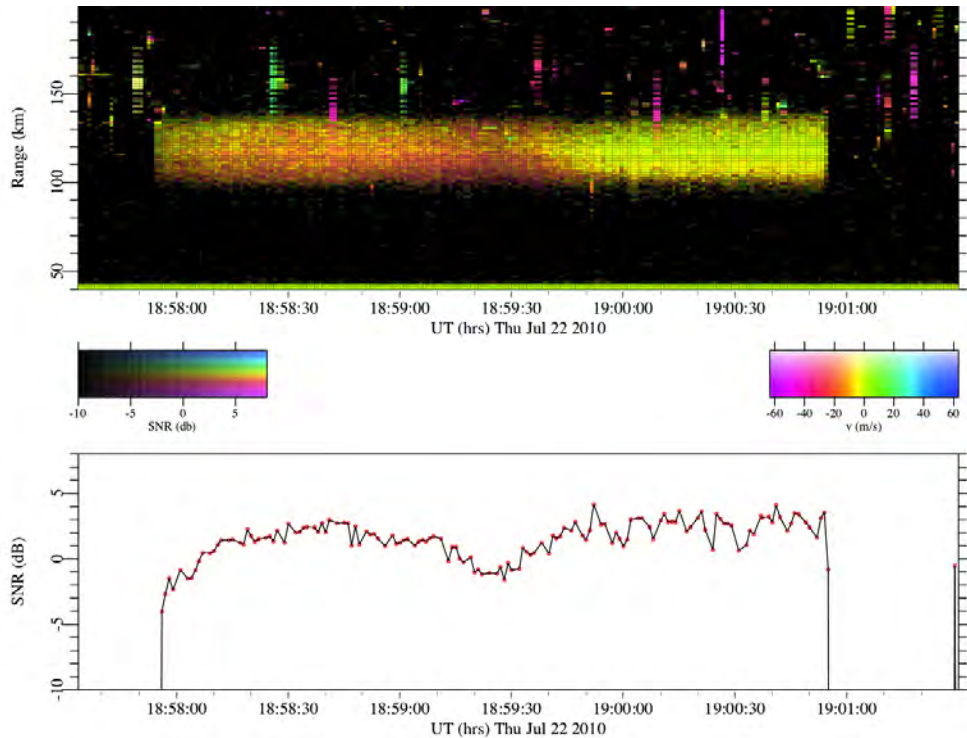
Figure 40: Experiment to detect the instabilities present during heating at 2Ωe (pulses at 20% of full power)

Figures 39 and 40 are examples of results for pulses respectively below and above the power threshold for resonance instability. In each figure, the first panel is the range-time-Doppler-intensity plot for the pulse. The second panel is the average of the Signal-to-Noise ratio (S/N) for the lower ranges of the heated area. Frequency is changing in equidistant steps from 2.95 MHz to 3.05 MHz and then back down to 2.95 MHz, followed by one minute without heating.

The suppression was barely present when TOTSI was isolated (power below the resonance threshold). Meanwhile, the suppression was almost nonexistent for pulses with resonance instability present (>18% of full power).

This experiment presents many challenges because when the power is decreased, the SNR also decreases. For that reason, this experiment should be performed when a higher F_oE exists. Also, higher resolution is desirable.

Experiment 2: Filament size

Effects of preconditioning have been observed in previous experiments (Hysell et al, 2010). When the ionosphere is quiescent (no immediately previous heating), echoes are registered by the coherent radar 30 seconds after the starting time of an AM heating pulse. When the ionosphere is preconditioned, the echoes start after just 5 seconds due to wave trapping or resonance instability, as it was called in the previous experiment.

To see how long the filaments could persist before the resonance instability was extinguished, a series of pulses with different inter-pulse periods (IPP) was performed. First, the heating is ON for 20 seconds at full power then OFF for a specific time, $\tau = 0, 5, 10, 20, 30, 40$ seconds. Then, a small perturbation is generated using 2 % of full power. When $\tau < 5$, the perturbation produces

an increase in the signal, but at $\tau \geq 5$ seconds, there is no perturbation. Figure 41 shows the total sequence used.   The perturbation is always visible when $\tau = 0$.
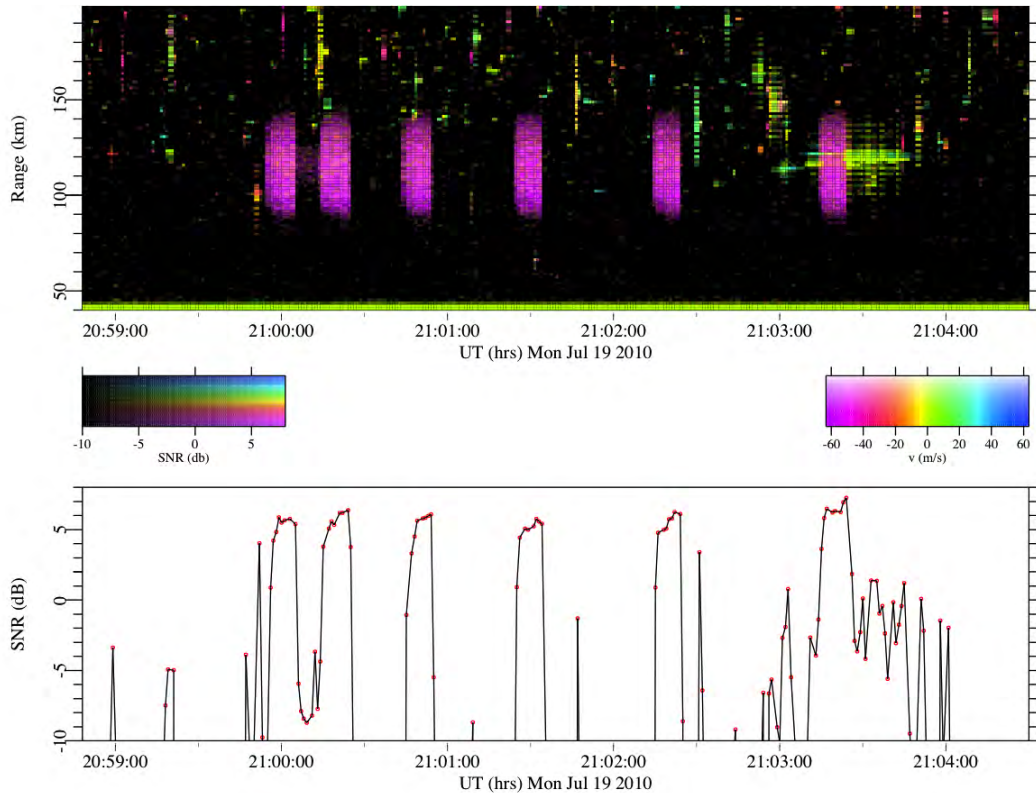
Figure 41: Filament size experiment

The sequence of the filament size experiment was: "o-ox-oxx-oxxx-oxxxx-oxxxxx-xxx", where every symbol lasts 10 seconds, "o" is 100 % power, "-" is 2 %, "x" 0 %. The perturbation after the first full power pulse ($\tau =0$) is always present. Perturbations after the second pulse were expected but were not observed. This is a topic to explore further. The echo detected after the last pulse corresponds to a meteor and it is not an effect of the heating.

These results demonstrate the nonlinearity associated with the irregularity because the timing required to stimulate the perturbation is different for a square pulse than for an amplitude modulated pulse.   Refined experiments to explore the hysteresis with shorter IPPs will be conducted in future campaigns.

In experiments performed during the BRIOCHE Summer 2010 campaign, some filaments persisted for 10 or more seconds. The reason of the variability is unknown and will be a topic of future research.

3.14.   Generation of Acoustic Gravity in the Ionosphere by the HAARP Heater

3.14.1. Investigators

R. Pradipta, J. Gancarz and Min-Chang Lee (Advisor), *MIT, Cambridge, MA*
K. Hu,. *Boston University, Boston, MA*

3.14.2. Objective

The objective of this experiment is to investigate HF heater-induced gravity waves at HAARP based on the following scenario. The HAARP HF heater, operated in CW mode with O-mode polarization can heat ionospheric plasmas effectively to yield depleted magnetic flux tubes as rising plasma bubbles. Two processes responsible for the depletion of magnetic flux tubes are: (1) thermal expansion and (2) chemical reactions caused by heated ions. The depleted plasmas create large density gradients that augment spread F processes via generalized Rayleigh-Taylor instabilities [Lee et al., 1999]. It is thus expected that the temperature of neutral particles in the heated ionospheric region can be increased. A heat source such as this in the neutral atmosphere may potentially generate acoustic gravity waves (AGWs) in the form of traveling ionospheric disturbances (TIDs). In our experiment during the 2009 Summer Student Research Campaign (SSRC) we obtained some exciting results, which support the aforementioned scenario [Pradipta et al., 2009]. We should point out that these TIDs have features that are distinctively different from **E X B** drifts of HF wave-induced, large-scale, non-propagating plasma structures. Moreover, it is noted in our recent study of naturally-occurring AGW-induced TIDs that only large-scale AGWs can propagate upward to reach higher altitudes. Thus, in this experiment, we select optimum heating schemes for HF wave-induced AGWs that can be distinguished from those occurring naturally.

3.14.3. Observation Technique

HAARP IRI Operation:

Polarization:	O-mode with beam pointed at zenith (vertically)
Modulation:	Square Root Sine Amplitude Modulation starting at a zero crossover with a 12 minute period.
HF frequency:	Below foF2.
Transmission Sequence:	Square Root Sine modulation for 24 minutes (power reaches maximum twice)
	OFF for 12 minutes
	Square Root Sine modulation for 12 minutes (power reaches maximum once)
	OFF for 12 minutes
	Repeat

Diagnostics Required:

HAARP Digisonde:	1 ionogram & 4 F-region skymaps within each 5 minute period
MUIR	Beam pointed along magnetic field (B) direction, record ion line using uncoded pulse

GPS/LEO Satellite Pass:	Measurement/scan of TEC (ideally satellite pass in the middle or the end of the heating period)
SuperDARN:	3 look directions (beam #2, #8, #14)
Magnetometer:	Normal measurements
Riometer:	Normal measurements
GMOS/VLF Receivers	MIT to deploy & operate

Conditions Required

The ideal ionospheric condition for this experiment are daytime (significantly high f_oF_2), no spread F.

3.14.4. Preliminary Results

Figure 42, shown below, presents a set of sky maps recorded on 19-20 July 2010 during the period 22:30-00:30 UT.   In the sky maps Doppler shifts are color-coded as follows. The red color denotes large negative Doppler shifts, while the blue color indicates large positive Doppler shifts. It is seen that sky map echoes with large Doppler shifts were present both during and after the Square Root Sine modulation of HF heater waves. But, prior to the heater wave modulation, no large Doppler shifts were found in the sky maps. In other words, we can see that large-scale waves were excited and propagated in directions different from the **E X B** drift directions on the sky maps. This is evidence of HAARP heater-induced TIDs.
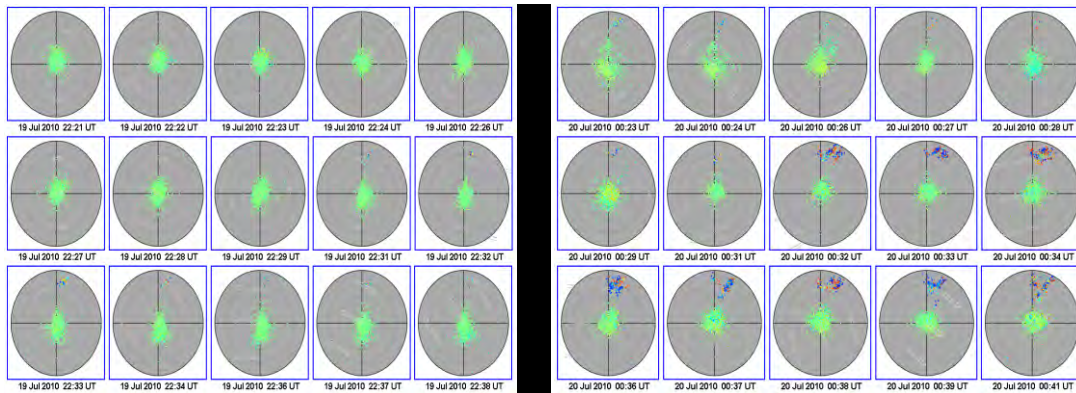

Figure 42: Sky map sequence obtained from the HAARP digisonde for the period of this experiment

We are still analyzing GPS/LEO, and MUIR data to derive the total electron content perturbation (TECP) and monitor the occurrence of HAARP heater-excited large-scale perturbations, respectively. We anticipate being able to see more cases where the power spectra of TECP contain wave structures with periods of ~ 12 minutes equal to the HAARP power modulation period, as we found in our previous experiments.   We noted that plasma lines were continuously excited during operation of the HAARP heater in pulsed mode in the first 12 minute period. However, after the large TIDs were generated as seen in sky maps, plasma lines disappeared as expected. Results of this experiment support the Ph.D. research for Rezy Pradipta.

3.15.   Coordinated Studies of the HF Interaction Region at HAARP

3.15.1. Investigators

R. G. Roe, N. Adham, and J. P. Sheerin (Advisor), *Eastern Michigan University, Ypsilanti, MI*

B. J. Watkins, W. A. Bristow and J. Spaleta, *Geophysical Institute, University of Alaska, Fairbanks, Fairbanks, AK*

C. Selcher, P. Bernhardt and G. San Antonio, *Naval Research Laboratory, Washington, DC*

3.15.2. Objective

The full HAARP IRI was operated at low-duty cycle to generate and study Langmuir plasma waves recorded in the MUIR UHF backscatter spectra (the HF-induced plasma line or „HFPL‟) for a wide range of HF pointing angles. High time resolution (3.3 ms) achieved in the MUIR spectra enabled the study of the development of HFPL spectra during each HF pulse. Stimulated electromagnetic emissions (SEE) spectra were recorded for comparison to MUIR radar backscatter from plasma waves.

3.15.3. Observation Technique

The HAARP IRI was operated at full power (3444 kW) in O-mode at 4.5 MHz and 4.3 MHz (third gyroharmonic) during periods when the ionosphere was overdense. Based on our previous results, a HF pulse width („on‟) of 50 ms in an inter-pulse period (IPP) of 12 - 15 sec (for a low-duty cycle of 0.3 - 0.5%), was necessary and sufficient to prevent onset of Artificial Field-Aligned Irregularities (AFAI) enabling comparison to theoretical predictions for HFPL spectra. The HF pump pointing was varied in zenith in 3° steps from vertical to magnetic zenith (14°) in the magnetic meridian. MUIR recorded the downshifted plasma line (PL) spectra with 250 kHz bandwidth (sufficient to record expected outshifted plasma line (OPL) and 3.3 ms resolution. The MUIR radar recorded the HFPL spectra along zenith angles at the magnetic zenith, and for the first time, rapid scans from 9 to 15 degrees south of vertical. The Kodiak SuperDARN HF radar was operated to monitor ionospheric conditions and any development of AFAI. On-site HAARP diagnostic instruments (e.g. ionosonde) were used to obtain ionospheric density profiles, absorption measurements, and to assess ionospheric conditions. HF receivers operated by NRL measured the SEE with high frequency and time resolution.

3.15.4. Preliminary Results

The HAARP HF beam pointing angle was varied stepwise and pulse-to-pulse typically from directly overhead to magnetic zenith. The HFPL spectra are expected to be characterized by strong cascades when observed by MUIR along the magnetic zenith. Our results confirm these observations. Results shown in Figure 43 reveal details of the PL spectra evolution. The mini-overshoot is observed. The OPL appears as intense transients with frequency offsets in excess of the HF pump frequency. The initially intense PL decays (called mini-overshoot) over 10 ms. Two very intense transients approximately 25 kHz beyond the HF offset (OPL) occur around 25 and 40 ms after the start of the HF pulse.

Figure 44 shows the SEE spectra as a function of time for a single HF pulse. There appears a narrow continuum (NC) downshifted from the HF pump frequency offset of 4.5 MHz. The evolution of the narrow continuum associated with strong PL turbulence is evident at negative frequency shifts. The NC is associated with the strong PL turbulence recorded by MUIR backscatter. Coordinated multi-instrument observations such as these help to understand the electromagnetic as well as electrostatic wave turbulence generated in these experiments. Analysis of this data is continuing.
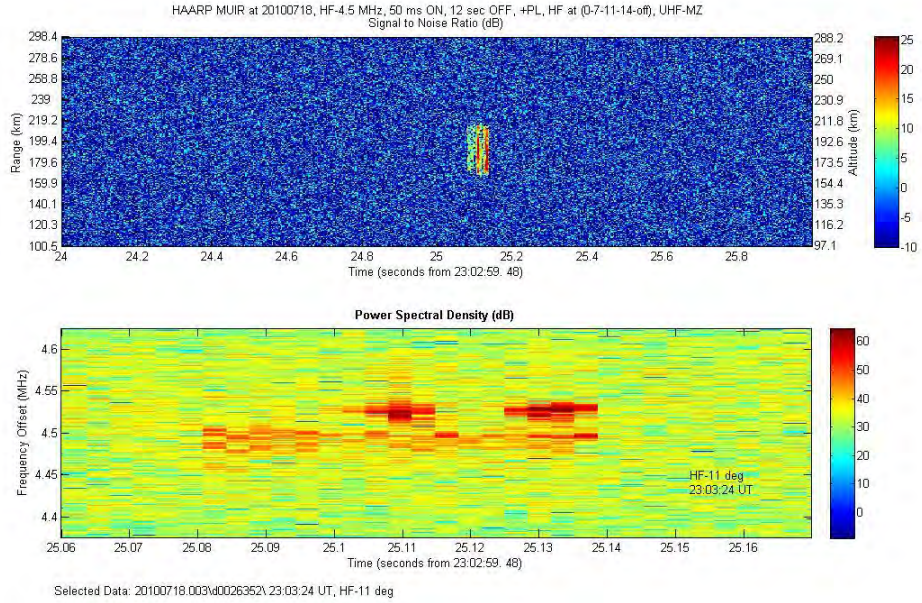
Figure 43: MUIR Plasma Line backscatter for a single 50 ms HF 4.5 MHz pulse at 11 degrees of zenith angle   (labeled in the figure) recorded with MUIR diagnostic radar pointed at magnetic zenith
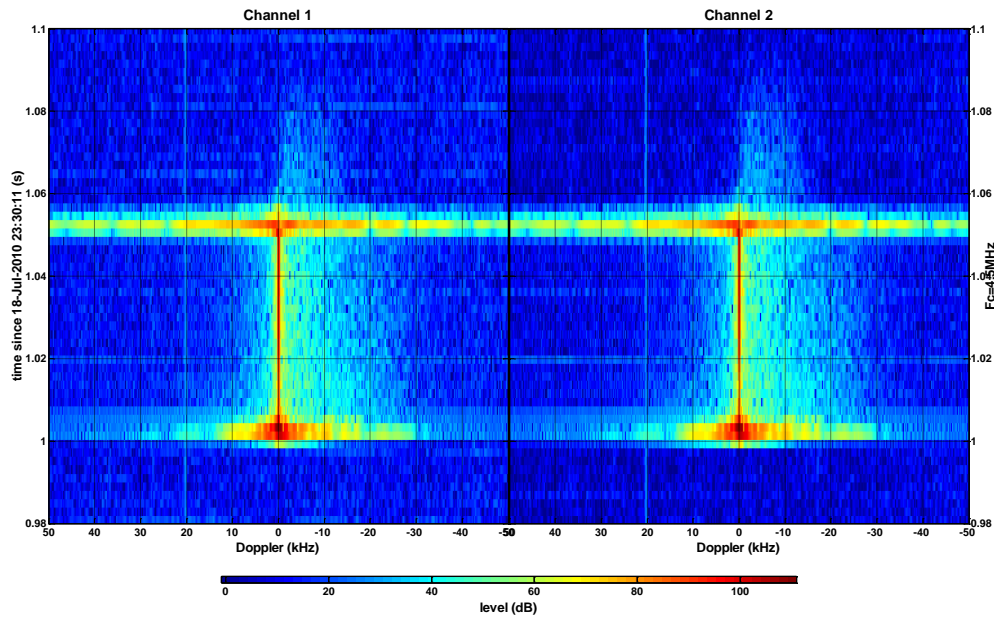

Figure 44:   SEE recorded for a single HF pulse in E-W (Ch 1) and N-S dipoles

3.16. Frequency-Dependent VLF Scattering by HAARP-Induced Ionospheric Disturbances

3.16.1. Investigators

T. Wang and R. Moore (Advisor), *University of Florida, Gainesville, FL*

3.16.2. Objective

The purpose of this experiment is to study the scattering of subionospherically-propagating VLF signals by HAARP-induced ionospheric disturbances. The VLF signals to be tracked are generated by Navy VLF transmitters used for communications with submarines, and the NPM transmitter in Hawaii (21.4 kHz) is of particular interest to this experiment. Recent theoretical analysis indicates that the VLF fields scattered by HAARP-generated ionospheric conductivity changes are likely to consist of a single propagation mode, although this conclusion depends on ionospheric conditions. Additionally, a new measurement technique provides the ability to assess the scattered field amplitude and phase across the 200-Hz bandwidth of the narrowband VLF signal. This new measurement technique will be used to determine whether the scattered field consists of a single mode since theoretical predictions indicate that multi-mode scattered fields will exhibit a ~2 dB fluctuation in amplitude over the 200-Hz band, whereas single-mode fields exhibit much more stable (~0.1 dB) behavior (both of these signal levels are typically measurable). If the VLF scattered field does indeed consist of a single-mode, a series of HAARP transmissions may be used to determine the change in ionospheric refractive index produced by HAARP heating and may also be used to determine the dominant altitude of VLF scattering using only one VLF receiver. Our experiment will perform this series of HAARP transmissions under the assumption that the scattered field is single-mode, and assess this assumption after the fact. We have identified Tanacross, AK (between Tok and Delta Junction) as the preferred site to perform successful VLF scattering observations. This experiment will serve as a proof-of-concept experiment. If successful, similar experiments may be used to assess the change in ionospheric conductivity and the altitude of VLF scattering as a function of HF power and HF frequency in order to provide a deeper understanding of HF absorption within the D-region ionosphere.

3.16.3. Observation Technique

Two broadband (300 Hz - 45 kHz) ELF/VLF receivers were deployed, one at Sportsman's Paradise in Wrangell-Saint Elias National Park, the other one at Tok, AK. The systems consist of two orthogonal magnetic loop antennas oriented to detect the radial and azimuthal magnetic fields at ground level, a preamplifier, a line receiver, and a digitizing computer that samples at 100 kHz with 16 bit resolution. Figure 45 shows the picture of receiver at Tok, AK.

These locations were chosen by a combination of theoretical calculation and availability during the

Figure 45: Photograph of the ELF/VLF receiver installed at Tok, AK

campaign. As shown in Figure 46, the propagation paths (blue line) from NPM to the receiver sites were as close to the HAARP facility as possible, so that the scattered field would be strong enough to be detected when a direct path field was present.

We requested the latest operating hours of all the available experiment slots to have the VLF signal propagating in its night hours.

Our transmission pattern was to use the full 12x15 HAARP array to transmit at 3.25 MHz using X-mode polarization and with square wave amplitude modulation. The modulation frequency was 0.05 Hz (10 seconds ON and 10 seconds OFF alternatively). Three beam directions were selected to achieve variability of the disturbance locations. We began with 10 seconds ON and the beam pointed at 15° off zenith, 109° azimuth, followed by 10 seconds OFF.

Figure 46: Map showing the locations for HAARP, NPM, and the receiver sites for PARS 2010

Next the transmitter was turned ON for 10 seconds with the beam pointed at 30° off zenith, 109° azimuth followed by another 10 seconds OFF. Finally the transmitter was turned ON for 10 seconds with the beam pointed at 24° off zenith, 141° azimuth, followed by a 10 seconds OFF. This 60 second sequence was repeated multiple times.

3.16.4. Preliminary Results

Because of a hard drive failure at our Tok site, we lost two full days" of data. We were able to recover a 30-minute block and a 6-minute block of data at both Paradise and Tok sites. While we are still validating the single mode assumption, the preliminary results are quite encouraging. Figure 47 shows the amplitude of the measured field, after normalizing consecutive ON/OFF pairs and averaging every 60 second sequence. It is obvious that the observation on 22 July is of regular patterns when 21 July isn"t that clear. Figure 48 shows data from the HAARP fluxgate magnetometer indicating a relatively active electrojet.

Although the data from the Paradise site is not as clean, it is of high SNR and could be a potential source of important information. The plots weren"t attached for simplicity.

This experiment was proposed as a proof-of-concept experiment. Future work would include verification of the basic theory. If successful, the results could be used to determine the change in ionospheric conductivity and the altitude of VLF scattering as a function of HF power and HF frequency.
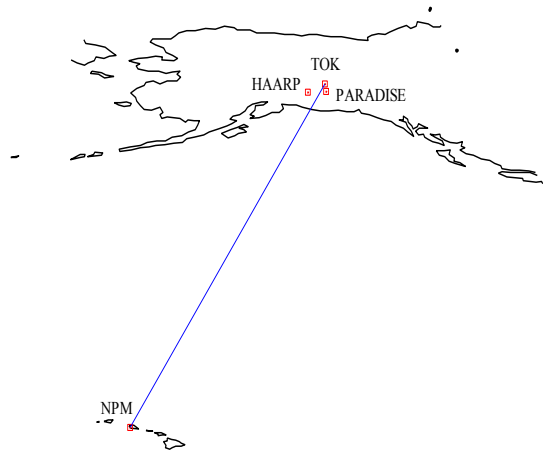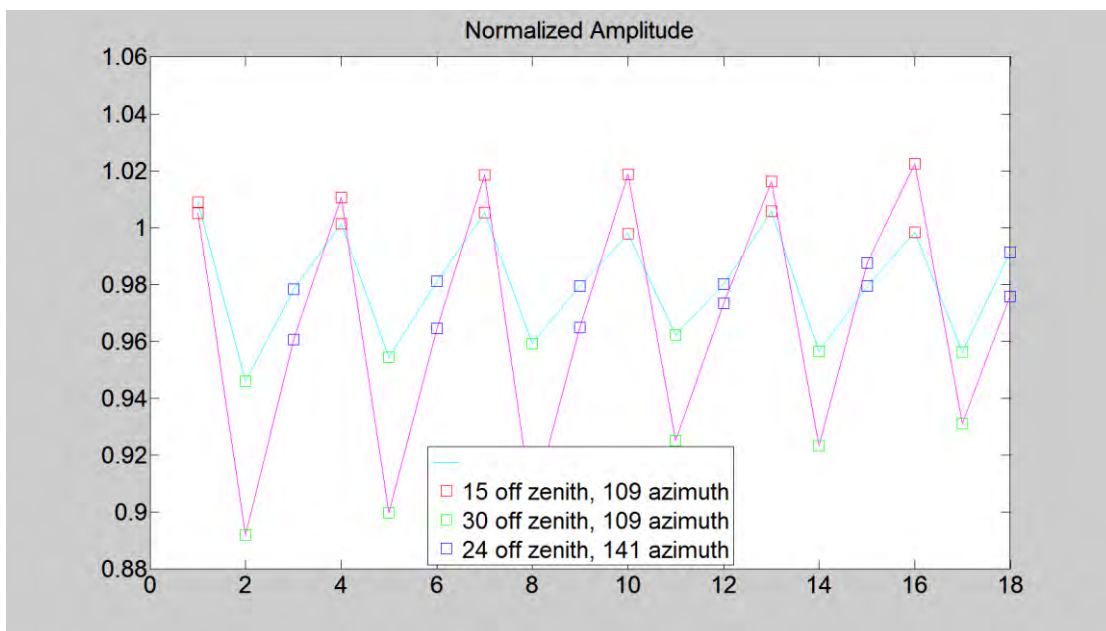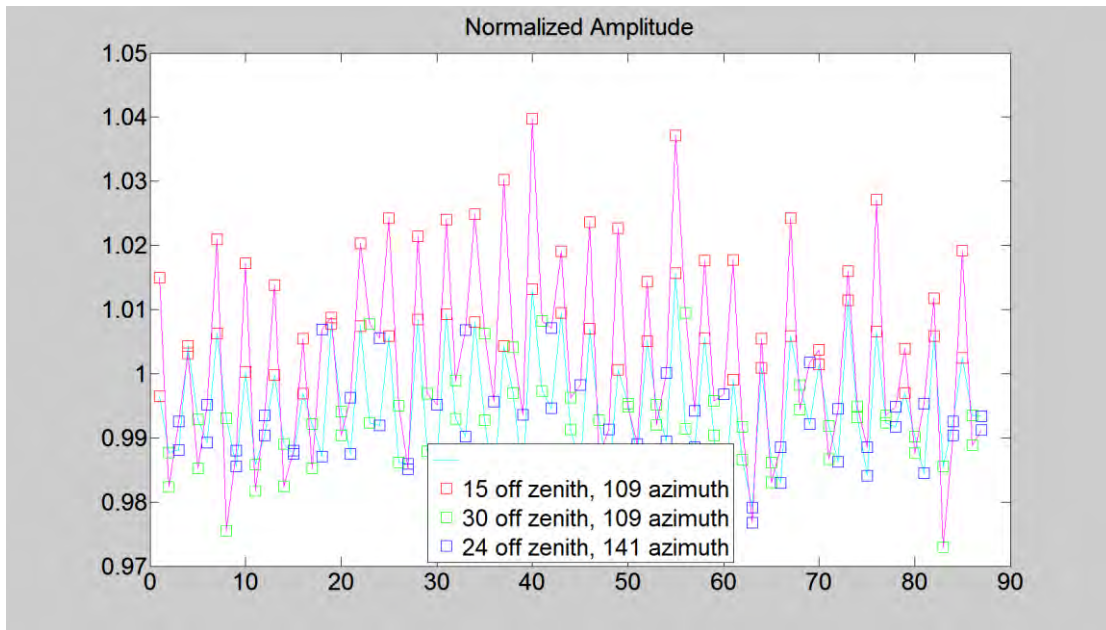
Figure 47: Plots of the measured magnetic field at Tok

 In Figure 47, the N-S channels is shown in cyan and E-W channel is shown in magenta. The top figure represents 21 July 09:00-09:29 UT; the bottom figure represents 22 July 09:00-09:06 UT.
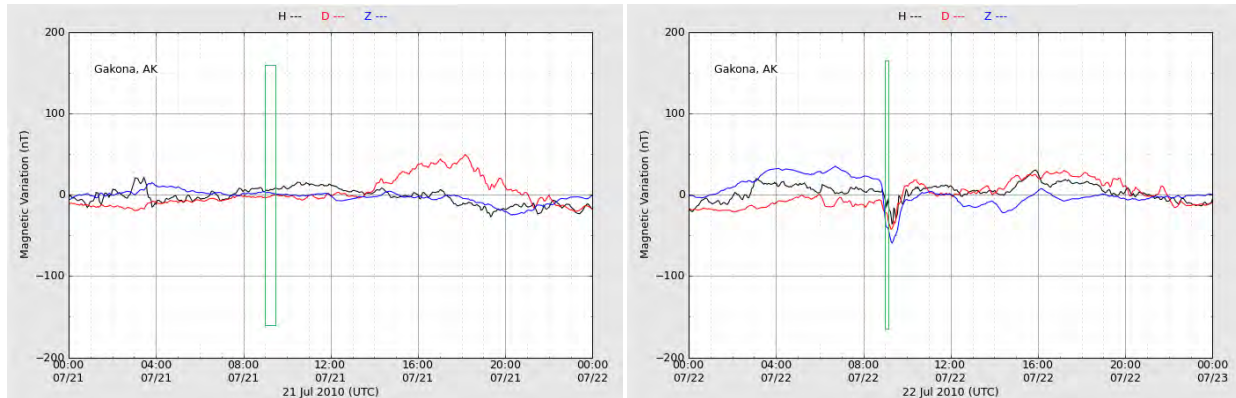
Figure 48: Plots of the readings taken from the HAARP fluxgate magnetometer

As seen above, the left figure represents 21 July 00:00UT-22 July 00:00UT; the right figure represents 22 July 00:00UT-23 July 00:00UT. The green rectangles mark the time slots for this experiment.

3.17. Time-of-Arrival of HAARP-Generated VLF Waves

3.17.1. Investigators

M. Webb and M. Golkowski (Advisor), *University of Colorado Denver, Denver, CO*

3.17.2. Objective

The Generation of VLF waves by modulated ionospheric heating has been pursued for many years, but many physical details of the process are still poorly understood. It has been theoretically predicted that using higher HF frequencies shifts the modulation of the electrojet to higher altitudes. This modulation in turn produces radiating ELF/VLF waves back towards the earth's surface, which can be measured by receivers. It has been experimentally verified that using higher HF frequencies generates weaker amplitudes of VLF waves observed on the ground, but clear evidence of a shift in altitude has not yet been observed. The goal of this experiment is to determine if higher HF frequencies lead to an increased modulation altitude and perhaps more radiation of VLF energy outward toward the magnetosphere.

Figure 49: The HAARP antenna array, Gakona, Alaska

3.17.3. Observation Technique

Using the HAARP facility (Figure 49), VLF waves were generated using HF carrier frequencies of 2.75 MHz (lowest available), 4.5 MHz, 5.8 MHz, and 9.4 MHz (highest available). A time of arrival technique developed by Dr. Robb Moore from University of Florida was used to investigate modulation altitude differences as a function of HF carrier frequency. The differences in altitude for the applied HF frequencies are expected to be on the order of 10 km, leading to an expected propagation delay time on the order of tenths of a

58

millisecond. In order to observe a delay this short in the VLF band, the transmitted bandwidth was maximized. By transmitting frequency-time ramps from 1 kHz to 5 kHz, a sufficient signal-to-noise ratio (SNR) was achieved, to allow for a measurement of time of arrival for each transmitted frequency-time ramp. The ramps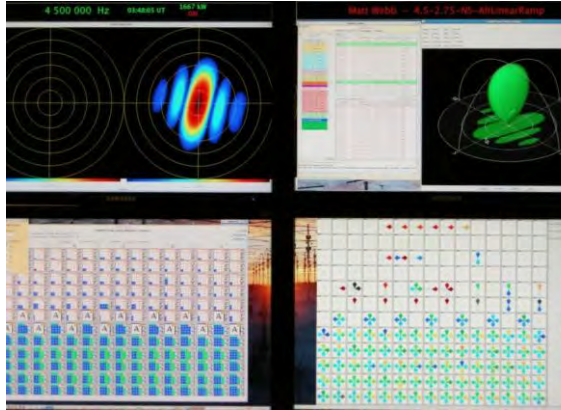 had a slope of 500 Hz/s, lasting 8 seconds. In the first transmission sequence, the HAARP array was split in half with different HF frequencies used for each half of the array. A control ramp at 2.75 MHz was transmitted along with one of the higher frequencies listed above. This transmission format was repeated for five minutes, after which the next highest HF frequency was transmitted with the 2.75 MHz control. This sequence was repeated twice in the allotted thirty-minute intervals. Transmitting two different frequencies required splitting the HAARP array to produce two separate beams (Figure 50). A second transmission sequence was used for half of the experiment time. In the second transmission format, the entire array transmitted the frequency-time ramps at alternating carrier frequencies of 2.75 MHz and 5.8 MHz, alternating between the two over the thirty-minute time slot.

Figure 50: Split-beam configuration of the HAARP array, transmitting at 4.5 MHz

The VLF waves generated by this electrojet modulation scheme were observed at receiver sites operated by University of Florida at Paradise Lodge (99 km distance) and by Stanford University"s Chistochina receiver site (36 km distance).

3.17.4. Preliminary Results

Unfortunately, ambiguities in portions of the data have prevented a full analysis. Specifically, in the split array, alternating carrier frequencies format, an unexpected 45 ms offset was observed. At this point it is not clear if this resulted from a timing discrepancy in HAARP transmissions or is a signal processing artifact. The more available data came from the second transmission sequence described in the previous section. Figure 51 shows a typical spectrogram of the frequency-time ramp measured by the receivers.
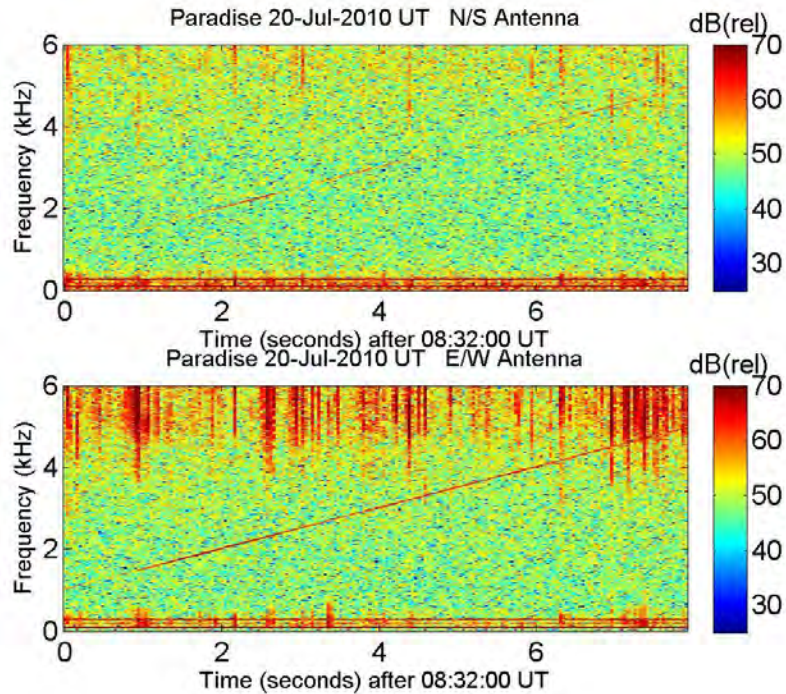
Figure 51: Spectrogram showing frequency-time ramp of generated VLF waves, 2.75 MHz carrier frequency

In the spectrogram, it is apparent that the electrojet conditions were sufficient to produce detectable propagating ELF/VLF waves observed at Paradise. The particular spectrogram in Figure 51 is that of a ramp transmitted at the 2.75 MHz carrier frequency. It was observed that at the higher carrier frequency of 5.8 MHz, the signal was attenuated by 5-10 dB (relative), consistent with previously published results.

The time-averaging of the arrival of the frequency-time ramp was accomplished using mix-down and Fourier analysis techniques. For each ramp, an impulse response was generated and the delay of the impulse correlated to modulation height (Figure 52). The earth-reflected VLF waves are also detected in the analysis.
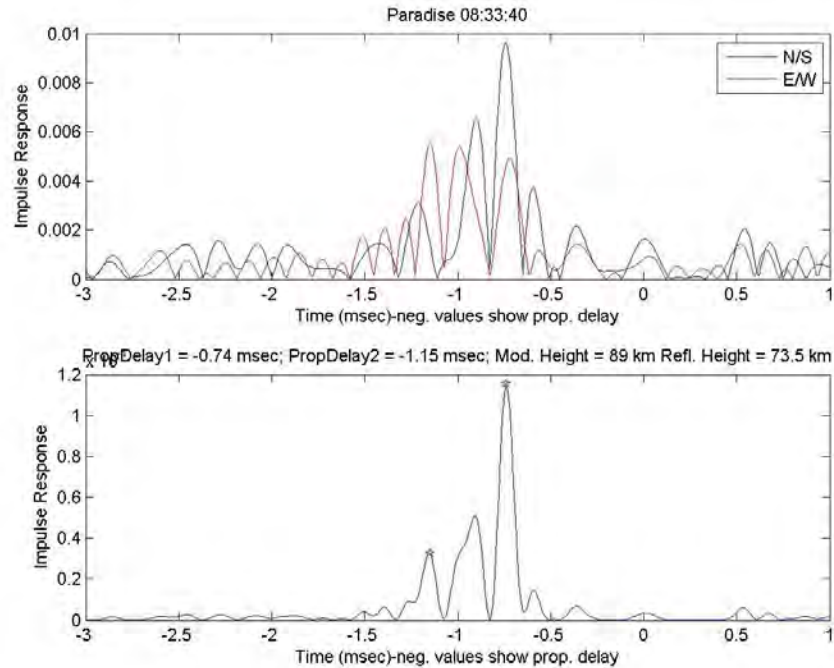
Figure 52: Impulse response of frequency-time ramp showing delay, modulation height, and reflection height

Averaging the modulation height and propagation delay times has thus far not provided significant evidence of a shift in the modulation altitude. Analyzing the alternating frequency-time ramp transmission sequence has yet to be done, and a definitive result is expected once the analysis can be completed. Furthermore, the relative signal strength at the Chistochina site will allow for analysis of the harmonics. The spectrograms from Chistochina show the second, third, and fourth harmonics of the VLF waves. Quantification of the effective altitude for HF frequency and harmonic number is an important step in being able to create ELF/VLF amplitude enhancement and directionality using multiple beams.

4.   Summary and Concluding Remarks

The goal of the Polar Aeronomy and Radio Science (PARS) Summer School is to acquaint graduate level university students with many of the scientific facilities located in Alaska including the HAARP Research Station. The program which is sponsored by HAARP, the National Science Foundation and the University of Alaska Fairbanks (UAF) is split between the Geophysical Institute in Fairbanks where students are presented with lectures and the HAARP Research Station in Gakona where students participate in a short experiment campaign. The campaign affords the students an opportunity to become familiar with the HAARP facility by using it for research purposes, planning and executing experiments of their own design in close cooperation with the facility operators. The period at the HAARP facility includes daily meetings at which tutorials or presentations are provided by a mentor or other visiting scientist. Students are encouraged to provide interim results of their experiments during these daily meetings to

obtain feedback and encouragement from their peers. At the end of the summer school, students present summaries including results of their experiments to the assembled group.

The 2010 PARS Summer School was organized and executed jointly by the UAF/GI and NorthWest Research Associates (NWRA). UAF/GI planned all of the school"s activities that took place in Fairbanks. NWRA was responsible for the experimental portion of the program at HAARP, including planning the program, developing the campaign schedule, coordinating with the UAF as necessary, and directing the research campaign activities.

Because the number of students responding to the announcement was 21, all were selected to participate. In addition to the students, there were 18 mentors or scientists who participated either at UAF/GI or at HAARP. A total of 12 universities were represented in the program. During the experimental program at HAARP, there were 22 unique experiments with a total operations time allocated to students of 45 hours which provided an average time per student experiment of approximately 2.4 hours.

The HAARP facility, including the high power HF Transmitter and phased array antenna along with all of its installed diagnostic instruments performed flawlessly with no interruptions during the campaign period. The HAARP operations staff demonstrated the maturity of the site and its usability by responding regularly and in a timely manner to requests for experimental changes in real time. The 2010 PARS Summer School was a success, meeting its academic and experimental goals while simultaneously providing a stimulating experience for all of its participants.

References

Hysell, D.L., E. Nossa, M. McCarrick. Excitation threshold and gyroharmonic suppression of artificial E region field-aligned plasma density irregularities. Radio Science 2010 (in press).

Hysell, D.L. 30 MHz radar observations of artificial E region Field-aligned plasma irregularities. Ann. Geophys., 26, 117-129, 2008. http://www.ann-geophys.net/26/117/2008/.

Appendix

Geophysical Data During the Campaign Interval

This appendix provides graphical and tabular information characterizing the geophysical conditions during the period July 18-22, 2010 which encompassed the experimental portion of the 2010 PARS Summer School.
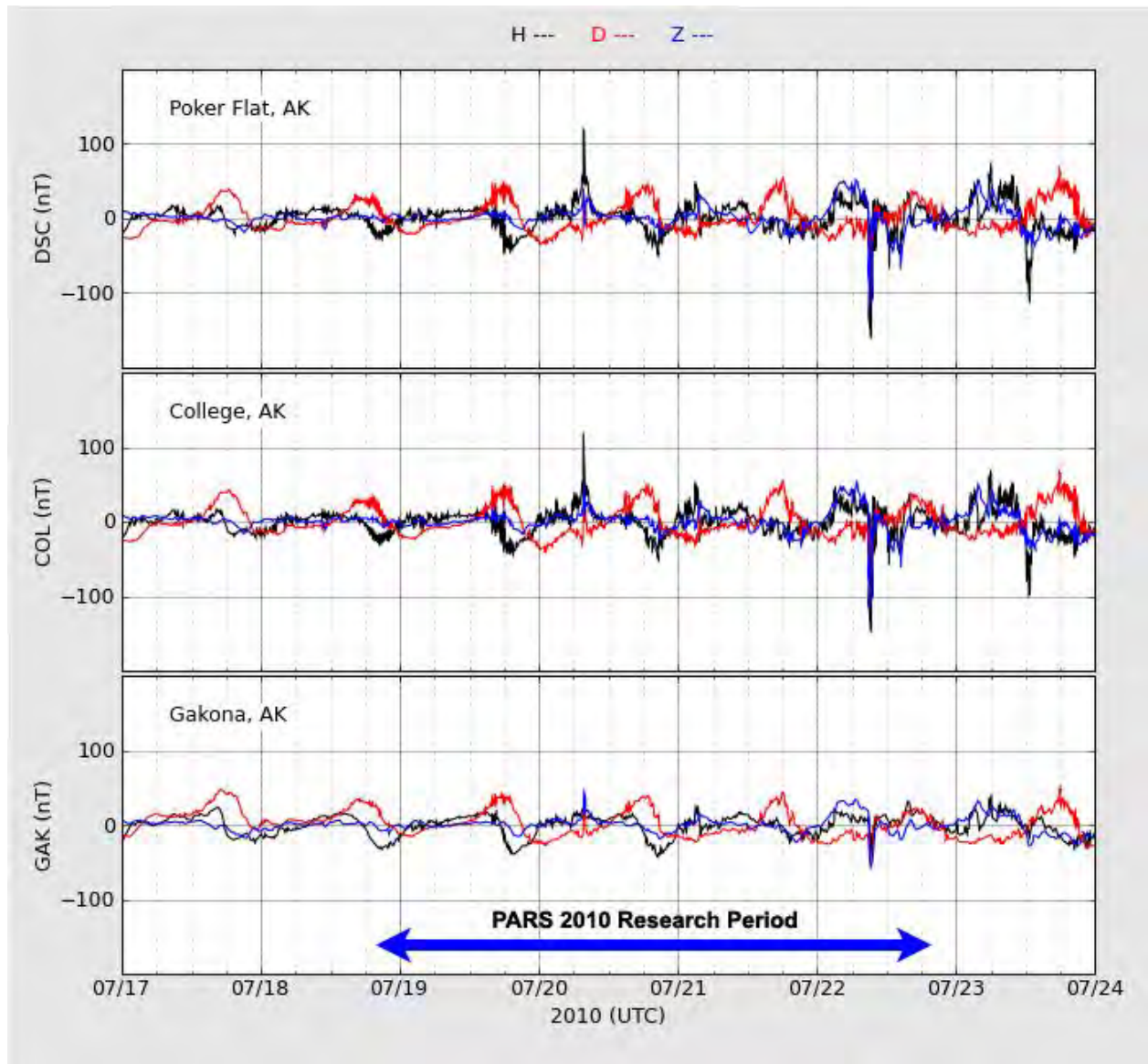

Figure A.1: Data from the University of Alaska Geophysical Institute Magnetometer Array for 17-24 July 2010 – Data from only three instruments in the string were available during this time
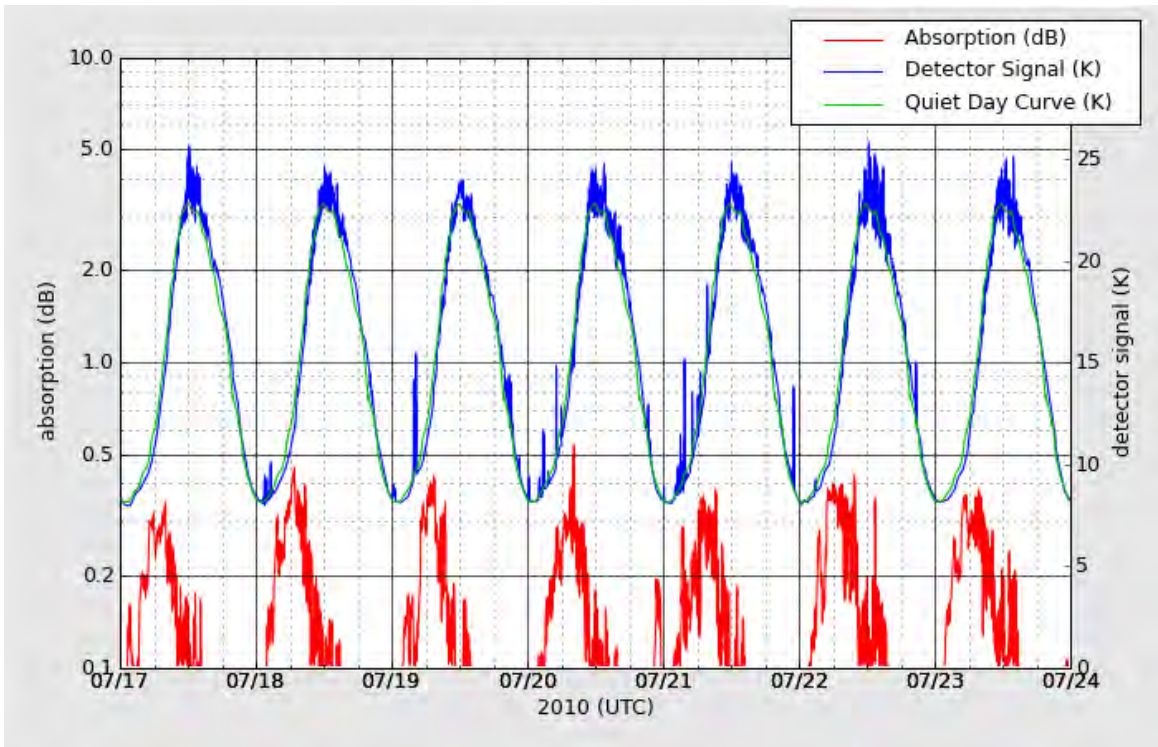
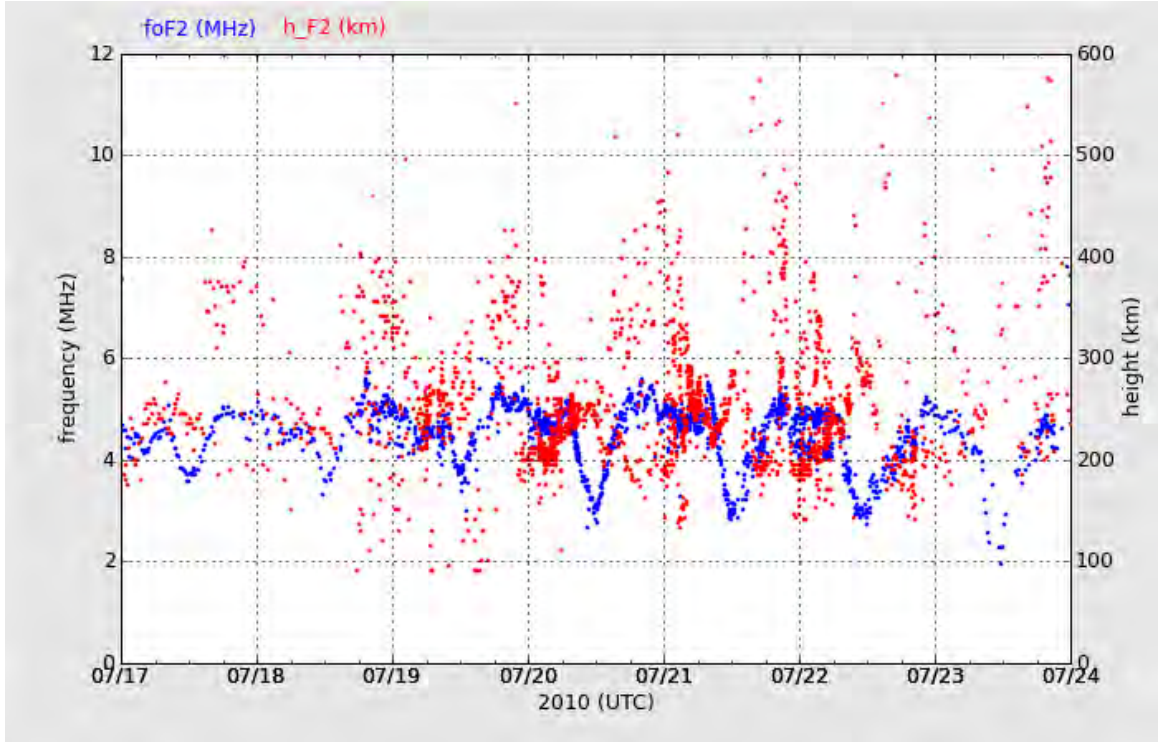**Figure A.2: Data from the HAARP riometer for 17-24 July 2010**

Figure A.3: Data from the HAARP Digisonde for 17-24 July 2010 – the observed f_0F_2 is plotted in blue, the observed h_mF_2 in red
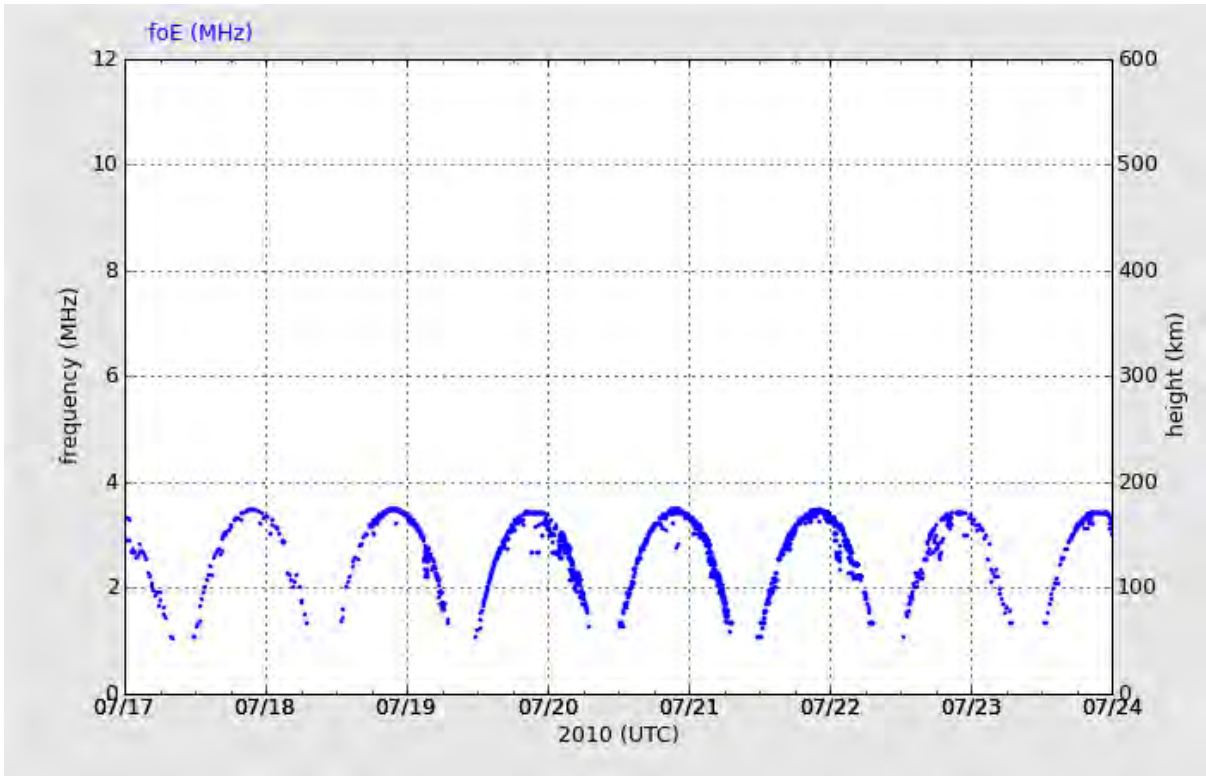
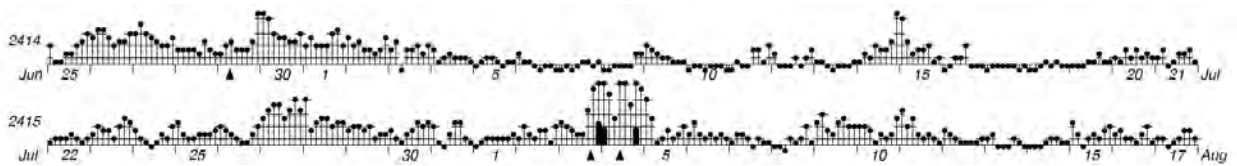**Figure A.4: E-region critical frequency F_0E from the HAARP Digisonde for 17-24 July 2010**

Figure A.5: Plot of the K_p "musical diagram" for two solar rotations which include the July 18-22, 2010 PARS Summer School experiment campaign
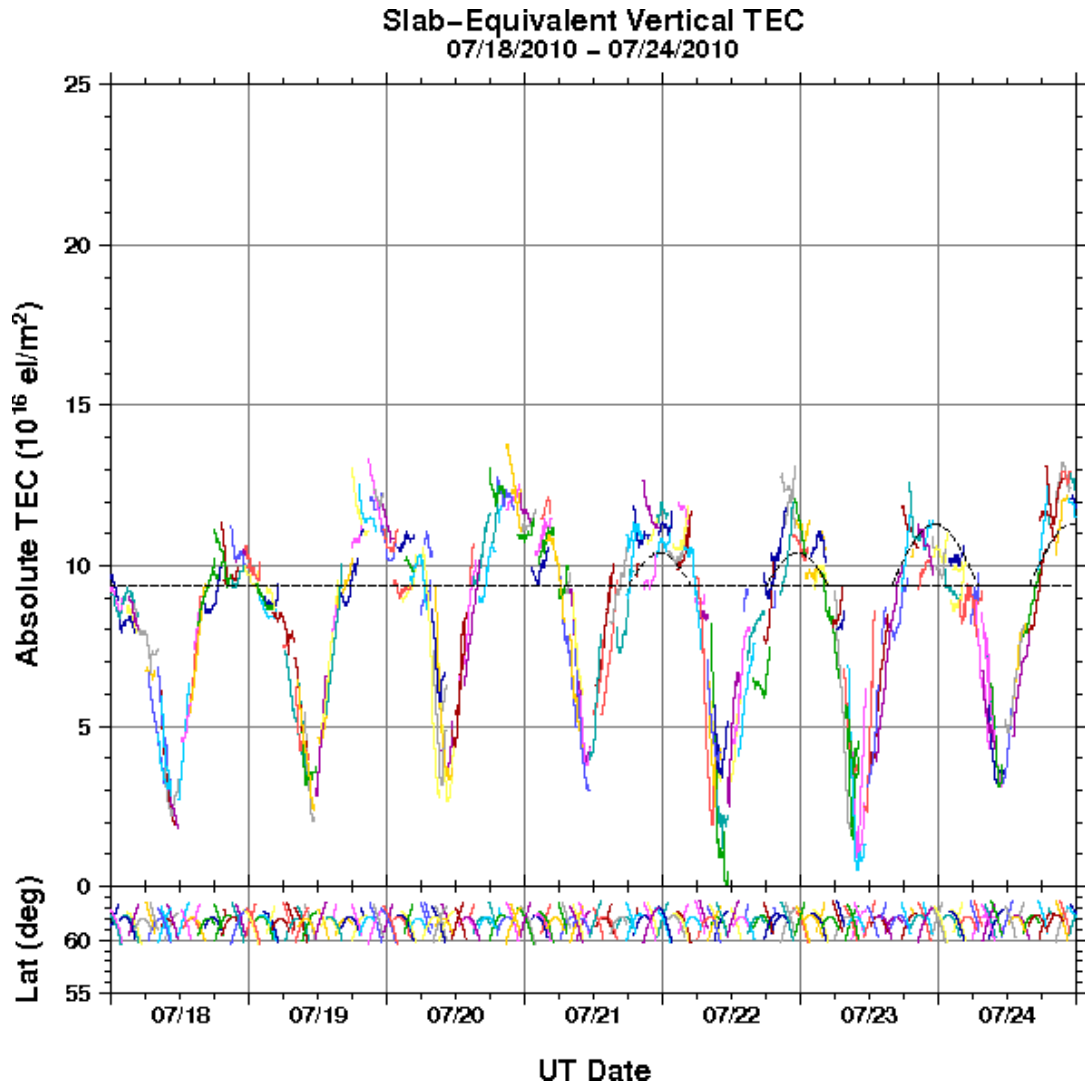
Figure A.6: **Total Electron Content derived from the HAARP GPS receiver for the period 17-24 July 2010 – Different colors indicate data from different GPS satellites**

List of Symbols, Abbreviations, and Acronyms

AFAI	Artificial Field Aligned Irregularities
AFRL	Air Force Research Laboratory
AMISR	Advanced Modular Incoherent Scatter Radar
DM	Downshifted Maximum
EIC	Electrostatic Ion Cyclotron wave
ELF	Extremely Low Frequency
eV	Electron volt
FAI	Field-Aligned Irregularities
f_0F_2	Critical frequency (O-mode) of the F_2 layer (MHz)
f_0E	Critical frequency of the E layer (MHz)
GIOS	NWRA GPS Ionospheric Observing System software
GPS	Global Positioning System
EISCAT	European Incoherent Scatter Scientific Association
ELF	Extremely Low Frequency (Frequencies in the range 3 - 3 kHz)
HAARP	High-frequency Active Auroral Research Program
HF	High Frequency (Frequencies in the range 3-30 MHz)
HFPL	HF-induced Plasma Line
IPP	Ionospheric Penetration Point or Inter-Pulse Period
IRI	Ionospheric Research Instrument
ITS	Ionospheric Tomography System
K	Kelvin (degrees)
kHz	Kilohertz (10^3 cycles/seconds)
kW	Kilowatt (10^3 watts)
L-band	Radio frequency band covering 1.0 GHz to 2.0 GHz (nominal)
MHz	Megahertz (10^6 cycles/seconds)
MSBS	Magnetized Stimulated Brillouin Scatter
MUIR	Modular UHF Ionospheric RADAR
NIMS	Navy Ionospheric Monitoring System
NLDN	National Lightning Detection Network
NRL	Naval Research Laboratory
NWRA	NorthWest Research Associates

ONR	Office of Naval Research
PARS	Polar Aeronomy and Radio Science
PCA	Polar Cap Absorption
PRN	Pseudo-Random Noise (GPS identification signature)
rms, RMS	root mean square
RTI	Range Time Intensity
S_4	Ionospheric intensity scintillation index (non-dimensional)
S-band	Radio frequency band covering 2.0 GHz to 4.0 GHz (nominal)
SEE	Stimulated Electromagnetic Emission
sps	samples per second
SRII	SRI International
SSRC	Summer Student Research Campaign
SuperDARN	Super Dual Auroral Radar Network
TEC	Total Electron Content (electrons/m^2)
TOA	Time of Arrival
UHF	Ultra High Frequency radio band (300 MHz – 3 GHz)
UML	University of Massachusetts at Lowell
UMLCAR	University of Mass Lowell, Center for Atmospheric Research
UPS	Uninterruptible Power Source
VHF	Very High Frequency radio band (30 MHz – 300 MHz)
VLF	Very Low Frequency radio band (3 kHz – 30 kHz)
VTEC	Vertical (or equivalent vertical) TEC (el/m^2)

DISTRIBUTION LIST

DTIC/OCP
8725 John J. Kingman Rd, Suite 0944
Ft Belvoir, VA 22060-6218   1 cy

AFRL/RVIL
Kirtland AFB, NM 87117-5776   2 cys

Official Record Copy
AFRL/RVBXI/Craig Selcher   1 cy